

Anatomía Comparada de Vertebrados

CRÁNEO



Sergio Soto Acuña

*Laboratorio de Ontogenia y Filogenia, Universidad de Chile
Área de Paleontología, Museo Nacional de Historia Natural*



Hippopotamus amphibius

Cresta Neural

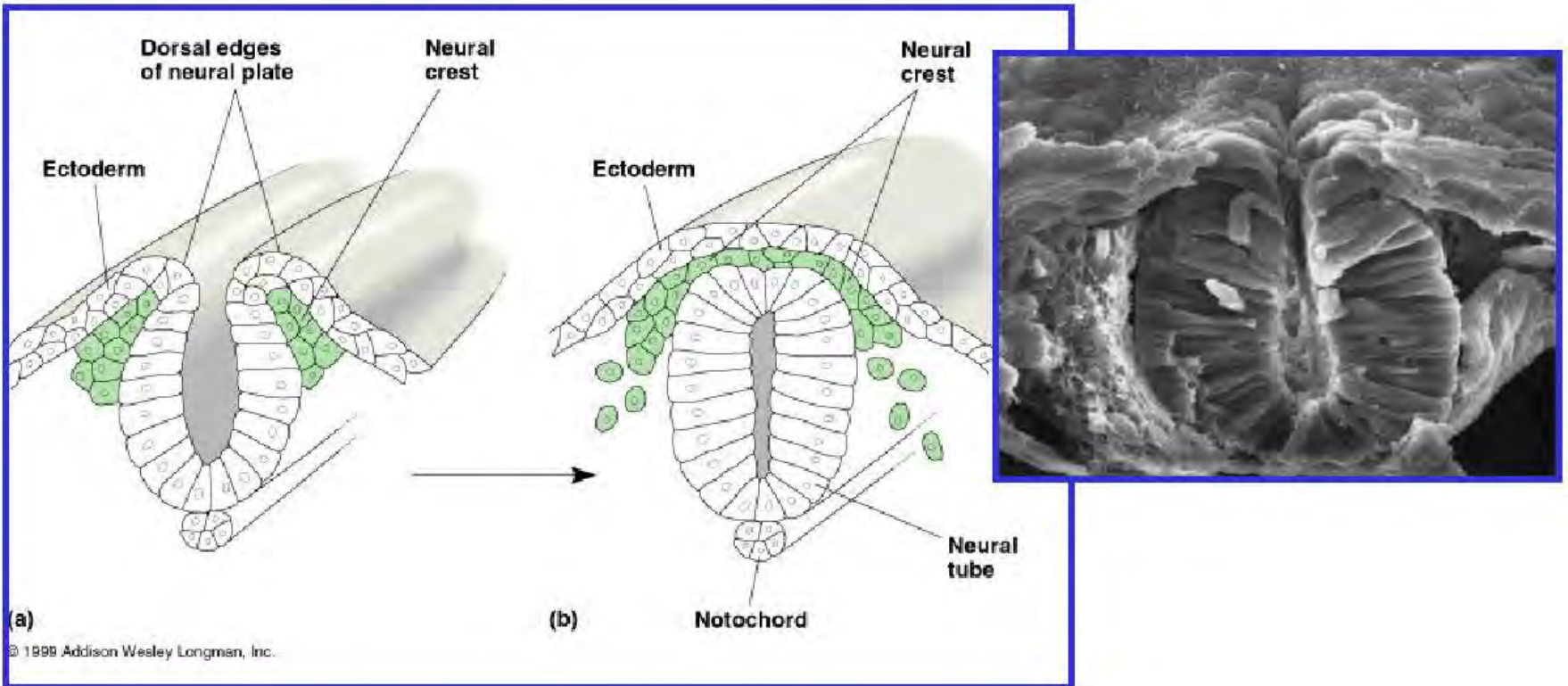


Tabla 1. Derivados de las Crestas Neurales. Según datos de Kardong (1999); Moore & Persaud (1999); Sadler, (2001)

- Neuronas de los Ganglios Sensoriales (Somáticos y Viscerales), y otros tipos de neuronas periféricas
- Ganglios Simpáticos y Parasimpáticos
- Células Productoras de Hormonas (Cromafines de la Médula Adrenal y productoras de Calcitonina)
- Células Pigmentarias (melanocitos, excepto los de la retina y SNC)
- Células de Schwann
- Células de Almohadillas conotroncales del corazón.
- Partes de las Meninges (Piamadre y Aracnoides)
- Huesos, Cartílagos y Tejidos Conectivos de los Arcos Branquiales y Estructuras Craneofaciales derivadas.
- Cápsulas Sensoriales y Partes del Neurocráneo, Dermatocráneo y dermis de la Región Facial
- Armadura Cefálica y Derivados
- Odontoblastos

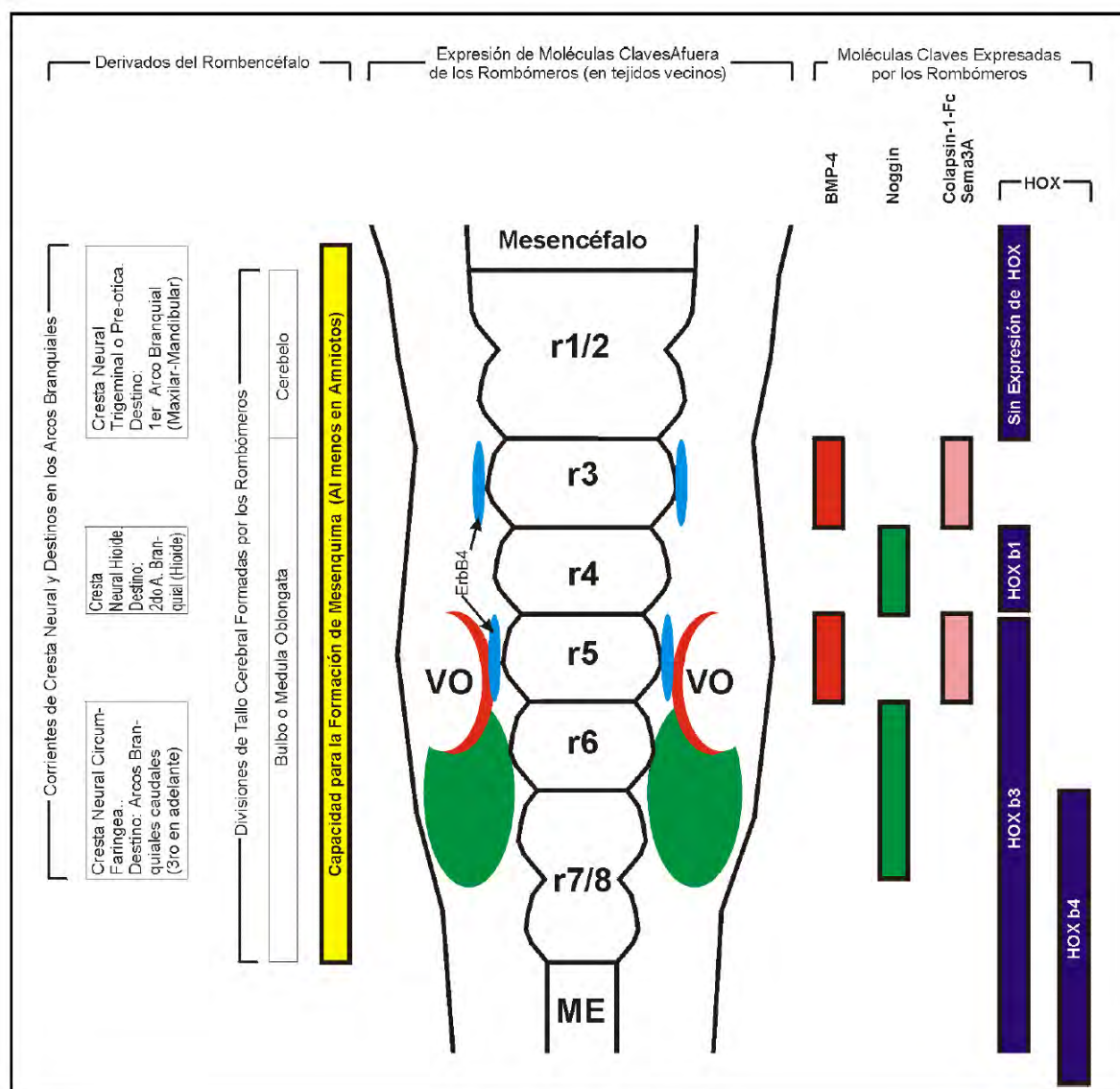


Figura 2. Aunque los límites entre las divisiones (ej: mes-, met [cerebelo + puente en mamíferos] y mielencéfalo), propiedades y moléculas expresadas por los rombómeros (r), son difusos y controvertidos, especialmente en los cefálicos (r1/2) y caudales (r7/8), para facilitar la comprensión de algunos aspectos claves del desarrollo del rombencéfalo y crestas neurales, se realizó esta representación esquemática, en la cual, a la izquierda se muestran los principales derivados del rombencéfalo y cresta neural, la cual se segrega en 3 corrientes: Pre-ótica o Trigeminal, Hioidea y Post-ótica o Circunfaringea. En la parte central de la figura, se ilustran moléculas clave expresadas por los tejidos vecinos del rombencéfalo. A la derecha, algunas moléculas expresadas por los rombómeros. Es de destacar la expresión del apoptótico de crestas neurales BMP-4 (rojo), el cual es producido por los r3, r5, y por las vesículas óticas (VO). Noggin (verde) funciona como anti-apoptótico, y es expresado por los rombómeros vecinos a r3 y r5, y especialmente por el r4, y por el mesénquima vecino a los r6 y r7. Además, las moléculas ErbB4 (azul), Colapsina-1-Fc y Sema3A (ambas en rosado), son inhibidoras de la migración de células de cresta neural. Se muestra el territorio de expresión de algunos genes Hox (azul oscuro), lo cual es compatible con los sitios donde hay patrones segmentarios globales, como r3 al r8 y niveles correspondientes al tronco, donde empieza la Médula Espinal (ME). Según datos y revisiones de Couly et al. (1998); Eickholt, et al (1999); Graham (2001); Golding et al. (2000); Holland & Chen (2001); Horigome et al. (1999); Kuratani (1997); Lumsden et al. (1991).

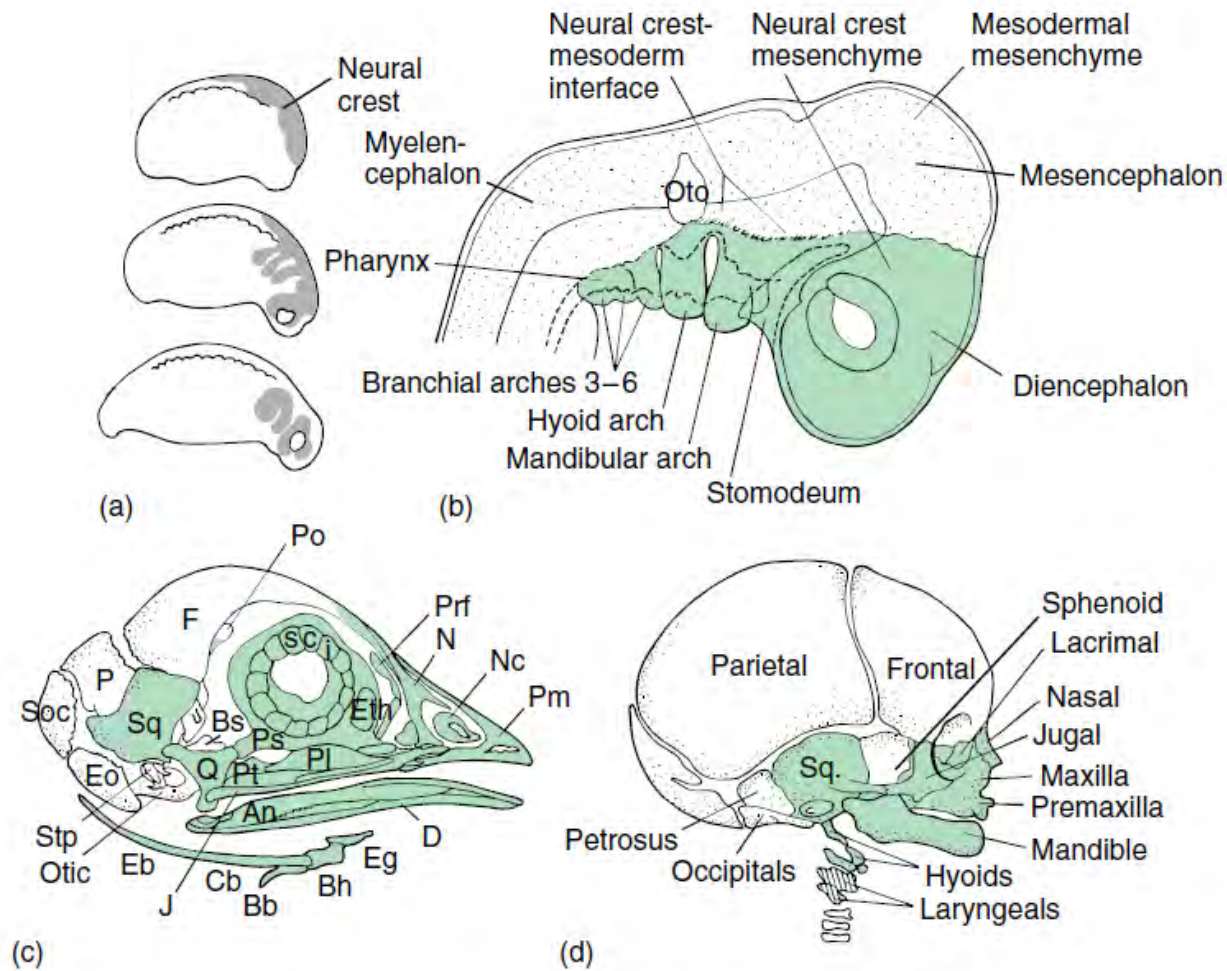
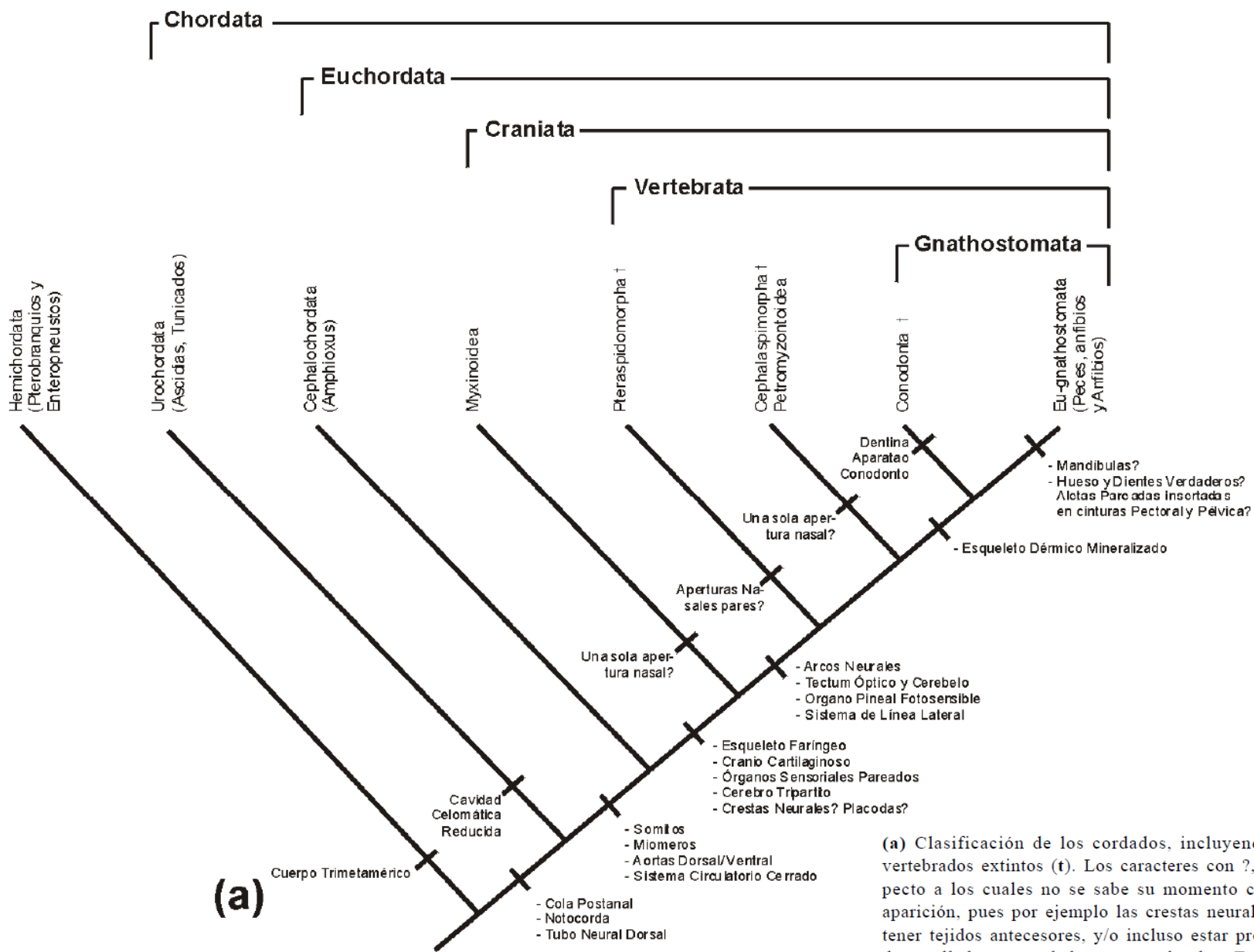


FIGURE 7.4 Neural crest contributions to the skull. (a) Salamander embryo illustrating the sequential spread of neural crest cells. During early embryonic development, neural crest cells contribute to the head mesenchyme, which is called the ectomesoderm because of its neural crest origin. (b) Also contributing to the head mesenchyme are cells of mesodermal origin, the mesodermal mesenchyme. The position of the mesodermal (stippled) and the neural crest (shaded) mesenchyme, and the approximate interface between them, are indicated in the chick embryo. Skull of a chick (c) and a human fetus (d) show bones or portions of bones derived from neural crest cells (shaded). Abbreviations: angular (An), basibranchial (Bb), basihyal (Bh), basisphenoid (Bs), ceratobranchial (Cb), dentary (D), epibranchial (Eb), entoglossum (Eg), exoccipital (Eo), ethmoid (Eth), frontal (F), jugal (J), nasal (N), cartilage nasal capsule (Nc), parietal (P), palatine (Pl), premaxilla (Pm), postorbital (Po), prefrontal (Prf), parasphenoid (Ps), pterygoid (Pt), quadrate (Q), scleral ossicle (Sci), supraoccipital (Soc), squamosal (Sq), stapes (Stp).



(a)

(a) Clasificación de los cordados, incluyendo algunos grupos de vertebrados extintos (†). Los caracteres con ?, son aquellos con respecto a los cuales no se sabe su momento cladográfico exacto de aparición, pues por ejemplo las crestas neurales y placodas, pueden tener tejidos antecesores, y/o incluso estar presentes en forma poco desarrollada, en cordados no vertebrados. Teniendo en cuenta que, entre otros datos controversiales, recientemente los conodontos son tomados como gnathostomados basales (**Donoghue et al., 2000**), el punto exacto de aparición cladográfica de los caracteres típicos de los gnathostomados (eu-gnathostomados), podría también ponerse en duda (?).

Placodas

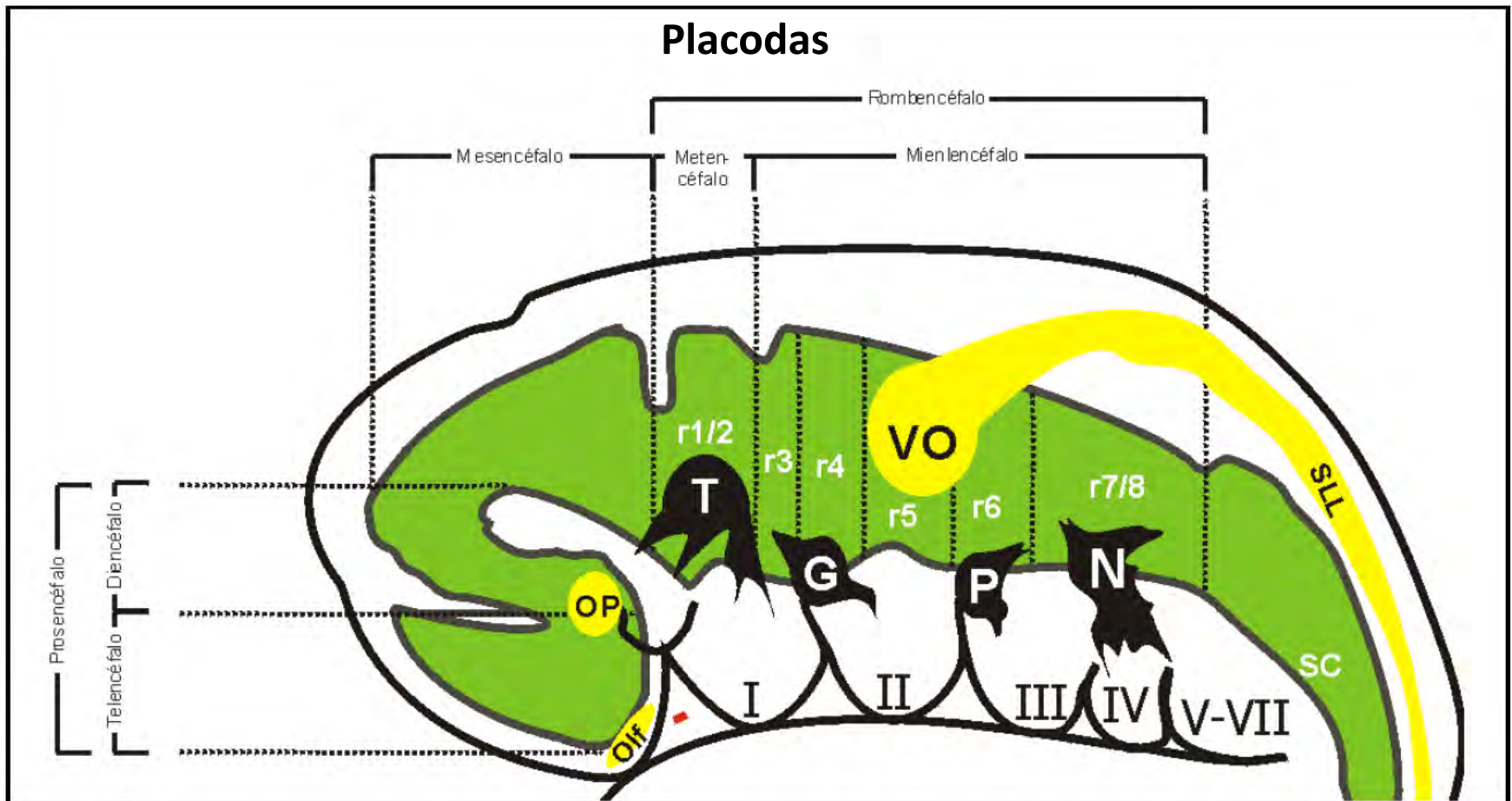


Figura 3. Representación esquemática de las placodas sensoriales (amarillo: Óptica [OP], Vesícula Ótica [VO], Olfativa [Olf]) y neurogénicas (negro), últimas que a su vez se dividen en placodas dorsolaterales o trigeminales (T), y epibránquiales (Geniculada [G], Petrosa [P] y Nodosa [N]). Para más detalles de esta clasificación y derivados placodales, ver la Tabla 2. Aunque como ya se dijo, la relación entre los límites de los rombómeros y las divisiones del tubo neural en formación son difusas (ver Figura 2), éste se ha esquematizado en verde, para ver su relación con la posición de las placodas, sin que esto quiera decir que estas últimas están en contacto directo con dicho tubo, pues las mismas son engrosamientos ectodérmicos. Esta representación, también pone de relieve las importantes relaciones de desarrollo entre las placodas y crestas neurales, pues juntas forman el sistema nervioso periférico cefálico, y además, las neuroglías derivadas de las crestas, se constituyen en importantes guías para la migración de las neuronas placodales que van a contribuir a la formación de los ganglios y nervios sensoriales cefálicos. Otro aspecto importante de este esquema es el hecho de que se le ha dado continuidad a la placoda ótica (que forma la vesícula ótica) y los primordios del sistema de línea lateral (SLL), pues aunque es una hipótesis controversial, es posible que todos los receptores acústico-laterales sean derivados de una misma placoda ancestral. Cada arco se ha denotado con un número romano y la cantidad total de los mismos es variable (V-VII aprox.): 5 amniotos, y típicamente 7 en peces. Según datos y revisiones de Begbie *et al.* (1999); Begbie & Graham (2001a); Begbie & Graham (2001b); Kardong (1999); Moore & Persaud (1999); Sadler (2001); Streit (2001).

Arcos Branquiales

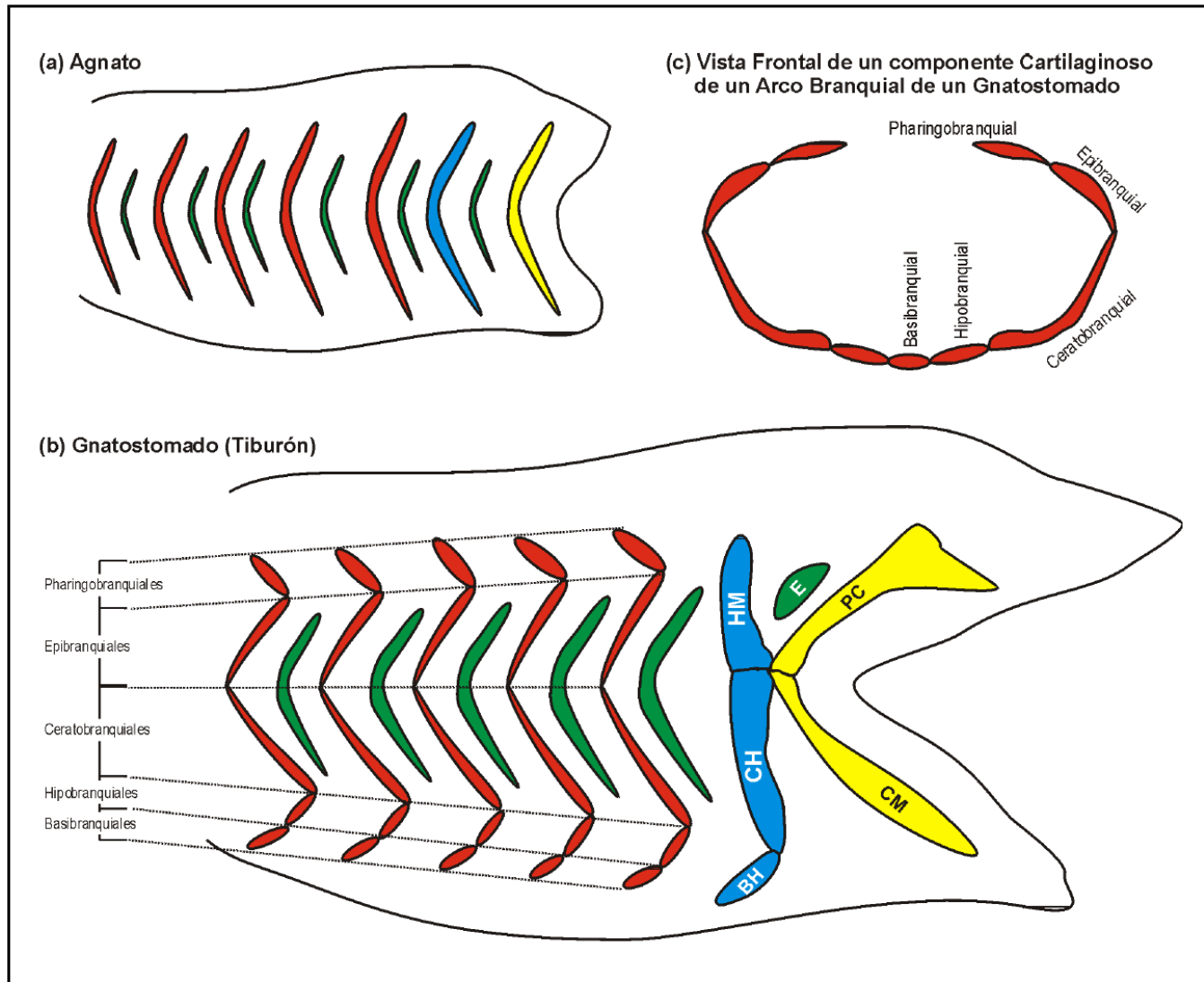
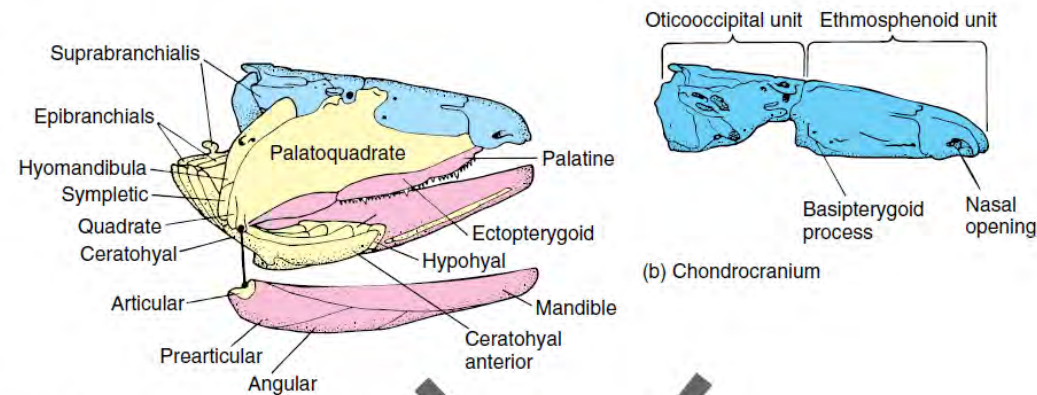


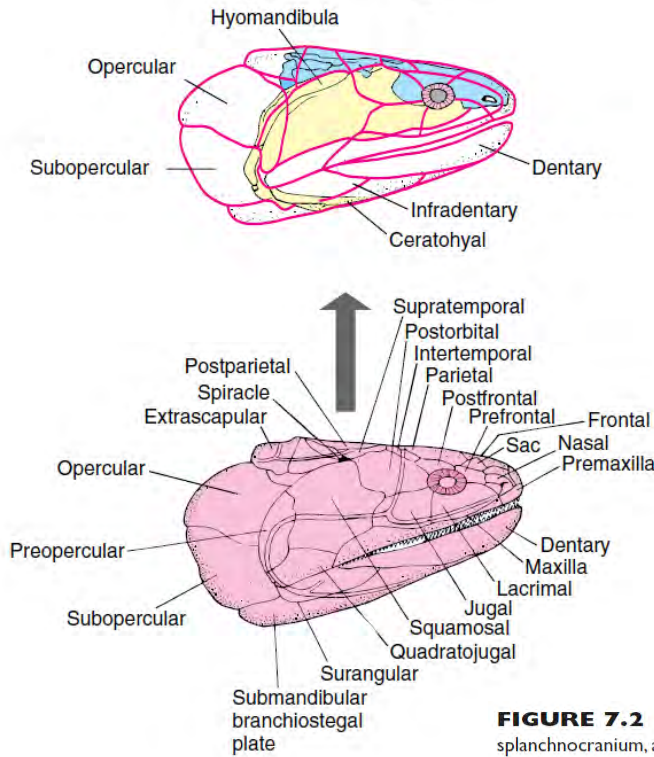
Figura 4. Esquema del esqueleto branquial. En amarillo el I arco o a. mandibular en gnatostomados (b) o dominio mandibular en agnatos (a)? En azul el II arco o a. hiodeo en gnatostomados o dominio hiodeo en agnatos? En rojo los arcos mandibulares caudales; en verde las hendiduras branquiales, de las cuales la primera se conserva en los elasmobranquios (tiburón) como espiráculo. Basihial (BH); Ceratohial (CH); Cartilago de Meckel (CM); Hiomandibular (HM); Palato Cuadrado (PC). La correspondencia en colores denota, de forma muy general, resumida e hipotética, como se pudo dar la evolución de las mandíbulas (hipótesis serial) a partir de algún agnato extinto del cual haya descendido el primer gnatostomado (animales extintos no representados en estos esquemas). Existen evidencias morfológicas y moleculares que apoyan esta hipótesis (ver texto). Nótese cómo en (b) cada bastón cartilaginoso se ha esquematizado en un solo elemento, para resaltar el hecho de que en los agnatos, el cesto branquial no está compuesto por elementos articulados como en los gnatostomados. En (c) se ve, desde un punto de vista frontal o caudal, cómo se disponen los elementos cartilagosos de cada arco, en los gnatostomados.

Componentes del Cráneo



(a) Splanchnocranium

(b) Chondrocranium



(c) Dermatocranium

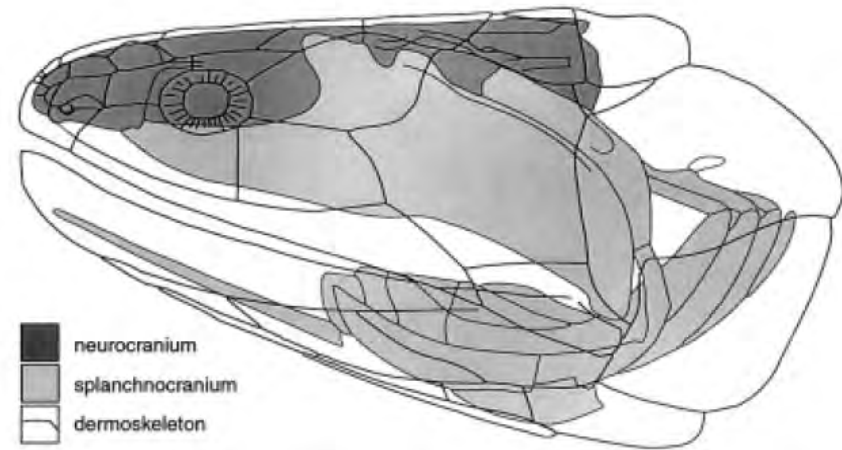


Fig. 1. The head of *Eusthenopteron foordi*, a sarcopterygian fish, demonstrating the different skeletal systems (after Jarvik, 1980). Neurocranium, dark gray; splanchnocranium, light gray; dermoskeleton, unshaded but margins between the cranial dermal bones are outlined in black.

FIGURE 7.2 Composite skull. The skull is a mosaic composed of three primary contributing parts: the chondrocranium, the splanchnocranium, and the dermatocranium. Each has a separate evolutionary background. The skull of *Eusthenopteron*, a Devonian rhipidistian fish, illustrates how parts of all three phylogenetic sources contribute to the unit. (a) The splanchnocranium (yellow) arose first and is shown in association with the chondrocranium (blue) and parts of the dermatocranium (red). The right mandible is lowered from its point of articulation better to reveal deeper bones. (b) The chondrocranium in *Eusthenopteron* is formed by the union between the anterior ethmosphenoid and the posterior oticooccipital units. (c) The superficial wall of bones composes the dermatocranium. The central figure depicts the relative position of each contributing set of bones brought together in the composite skull. (Sac: nasal series)

Dermatocráneo

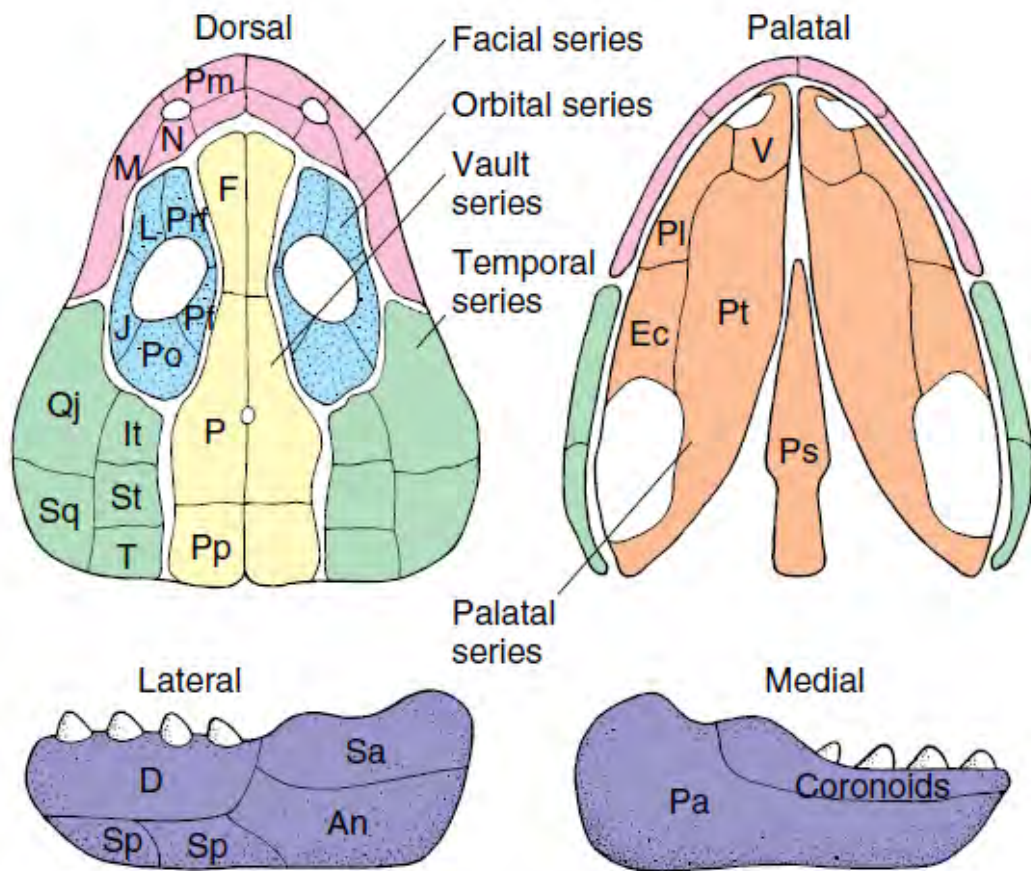
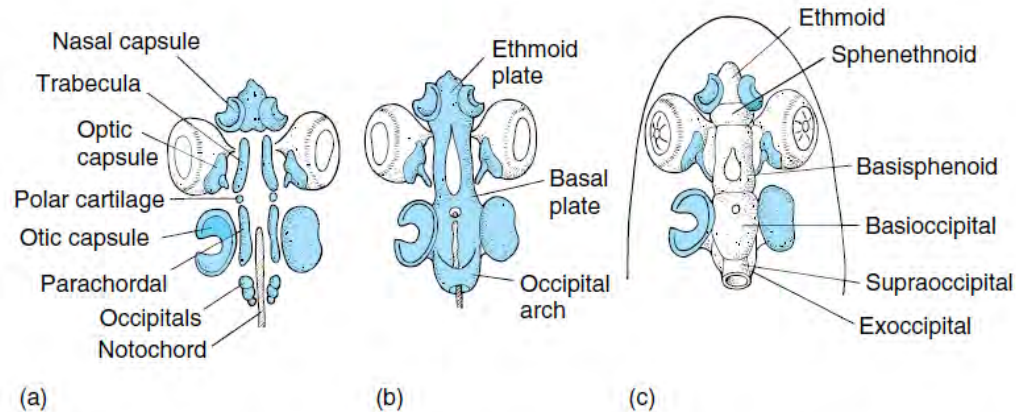


FIGURE 7.10 Major bones of the dermatocranium. Sets of dermal bones form the facial series surrounding the nostril. The orbital series encircles the eye, and the temporal series composes the lateral wall behind the eye. The vault series,

TABLE 7.3 Major Dermal Bones of the Skull		
B R A I N C A S E		
Facial Series	Orbital Series	Temporal Series
Premaxilla	Lacrimal	Intertemporal
Maxilla	Prefrontal	Supratemporal
Nasals (septomaxilla)	Postfrontal Postorbital	Tabular
	Jugal	Squamosal Quadratojugal
M A N D I B L E		
Vault Series	Palatal Series	Mandibular Series
Frontal	Vomer	Lateral bones:
Parietal	Palatine	Dentary (teeth)
Postparietal	Ectopterygoid	Splenials (2)
	Pterygoid Parasphenoid (unpaired)	Angular Surangular
		Medial bones: Prearticular Coronoids

Condrocráneo



Endochondral Structure	Fishes (Teleost)	Amphibians	Reptiles/Birds	Mammals	
Occipital bones	Supraoccipital Exoccipital Basioccipital	Supraoccipital Exoccipital Basioccipital	Supraoccipital Exoccipital Basioccipital	Supraoccipital Exoccipital Basioccipital	} Occipital bone
Mesethmoid bone	Mesethmoid ^a (internasal)	Absent	Absent	Mesethmoid (absent in primitive mammals, ungulates)	} Ethmoid
Ethmoid region	Ossified	Unossified	Unossified	Turbinals (ethmo-, naso-, maxillo-)	
Sphenoid bones	<i>Sphenethmoid</i> <i>Orbitosphenoid</i> <i>Basisphenoid</i> ^b <i>Pleurosphenoid</i>	<i>Sphenethmoid</i> <i>Orbitosphenoid</i> <i>Basisphenoid</i> ?	<i>Sphenethmoid</i> <i>Orbitosphenoid</i> <i>Basisphenoid</i> <i>Pleurosphenoid</i> (crocodilians, amphisbaenians)	<i>Presphenoid</i> <i>Orbitosphenoid</i> <i>Basisphenoid</i> Absent	} Sphenoid ^c
Laterosphenoid			Laterosphenoid (snakes)	Absent	
Otic capsule Periotic	{ Prootic Epiotic Sphenotic	Prootic Opisthotic	{ Prootic Opisthotic Epiotic (absent in birds)	Petrosal with mastoid process	

^aThis bone is of dermal origin, so it is not strictly homologous to tetrapod mesethmoid.

^bThis bone is usually absent or reduced in some fishes.

^cAlisphenoid from the splanchnocranium contributes.

Esplacnocráneo

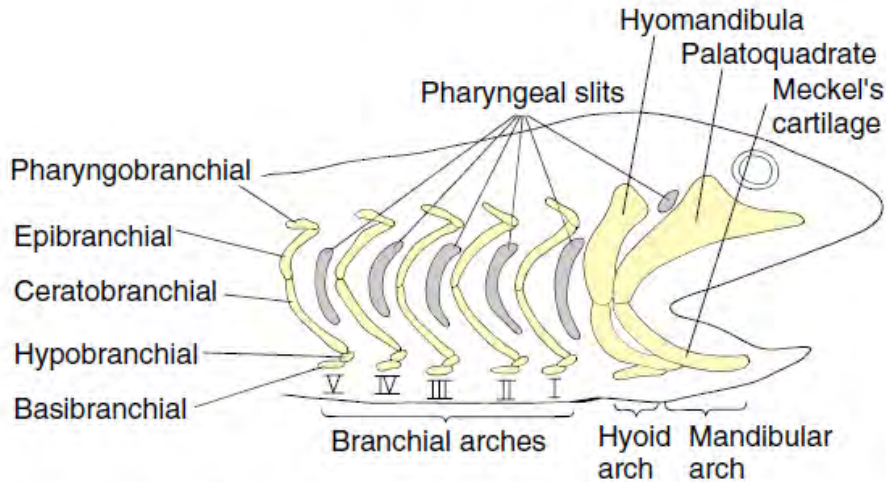


FIGURE 7.5 Primitive splanchnocranium. Seven arches are shown. Up to five elements compose an arch on each side, beginning with the pharyngobranchial dorsally and in sequence to the basibranchials most ventrally. The first two complete arches are named: mandibular arch for the first and hyoid arch for the second that supports it. The characteristic five-arch elements are reduced to just two in the mandibular arch: the palatoquadrate and Meckel's cartilage. The large hyomandibula, derived from an epibranchial element, is the most prominent component of the next arch, the hyoid arch. Behind the hyoid arch are variable numbers of branchial arches I, II, and so on. Labial cartilages are not included.

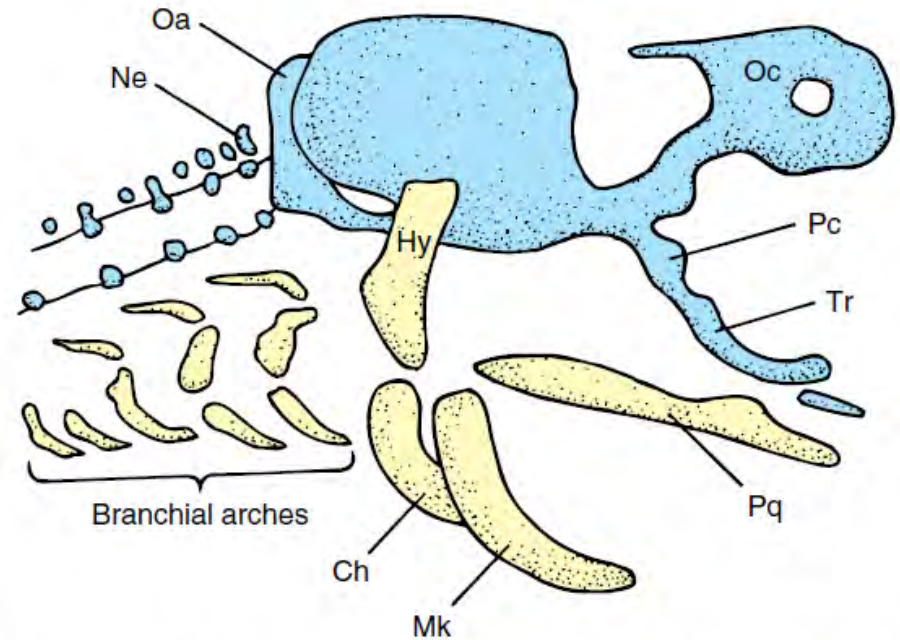


FIGURE 7.6 Shark embryo, the dogfish *Scyllium*. Jaws appear to be in series with the branchial arches. The mandibular arch is first, followed by the hyoid and then several branchial arches. Such a position of the jaws, in series with the arches, is taken as evidence that the jaws derive from the most anterior branchial arch. Abbreviations: ceratohyal (Ch), hyomandibula (Hy), Meckel's cartilage (Mk), neural arch (Ne), occipital arch (Oa), orbital cartilage (Oc), polar cartilage (Pc), palatoquadrate (Pq), trabecula (Tr). Labial cartilages are not included.

After deBeer.

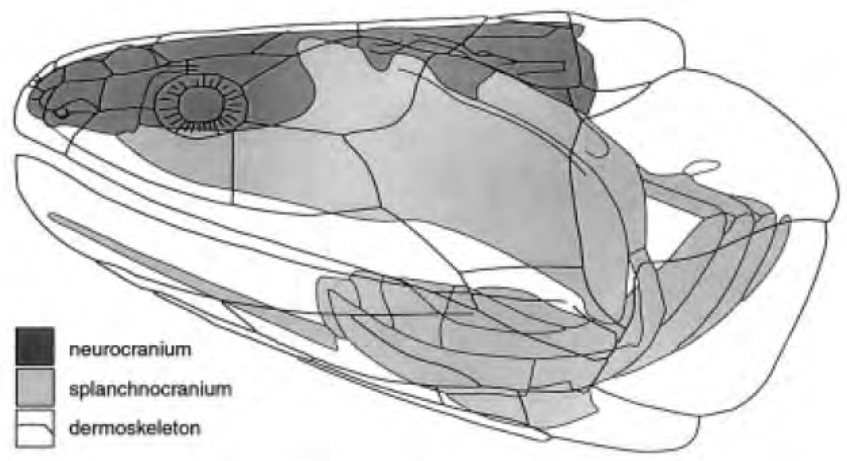
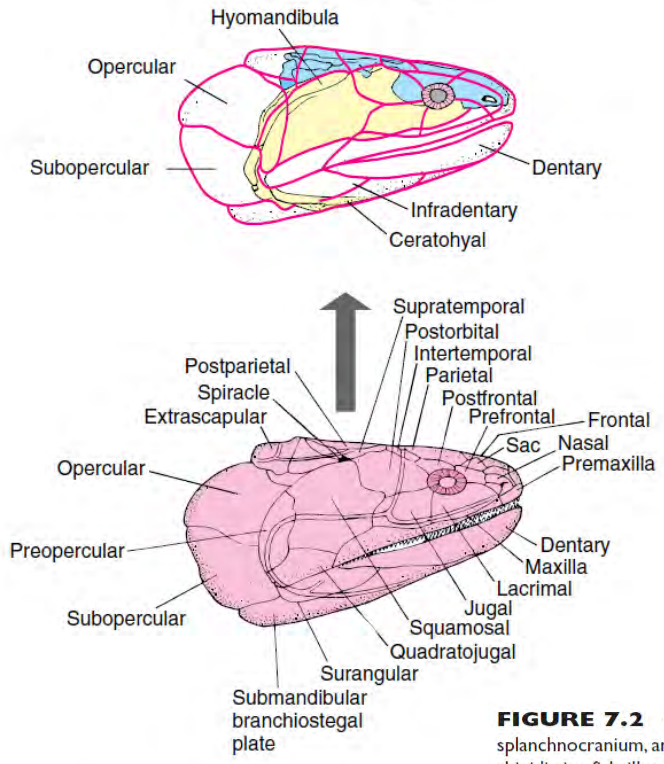
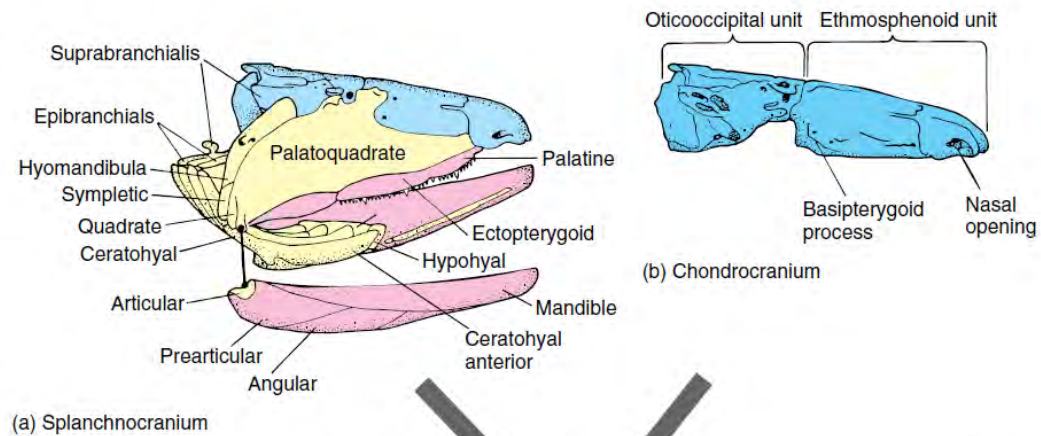


Fig. 1. The head of *Eusthenopteron foordi*, a sarcopterygian fish, demonstrating the different skeletal systems (after Jarvik, 1980). Neurocranium, dark gray; splanchnocranium, light gray; dermoskeleton, unshaded but margins between the cranial dermal bones are outlined in black.

FIGURE 7.2 Composite skull. The skull is a mosaic composed of three primary contributing parts: the chondrocranium, the splanchnocranium, and the dermatocranium. Each has a separate evolutionary background. The skull of *Eusthenopteron*, a Devonian rhipidistian fish, illustrates how parts of all three phylogenetic sources contribute to the unit. (a) The splanchnocranium (yellow) arose first and is shown in association with the chondrocranium (blue) and parts of the dermatocranium (red). The right mandible is lowered from its point of articulation better to reveal deeper bones. (b) The chondrocranium in *Eusthenopteron* is formed by the union between the anterior ethmosphenoid and the posterior oticooccipital units. (c) The superficial wall of bones composes the dermatocranium. The central figure depicts the relative position of each contributing set of bones brought together in the composite skull. (Sac: nasal series)

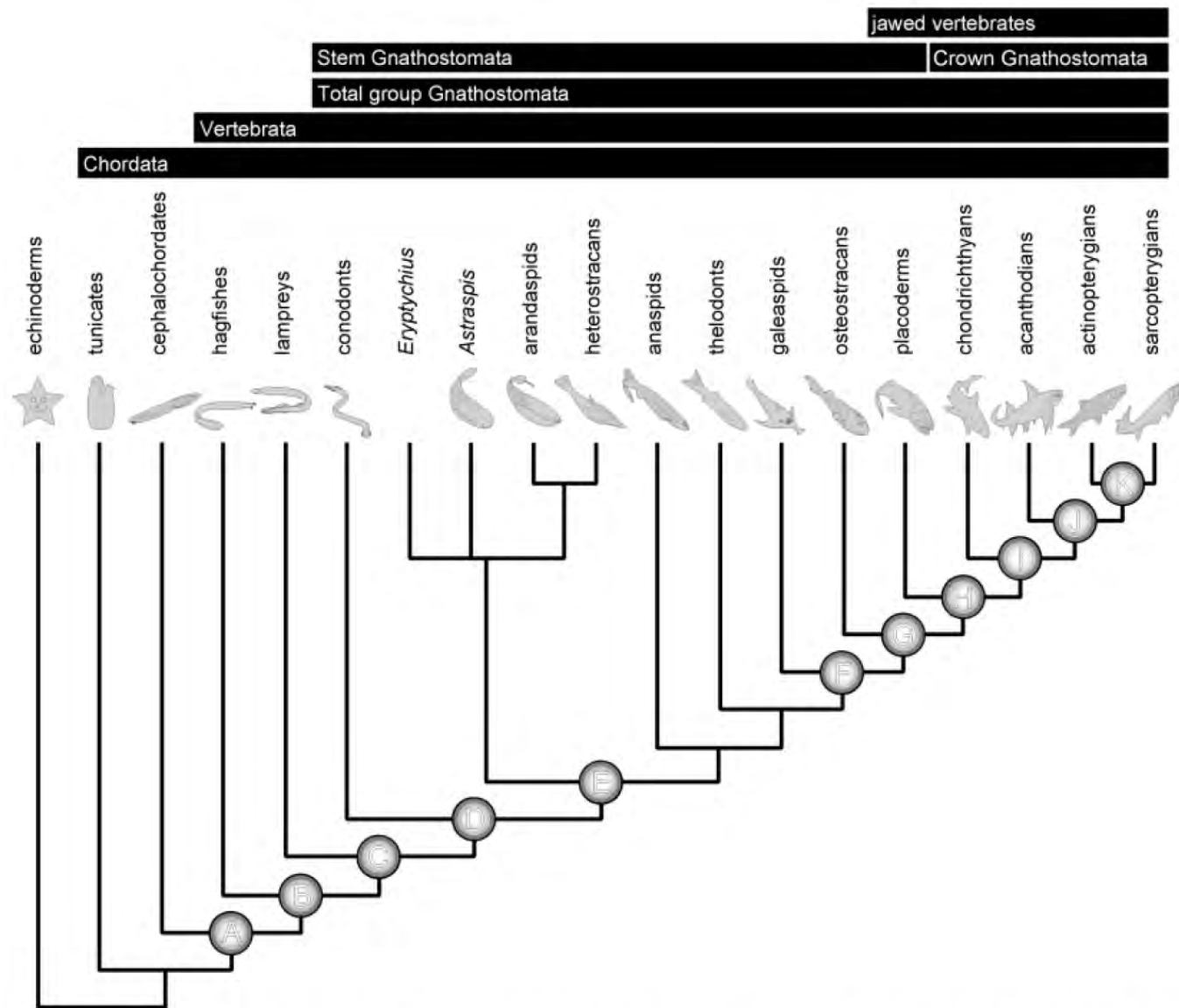


Fig. 3. Phylogenetic relationships between the groups of chordates considered in this study. The black bars across the top refer to the various taxonomic groups and grades of organization used; lettered nodes refer to significant events in the various chordate and vertebrate skeletal systems. **A:** Origin of the earliest skeleton in the vertebrate lineage—a splanchnocranium. **B:** Anatomical development of the splanchnocranium in concert with its takeover by neural crest; origin of a neurocranium. **C:** Further development of the splanchnocranium and neurocranium, origin of neural elements in the axial endoskeleton. **D:** Origin of mineralized splanchnoskeletal elements—the odontode, origin of dentine. **E:** Origin of a mineralized dermal

skeleton—multicomponent scales are primitive, origin of dermal bone. **F:** Origin of perichondral bone, origin of a mineralized endoskeleton. **G:** Origin of cellular dermal and endoskeletal bone, origin of an appendicular endoskeleton, splanchnocranial ossification-proper. **H:** Origin of a mineralized axial endoskeleton, ventral vertebral elements, centra (arcocentra), origin of “teeth.” **I:** Dental elements consistently associated with the splanchnocranium including branchial arches. **J:** neurocranium composed of distinct ossifications, splanchnocranium well ossified. **K:** origin of endochondral bone, dermoskeleton, and endoskeleton well ossified. [Color figure can be viewed in the online issue, which is available at www.interscience.wiley.com.]

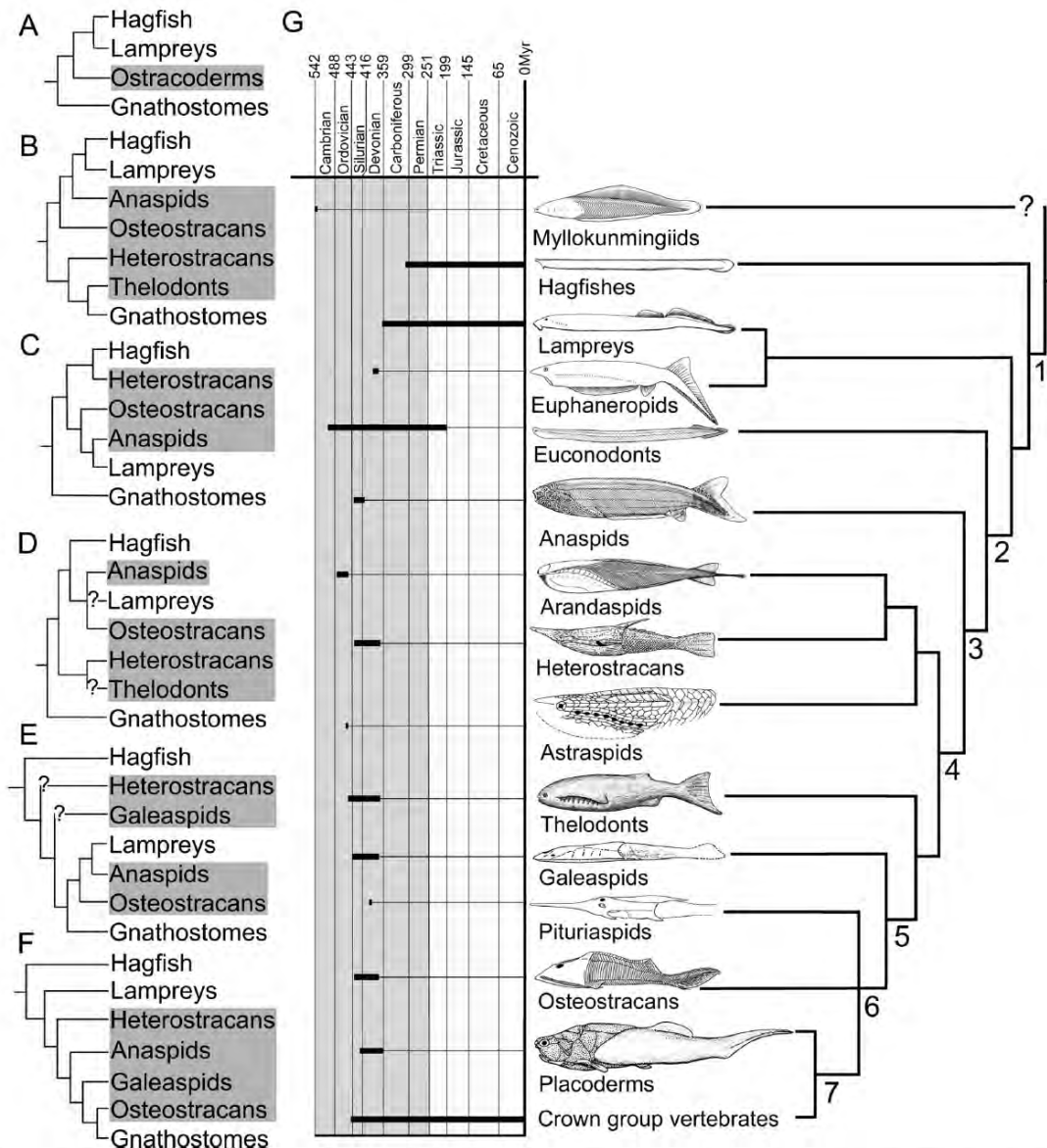


Fig. 1. Interrelationships of the major fossil and living vertebrate taxa since the late 19th century. **(A–F)** Phylogenetic position attributed to the major armored, jawless fossil vertebrate taxa (or ‘ostracoderms’; in grey box) according to various authors, showing the progressive shift from their status of ‘Agnatha’ to that of stem gnathostomes. **(A)** After Cope (1889). **(B)** After Kiaer (1924) and most other authors of the 20th century. **(C)** After Stensiö (1927). **(D)** After Moy-Thomas and Miles (1971). **(E)** After Janvier (1978). **(F)** After Janvier (1996a). **(G)** One of the recently published vertebrate tree topologies that entails cyclostome paraphyly (after Gess et al., 2007; possible position of mylokunmingiids modified according to Janvier, 2003); the distribution of the taxa through time is indicated by bold lines in the time scale to the left. Major synapomorphies at nodes: 1, neural crests, epidermal placodes, fin radials; 2, dermoskeleton in mouth and pharynx; 3, extensive dermoskeleton over the entire body; 4, extensive lateral-line system enclosed in grooves and canals, vertical semicircular canals forming loops, cerebellum; 5, endoskeleton lined with calcified cartilage or perichondral bone; 6, pectoral fins in postbranchial position; 7, jaws. (Illustrations of respective taxa after Janvier, 2007b).

Myllokunmingia fengjiao

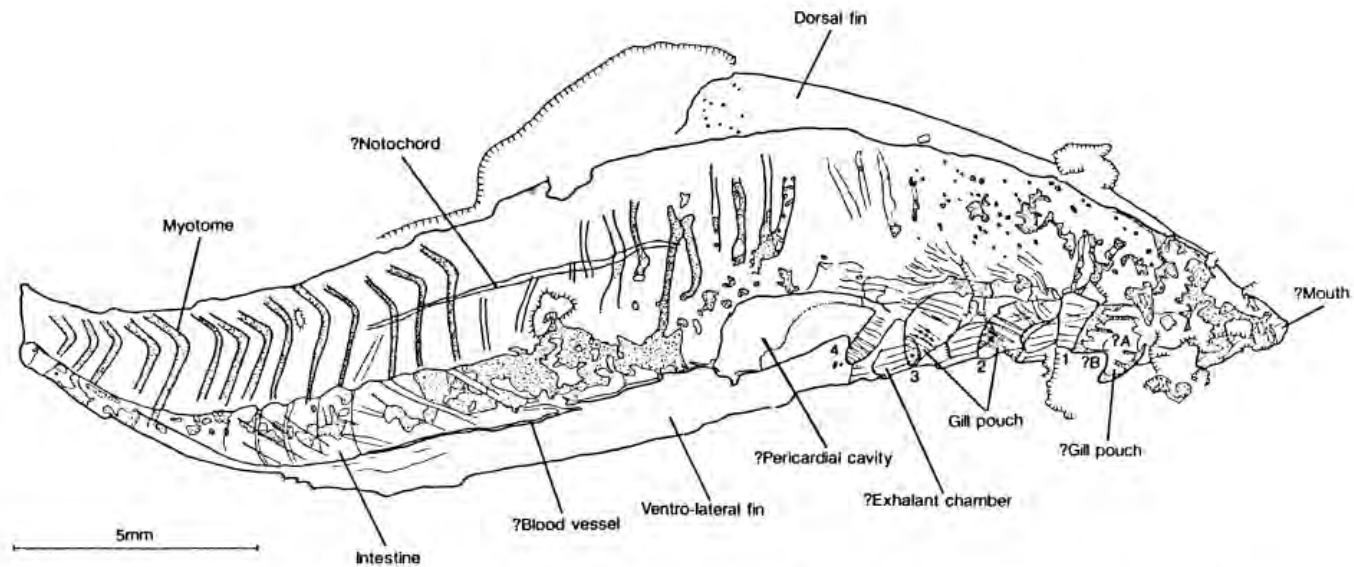


Figure 3 Camera-lucida drawing of specimen, with certain features (notably structures interpreted as extrabranchial atria) combined by reversal from the counterpart (Fig. 1c), to show interpretation. Numbers 1–4 refer to gill pouches identified with reasonable

certainty; ?A and ?B refer to more tentative identification of gill pouches, of which ?A is less certain than ?B.

Haikouichthys ercaicunensis

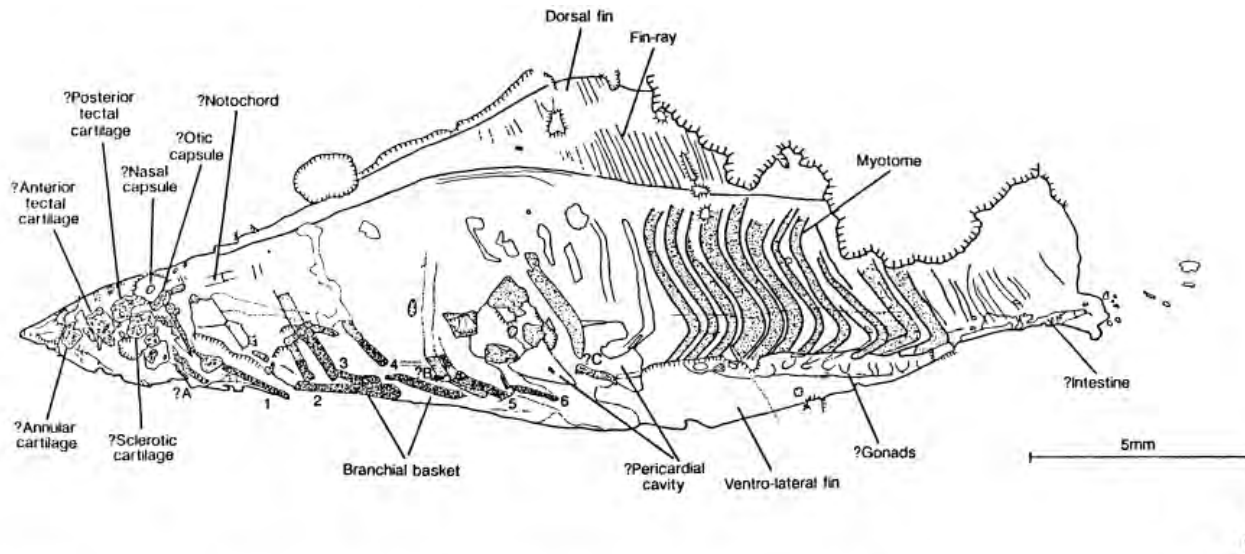


Figure 4 The Lower Cambrian agnathan vertebrate *Haikouichthys ercaicunensis* Luo, Hu & Shu gen. et sp. nov. from Haikou, Yunnan. Specimen HZ-f-12-127. **a**, Entire specimen, anterior to the left; more posterior region appears to fade out into sediment, possibly representing decay of body; attempts to excavate this area were not successful. Scale bar equivalent to 5 mm. **b**, Detail of anterior to show putative gill bars, possible elements of cranial endoskeleton, and pericardic area; scale bar equivalent to 5 mm. **c**, Camera-

lucida drawing of specimen to show interpretation. Numbers 1–6 indicate units of the branchial basket that are identified with some confidence; ?A–?C refer to less secure identifications. Two possible areas representing the pericardic cavity are indicated. To the anterior of ?C a triangular area with patches of diagenetic mineralization is one possibility; a fainter region to the posterior is the alternative location.

Origen esqueleto dérmico mineralizado

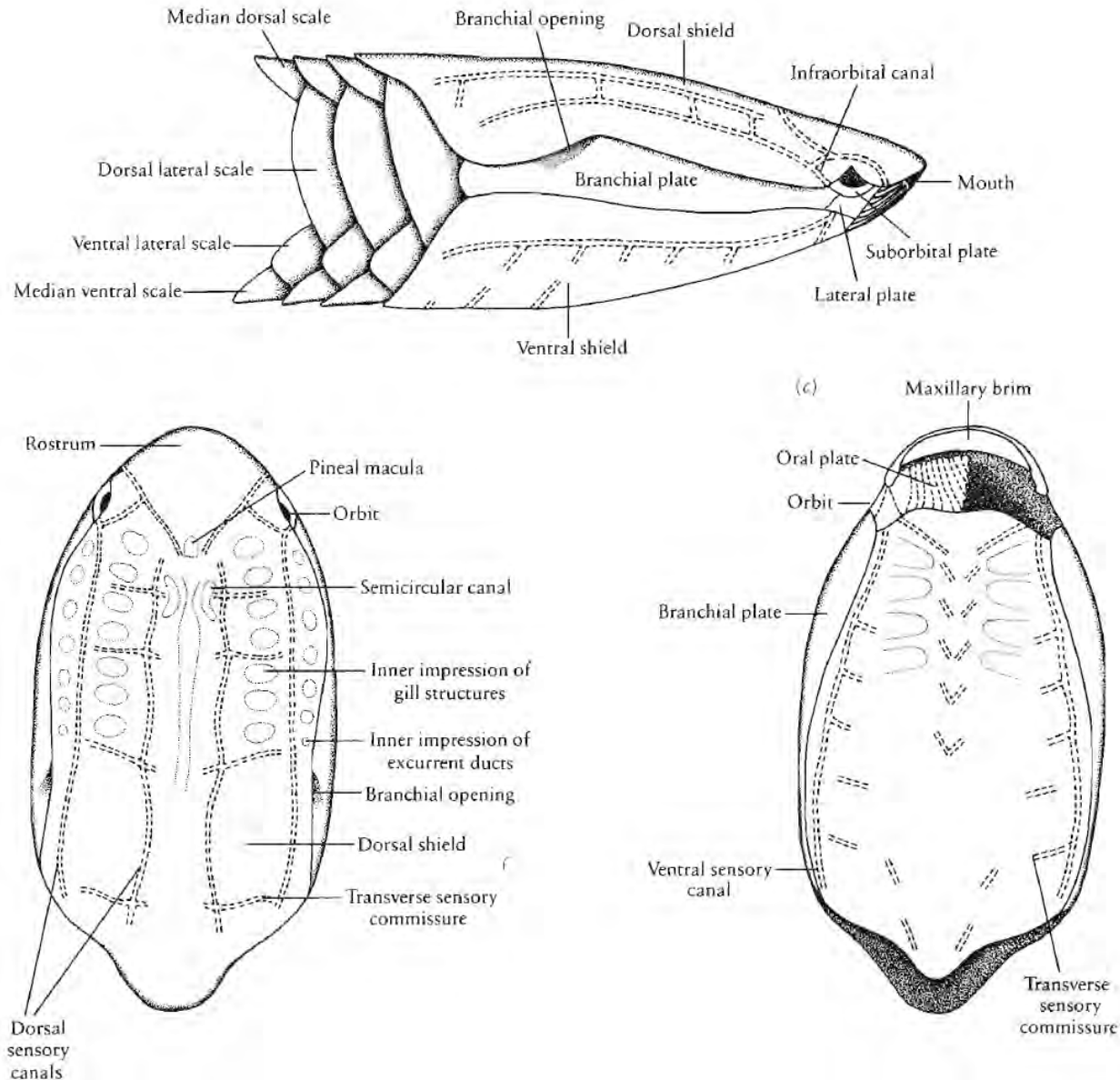


Figure 3-6. *PORASPIS*, A CYATHASPID HETEROSTRACAN. Restorations of shield in (a) lateral, (b) dorsal and (c) ventral views. Impressions on the inner surface of the shield indicated with dotted lines, $\times 2$. From Moy-Thomas and Miles, 1971. By permission from Chapman and Hall Ltd.

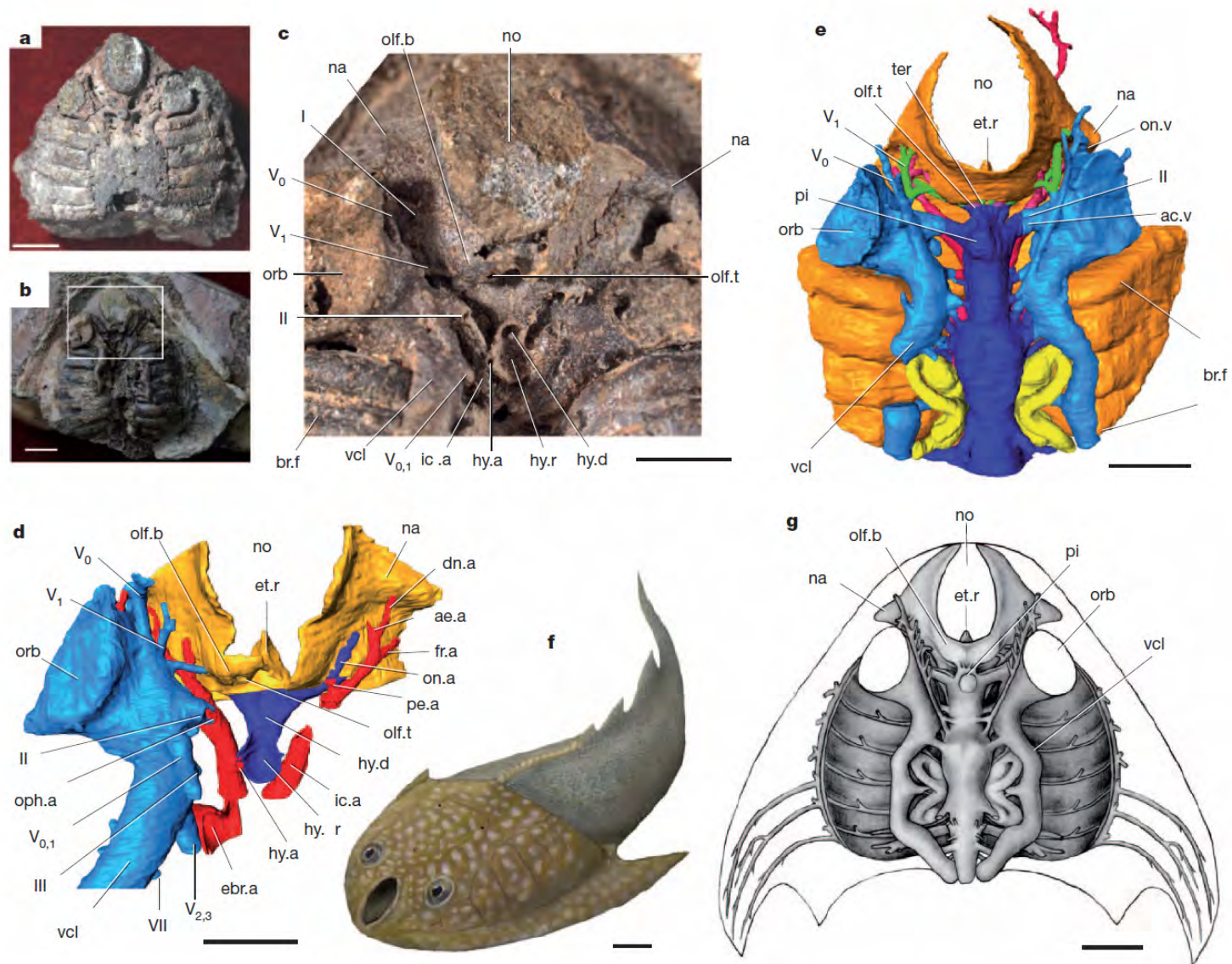


Figure 1 | *Shuyu zhejiangensis*, Silurian of Zhejiang, China. **a, b**, Two natural endocast specimens: V14334.1 (**a**); V14334.5 (**b**). **c, d**, Structure of nasal and hypophyseal region magnified from the boxed region of V14334.5: digital picture (**c**); three-dimensional (3D) reconstruction (**d**). **e**, Virtual endocast (V14334.3). **f**, Restoration of external morphology. **g**, Synthetic restoration. ac.v, anterior cerebral vein; ae.a, anterior ethmoidal artery; br.f, branchial fossa; dn.a, dorsal nasal artery; ebr.a, efferent branchial artery; et.r, ethmoid rod; fr.a, frontal artery; hy.a, hypophyseal artery; hy.d, hypophyseal or buccohypophyseal duct;

hy.r, hypophyseal recess; ic.a, internal carotid artery; na, nasal sacs; no, nostril; olf.b, olfactory bulb; olf.t, olfactory tract; on.a, orbitonasal artery; on.v, orbitonasal vein; oph.a, ophthalmic artery; orb, orbital opening; pe.a, posterior ethmoidal artery; pi, pineal organ; ter, terminal nerve; vcl, lateral head vein or dorsal jugular vein; I, II, III, V₀, V₁, V_{0,1}, V_{2,3}, VII, olfactory (I), optic (II), oculomotor (III), superficial ophthalmic (V₀), profundus (V₁), superficial ophthalmic plus profundus (V_{0,1}), maxillomandibular (V_{2,3}) of trigeminal (V), and facial (VII) nerves. Scale bars, 2 mm.

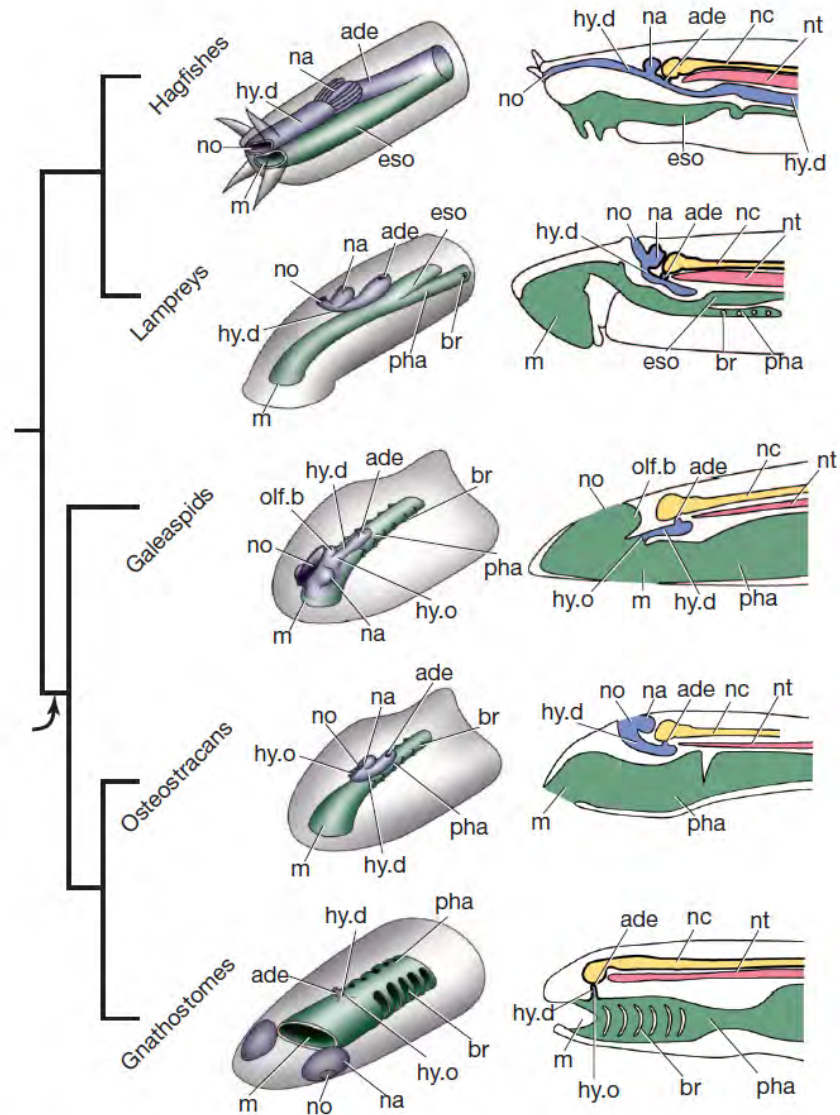


Figure 3 | The nasohypophyseal complex in craniates. Left, oblique view; right, sagittal section. The disassociation of the nasohypophyseal complex, an evolutionary prerequisite for the origin of jaws, happened at least in the common ancestor of galeaspids, osteostracans and gnathostomes (arrow). The condition of osteostracans probably converged with that of lampreys. ade, adenohypophysis; br, branchial duct or slit; eso, oesophagus; m, mouth; nc, neural cord; nt, notochord; pha, pharynx. See Figs 1 and 2 for other notation.

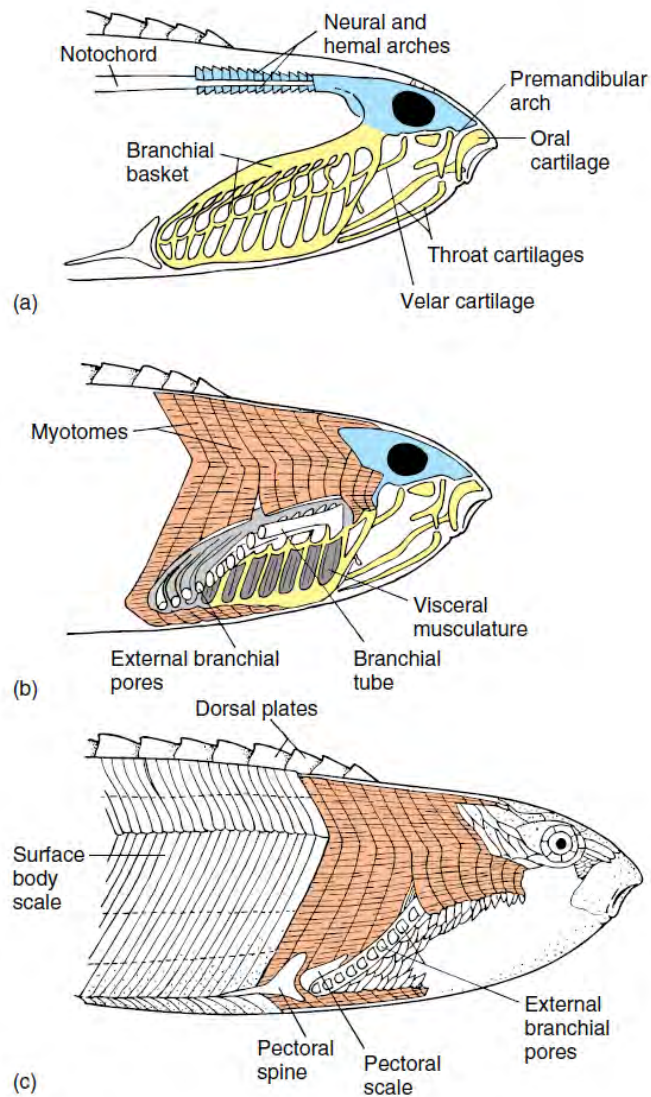


FIGURE 7.14 Ostracoderm *Pterolepis*, an anaspid.

(a) Exposed skull. The splanchnocranium included a few elements around the mouth, and the chondrocranium held the eye. A notochord was present and vertebral elements rested on it. (b,c) Restoration of muscles and some of the surface scales. The throat cartilages supported the floor of the buccal cavity, which might have been part of a pump to draw water into the mouth and then force it across the gills and out through the external branchial pores.

Placodermos

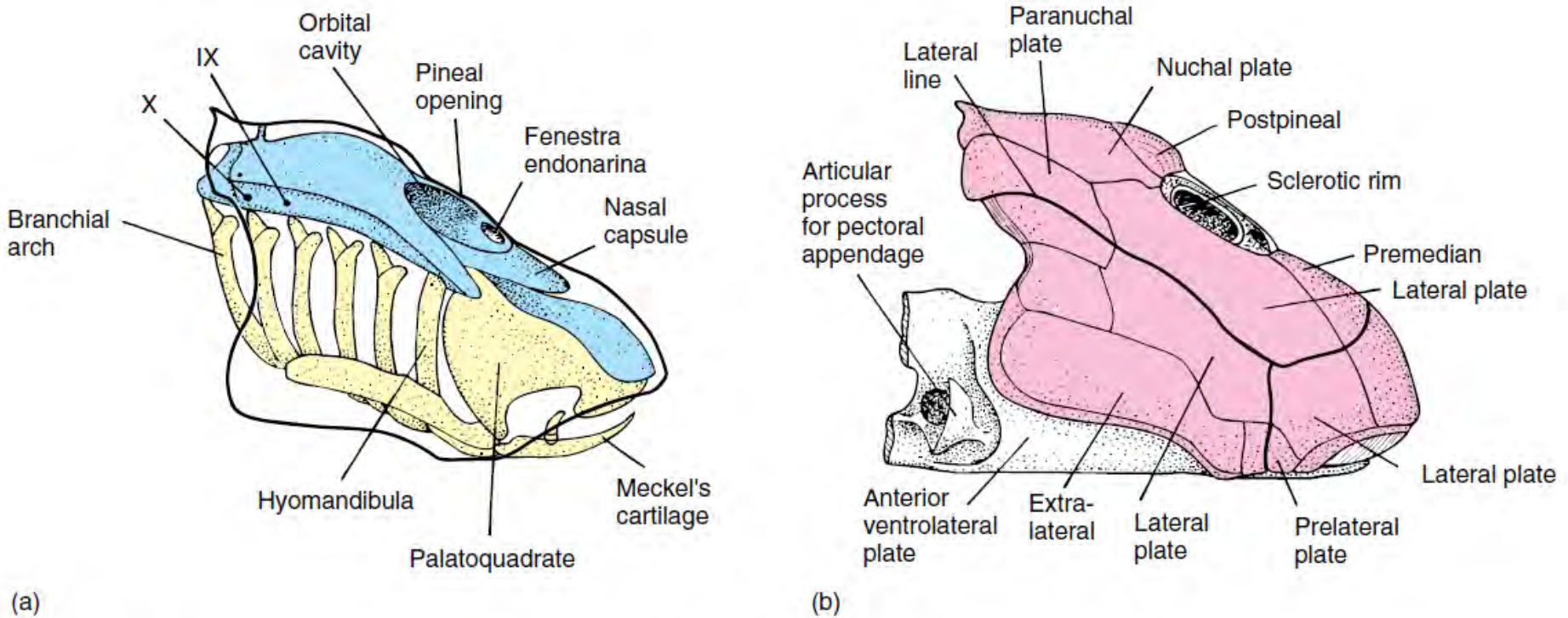
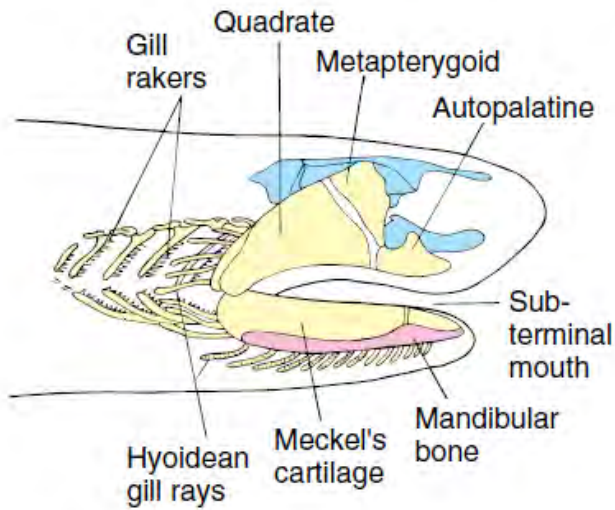


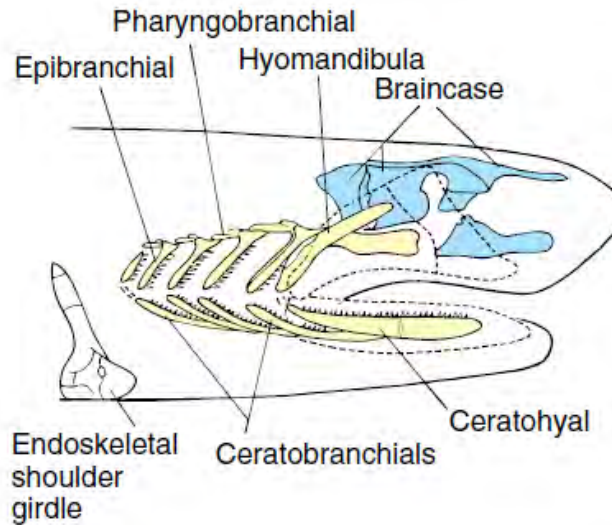
FIGURE 7.16 Placoderm skull. *Bothriolepis* was about 15 cm long and lived in the middle Devonian. (a) Lateral view of splanchnocranium and chondrocranium. (b) Skull with overlying dermatocranium in place. Note the dermal plates.

After Stensiö, 1969.

Acanthodios: Dientes asociados a arcos branquiales



(a)



(b)

FIGURE 7.17
Acanthodian skull, *Acanthodes*. (a) Lateral view with mandibular arch shown in its natural position. (b) Mandibular arch is removed to better reveal the chondrocranium, hyoid arch, and five successive branchial arches. (Red, dermal bone; yellow, splanchnocranium; blue, chondrocranium)

After Jarvik.

Elasmobranquios: Ausencia de dermatocráneo

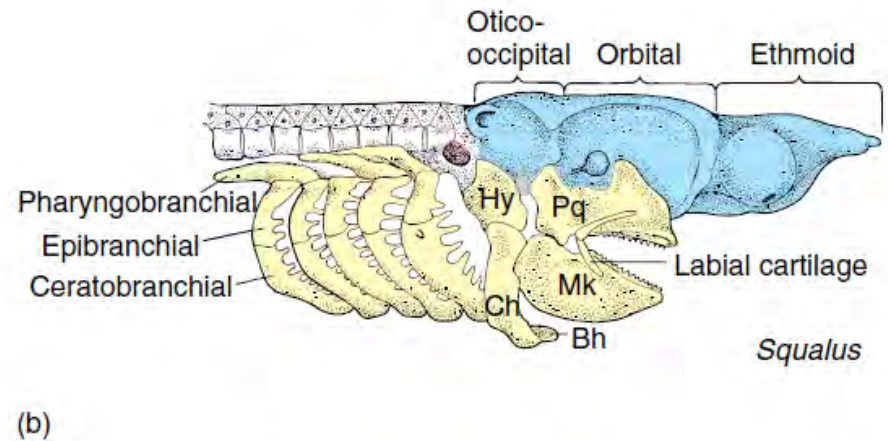
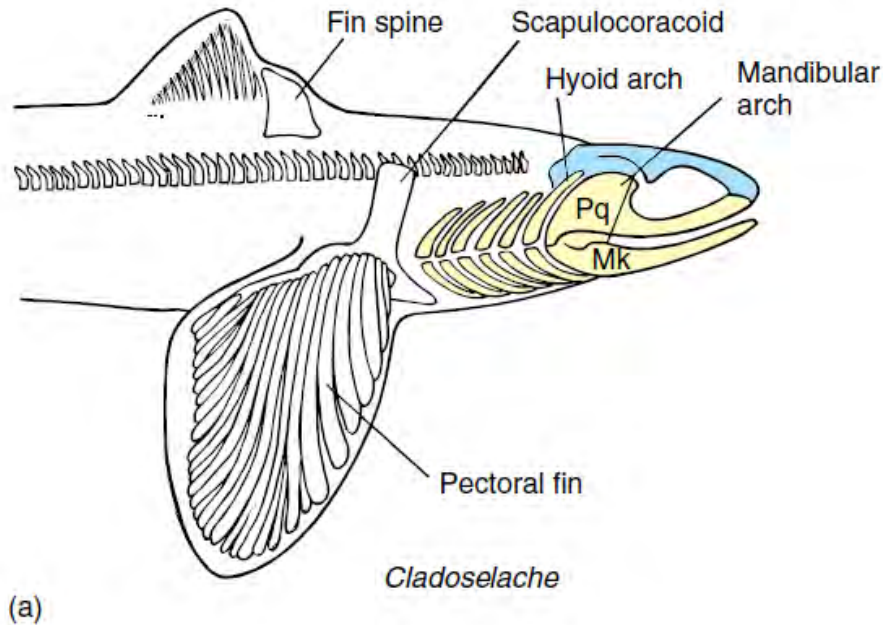


FIGURE 7.18 Shark skull. (a) Primitive shark *Cladoselache*, a late Devonian shark that reached perhaps 55 cm in length. Mandibles were followed by a complete hyoid arch and five branchial arches. Full gill slits were present between each arch. (b) Modern shark *Squalus*, the dogfish shark. The hyoid arch, second in series, is modified to support the back of the mandibular arch. As the hyoid moves forward to help suspend the jaw, the gill slit in front is crowded and reduced to the small spiracle. Although fused into one unit, the three basic regions of the chondrocranium are ethmoid, orbital, and oticooccipital. Abbreviations: basihyal (Bh), ceratohyal (Ch), hyomandibula (Hy), Meckel's cartilage (Mk), palatoquadrate (Pq).

(a) After Zangerl.

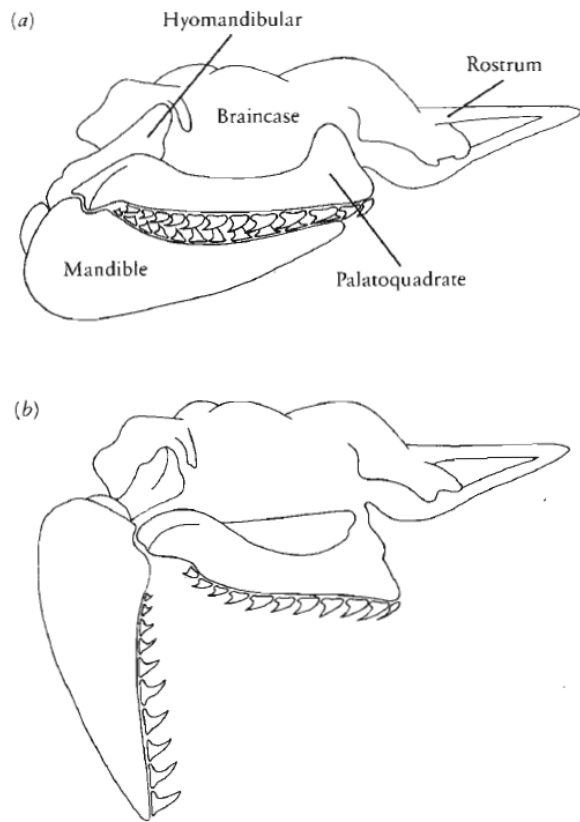


Figure 5-14. BRAINCASE AND JAWS OF THE MODERN SHARK *CARCHARHINUS*. Diagram showing movement of the palatoquadrate during feeding. The distal end of the hyoid and the posterior end of both jaws move laterally as the jaw is opened. From Moss, 1972. By permission of the Zoological Society of London.

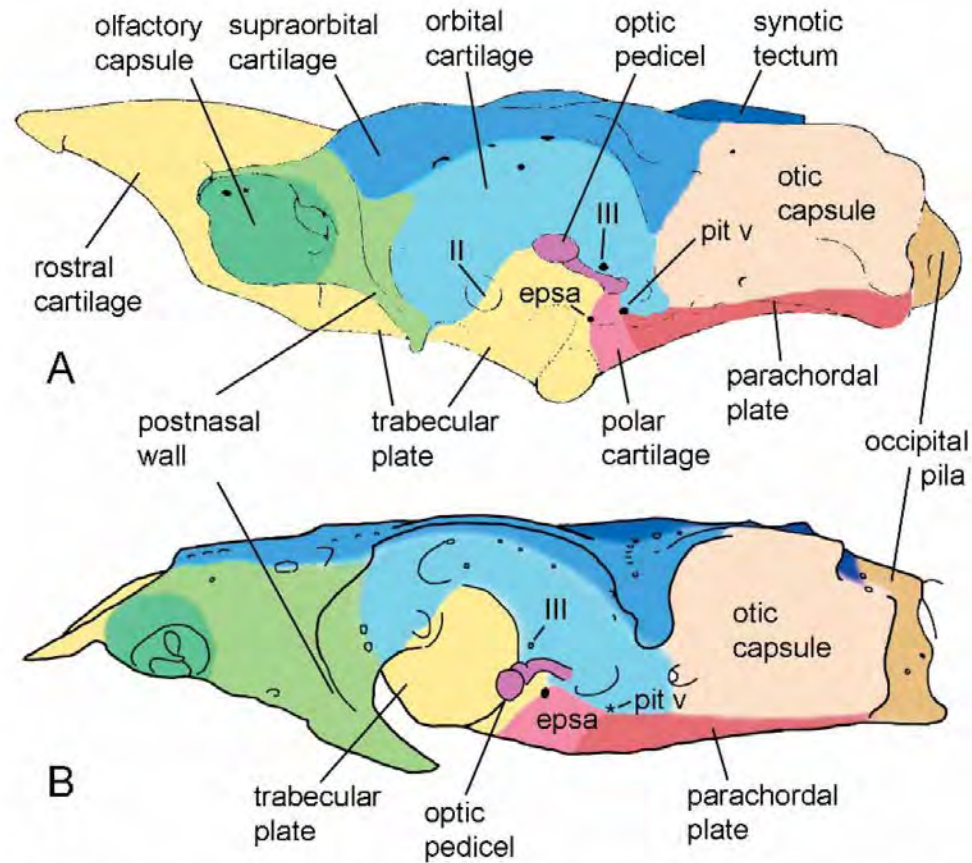
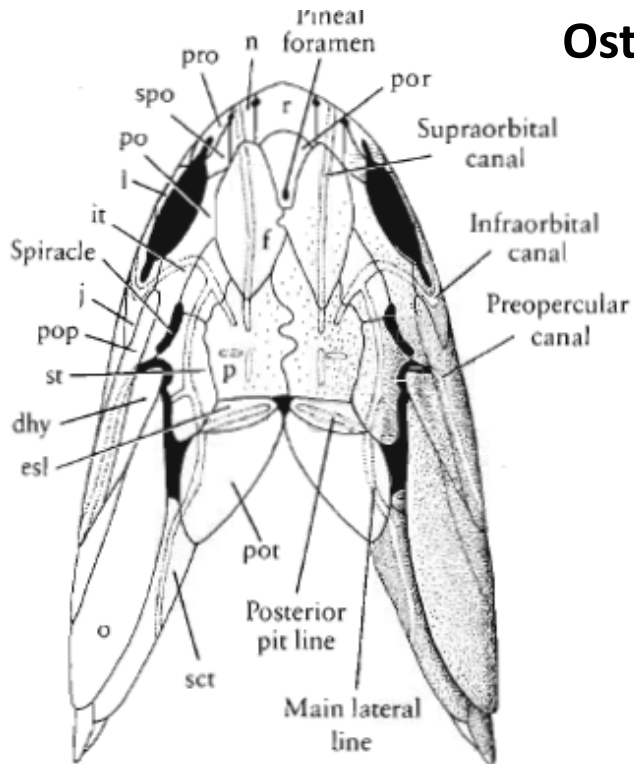


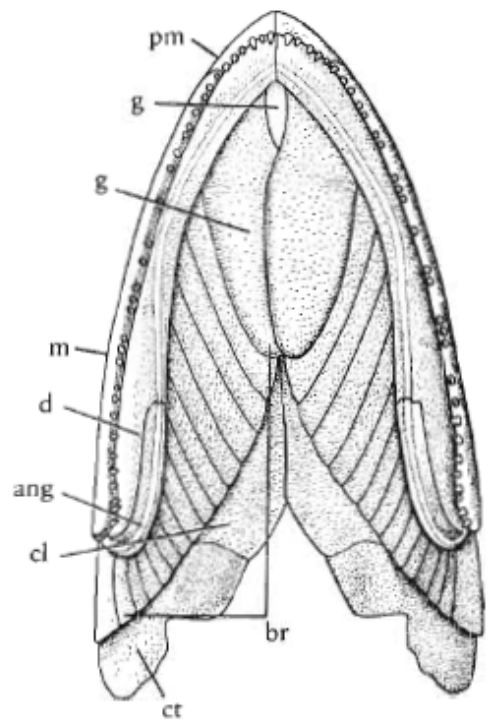
Fig. 1. Approximate extent of contributions made by major embryonic cartilages in the adult chondrocranium of two modern sharks. **A.** *Squalus acanthias* (based on ontogenetic data); **B.** *Chlamydoselachus anguineus* (hypothesized). Not to scale.

Osteichthyes

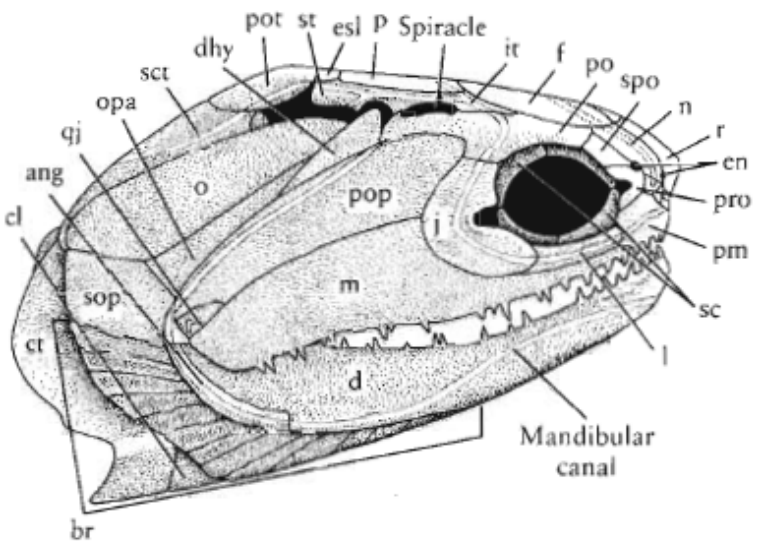
(a)



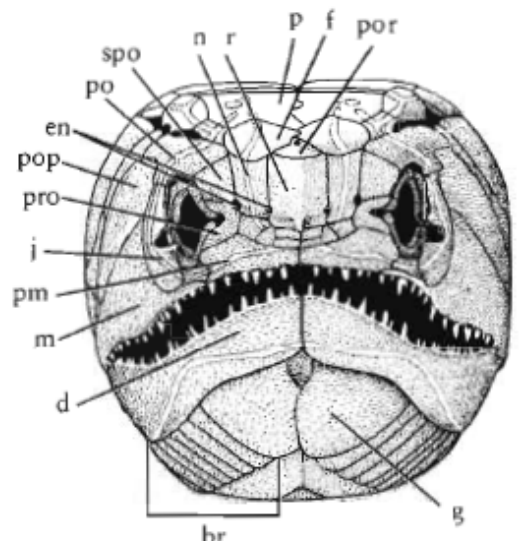
(b)



(c)



(d)



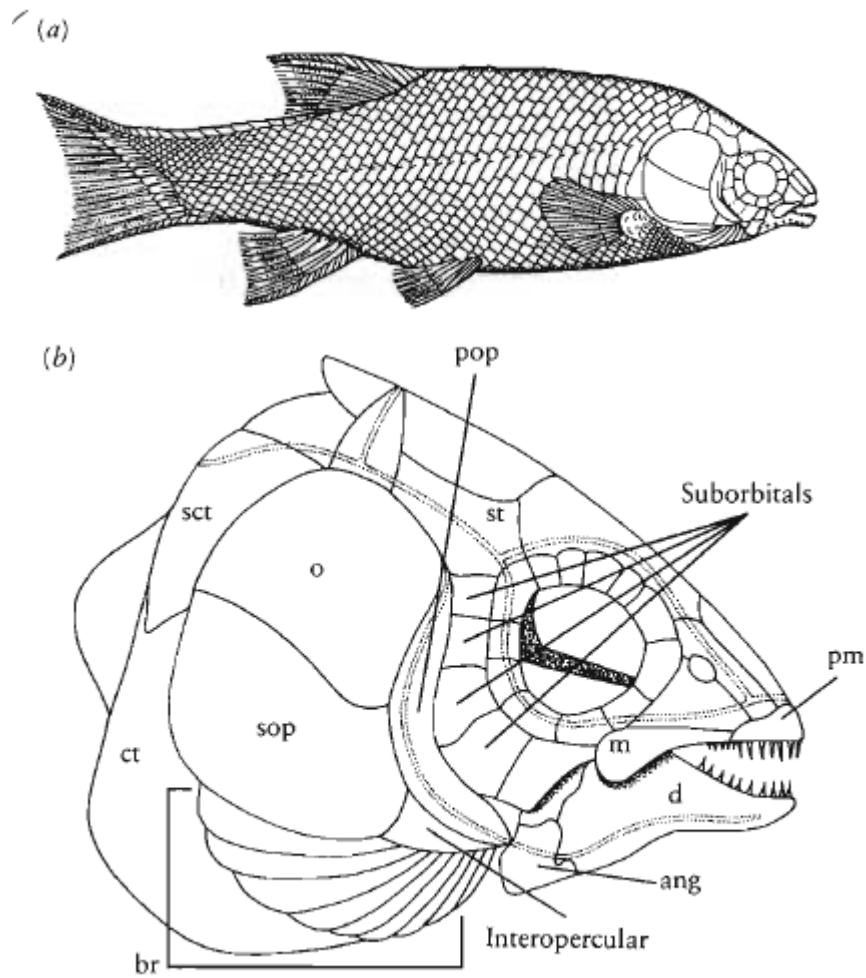


Figure 6-26. SEMIONOTID NEOPTERYGIANS. (a) Restoration of *Acentrophorus*, the oldest known neopterygian from the Upper Permian, approximately natural size. From Moy-Thomas and Miles, 1971. (b) Skull of *Acentrophorus*, $\times 4$. From Moy-Thomas and Miles, 1971. (a and b) By permission from Chapman and Hall, Ltd. (c) *Lepidotes minor* from the Jurassic, approximately 30 centimeters long. From Smith-Woodward, 1891–1901. (d) *Dapedium*, a deep-bodied genus, about 35 centimeters long. Photograph courtesy of Dr. Wild.

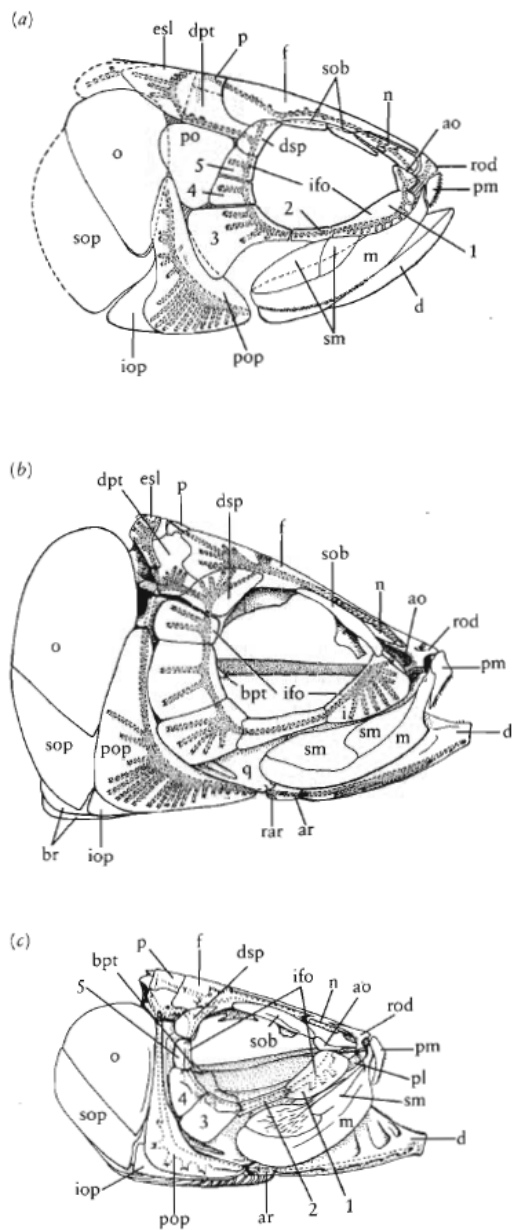


Figure 7-2. THE SKULLS OF PRIMITIVE TELEOSTS. (a) *Pholidophorus bechei*, Lower Jurassic, $\times 2$. From Nybelin, 1966. (b) *Tharsis* [*Leptolepis*] *dubius*, Upper Jurassic, $\times 1\frac{1}{2}$. From Patterson and Rosen, 1977. (b and c) Courtesy of the Library Services Department, American Museum of Natural History. (c) A primitive Upper Jurassic clupeocephalan, *Leptolepides sprattiformis*, $\times 5$. From Patterson and Rosen, 1977. For abbreviations see Figure 6-13.

Teleostei

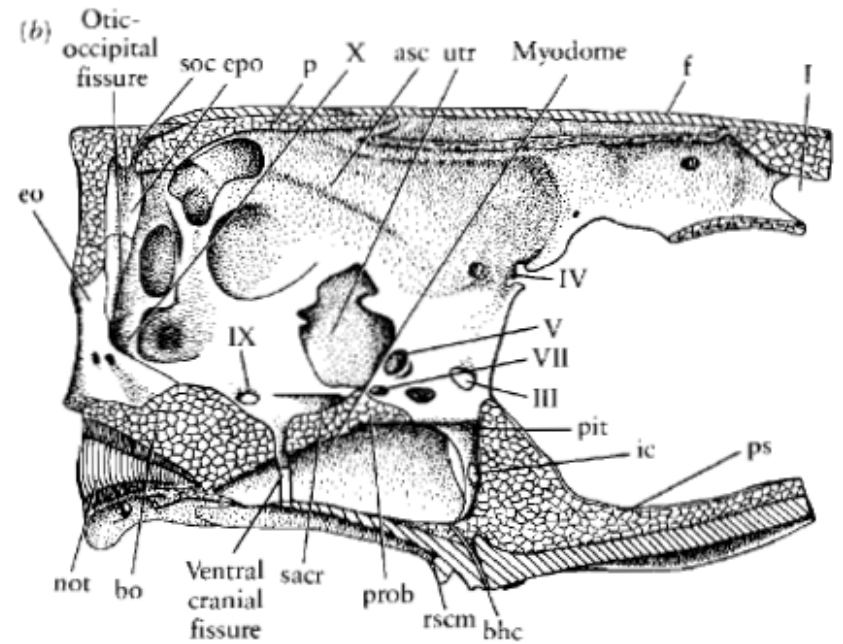
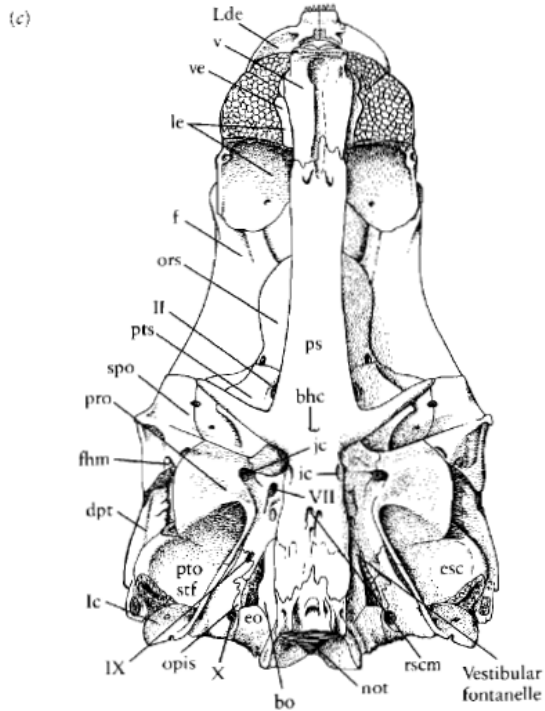
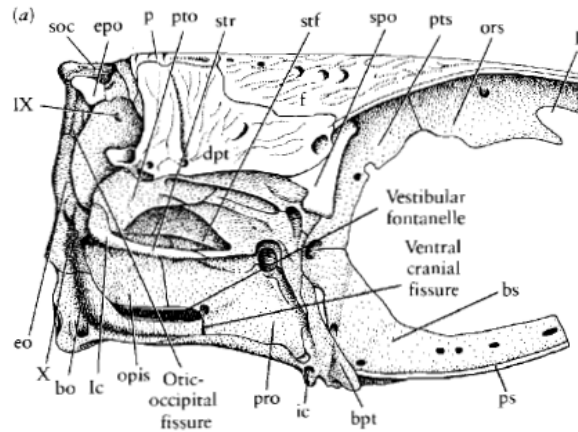


Figure 6-24. BRAINCASE OF THE PRIMITIVE TELEOST *PHOLIDOPHORUS*. (a) Lateral, (b) sagittal, (c) palatal, and (d) occipital views. We can see more individual centers of ossification here than in primitive actinopterygian fish (see Figure 6-11). Abbreviations as follows: asc, ridge over anterior semicircular canal; bhc, bucco-hypophysial canal; bo, basioccipital; bpt, basipterygoid process; bs, basisphenoid; dpt, dermopterotic; eo, exoccipital; epo, epioccipital; esc, ridge over external semicircular canal; f, frontal; fhm, hyomandibular facet; ic, foramina for internal carotid; lc, lateral ethmoid; not, notochordal calcification in notochordal pit; opis, opisthotic; ors, orbitosphenoid; p, parietal; pit, pituitary fossa; pro, prootic; prob, prootic bridge; ps, parasphenoid; pto, pterotic; pts, pterosphenoid; rscm, recess on parasphenoid housing origin of subcephalic muscles; sac, saccular recess; soc, supraoccipital; spo, sphenotic; stf, subtemporal fossa; str, prootic or intercalary portion of strut across subtemporal fossa; utr, utricle; v, vomere; ve, ventral ethmoid; I–X, foramina of cranial nerves. *From Patterson, 1975.*

Sarcopterygii

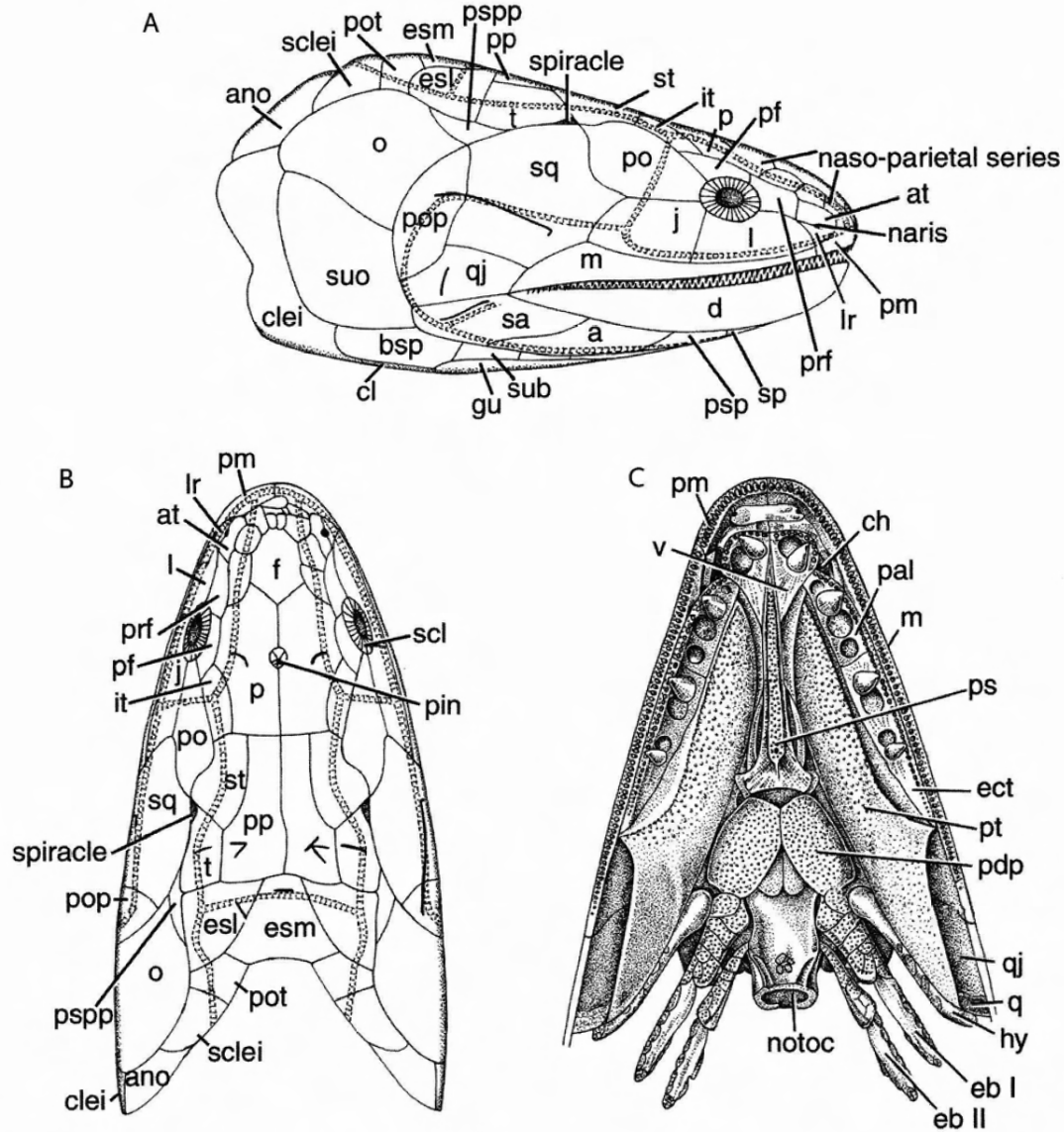


Figure 2.14. The skull of *Eusthenopteron*, the best-known of sarcopterygian fish, close to the ancestry of land vertebrates, in lateral, dorsal, and palatal views. Modified from Moy-Thomas and Miles, 1971.

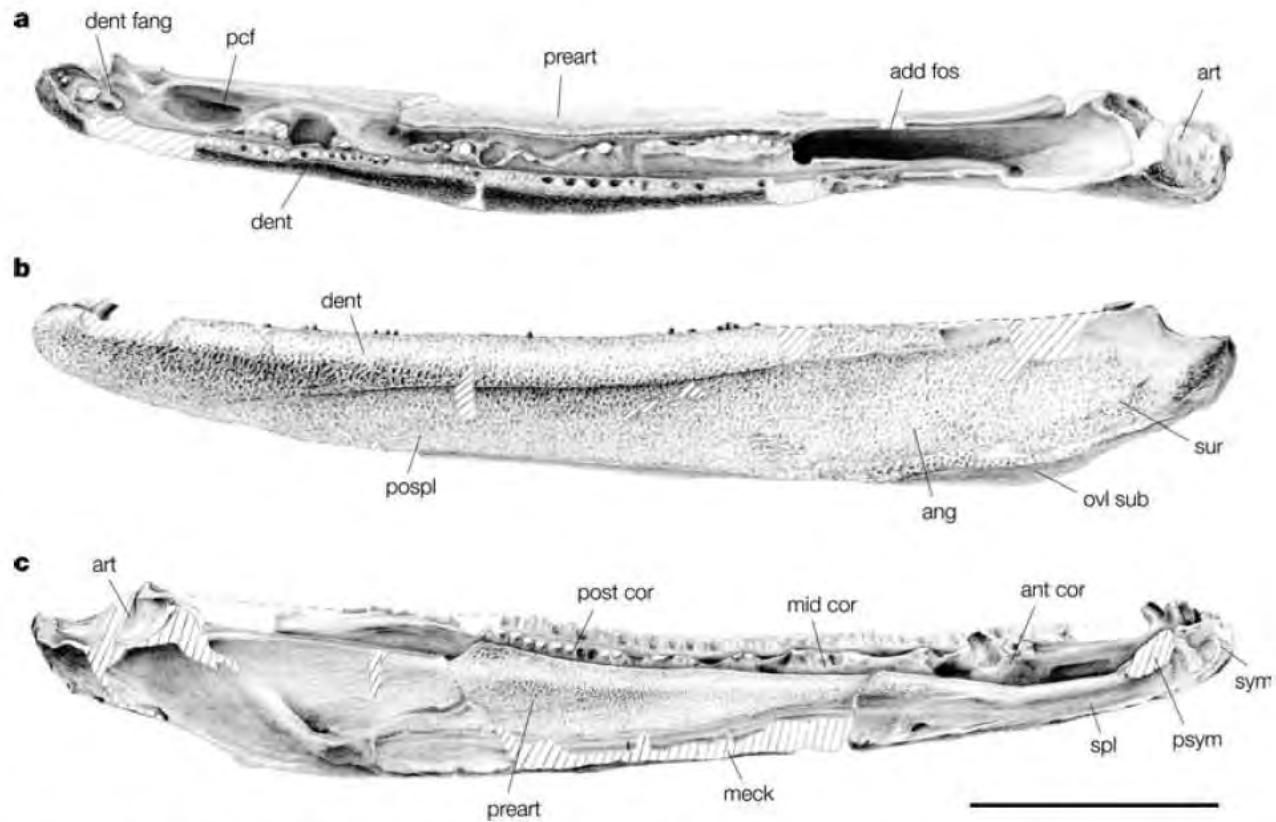


Figure 5 | NUFV 116, left lower jaw of *Tiktaalik roseae*. **a**, Dorsal view; **b**, lateral view; and **c**, medial view. Abbreviations: add fos, adductor fossa; ang, angular; ant cor, anterior coronoid; art, articular; dent, dentary; dent fang, dentary fang; meck, Meckelian bone; mid cor, middle coronoid; ovl

sub, submandibular overlap area; pcf, precoronoid fossa; pospl, postsplenial; post cor, posterior coronoid; preart, prearticular; psym, parasymphysial plate; spl, splenial; sur, surangular; sym, symphysis. Scale bar equals 5 cm.

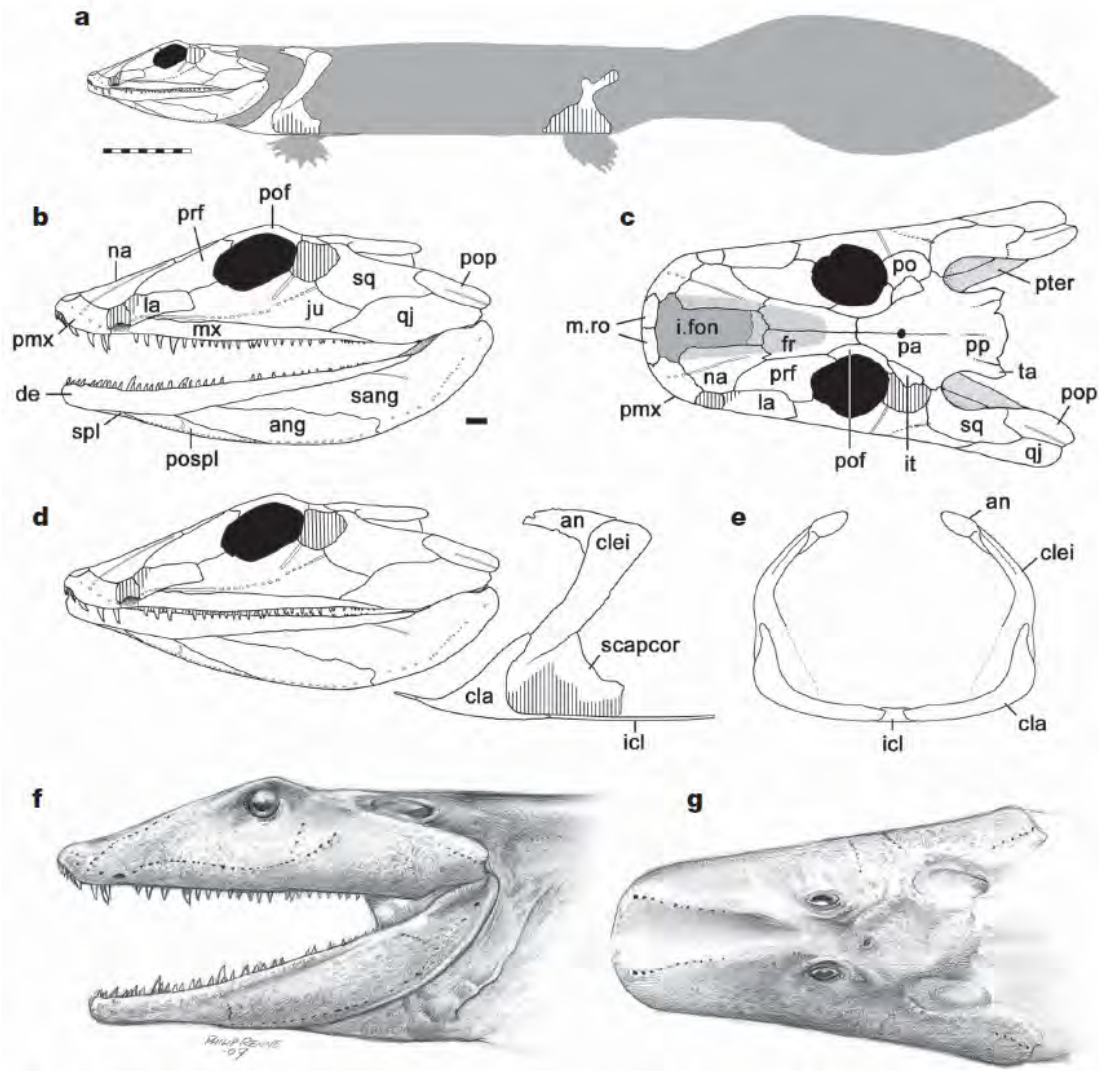


Figure 3 | Reconstructions of *Ventastega*. **a**, Whole-body reconstruction showing known skeletal elements on a body outline based on *Acanthostega* (modified from ref. 5; original *Acanthostega* body reconstruction by M. I. Coates). Scale bar, 10 cm. **b**, **c**, Skull reconstruction in lateral and dorsal views, based on material presented here and described previously²¹. **d**, Reconstructed association of skull and shoulder girdle in lateral view. **e**, Shoulder girdle in anterior view. Curvature of cleithrum based on LDM G 81/522 (ref. 21). Unknown bones are indicated with vertical hatching. Scale

bar for **b–e**, 10 mm. **f**, **g**, Life reconstructions of head in lateral and dorsal views (copyright P. Renne, 2007). an, anocleithrum; ang, angular; cla, clavicle; clei, cleithrum; de, dentary; fr, frontal; icl, interclavicle; i.fon, internasal fontanelle; it, intertemporal; ju, jugal; la, lacrimal; mx, maxilla; m.ro, median rostral; na, nasal; pa, parietal; pmx, premaxilla; po, postorbital; pof, postfrontal; pop, preopercular; pospl, postsplenial; pp, postparietal; prf, prefrontal; pter, pterygoid; qj, quadratojugal; sang, surangular; scapcor, scapulo-coracoid; spl, splenial; sq, squamosal; ta, tabular.

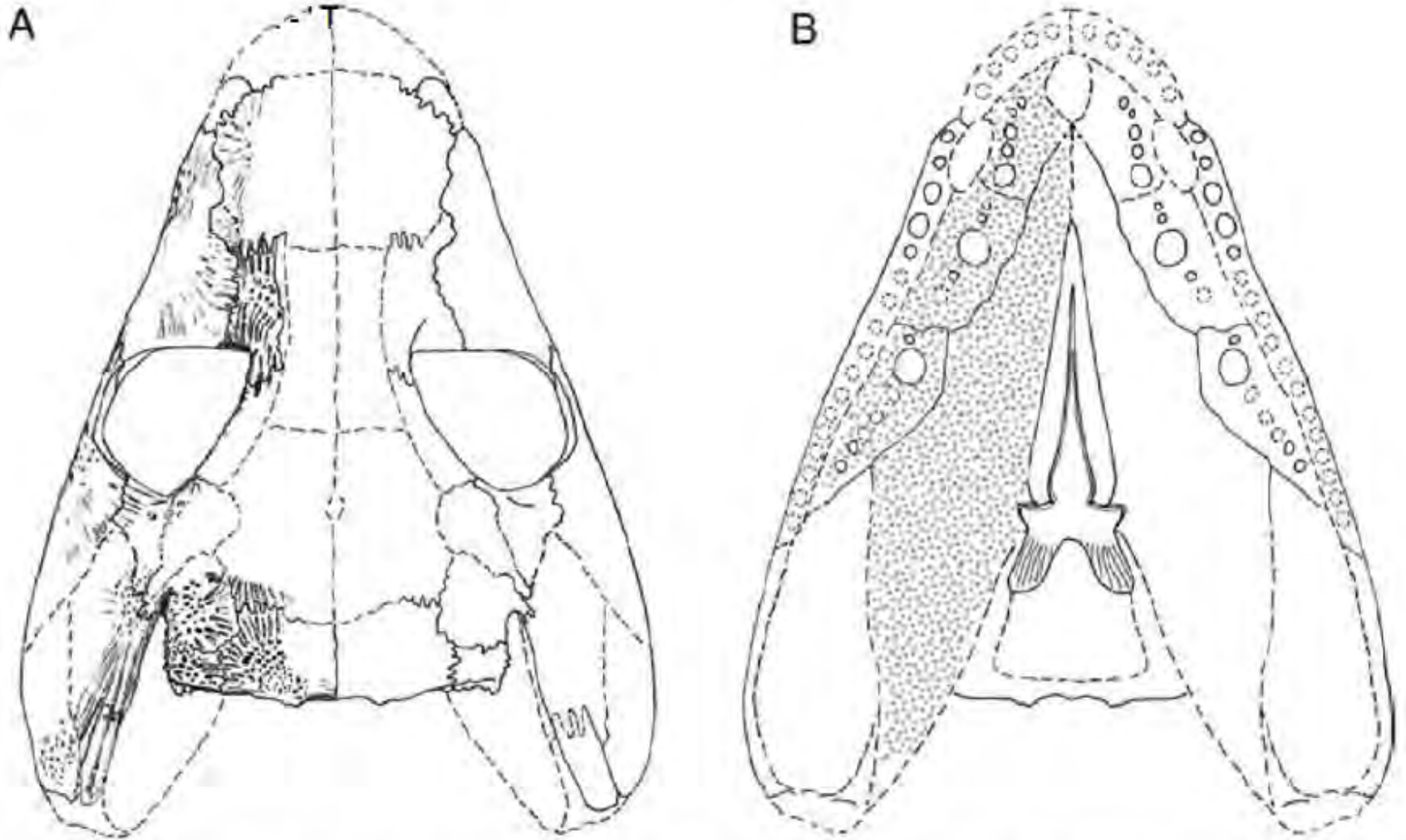


Figure 17 *Pederpes finneyae* Clack, 2002a: reconstruction of the skull in **A**, dorsal and **B**, palatal views. The distribution of denticles is shown schematically, because it has been inferred from a few selectively prepared areas.

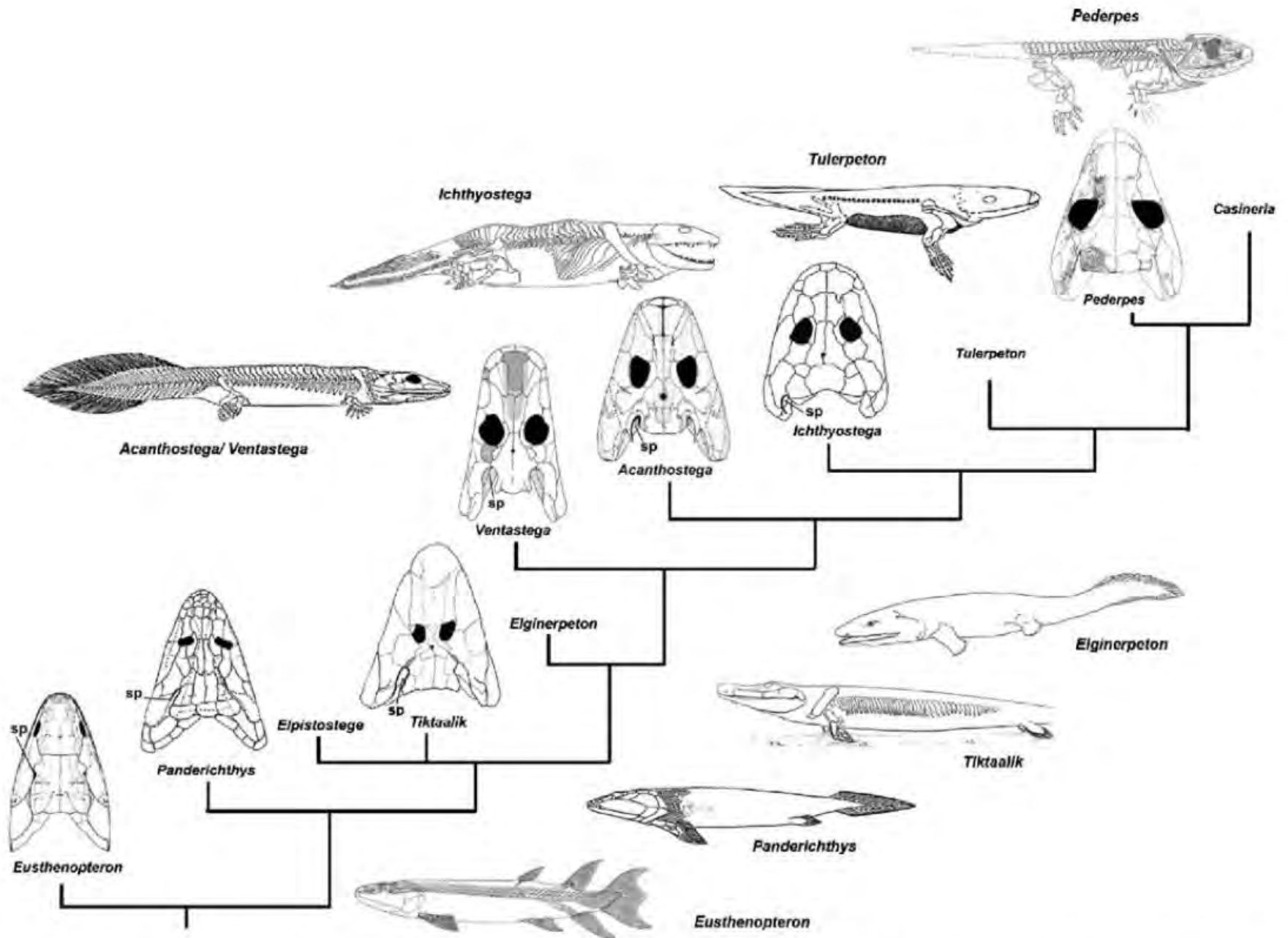
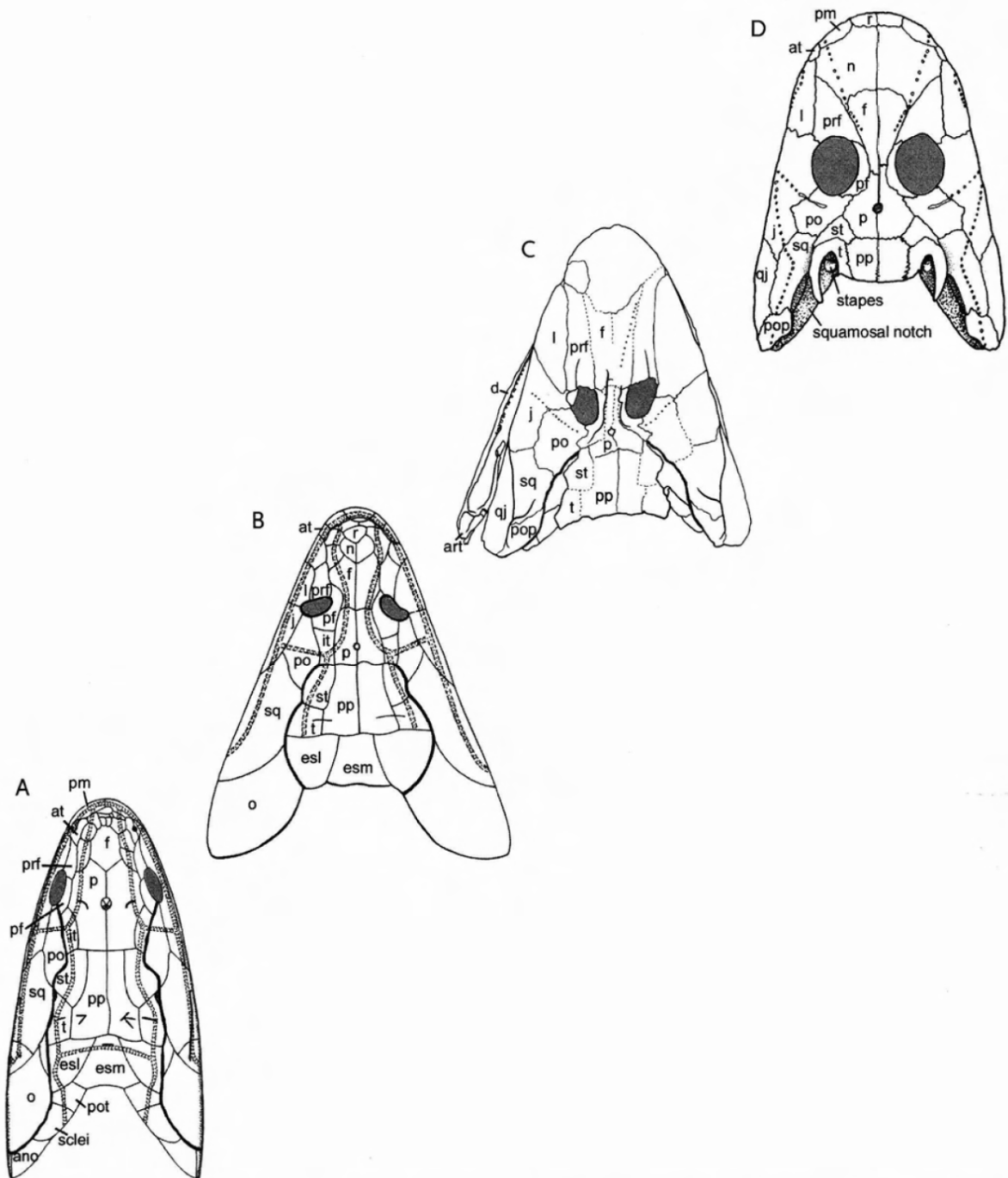


Fig. 1 Cladogram showing relationships of tetrapodomorphs according to a current consensus. Skulls and skeletal or body reconstructions are shown where these are available. Drawings are not to scale



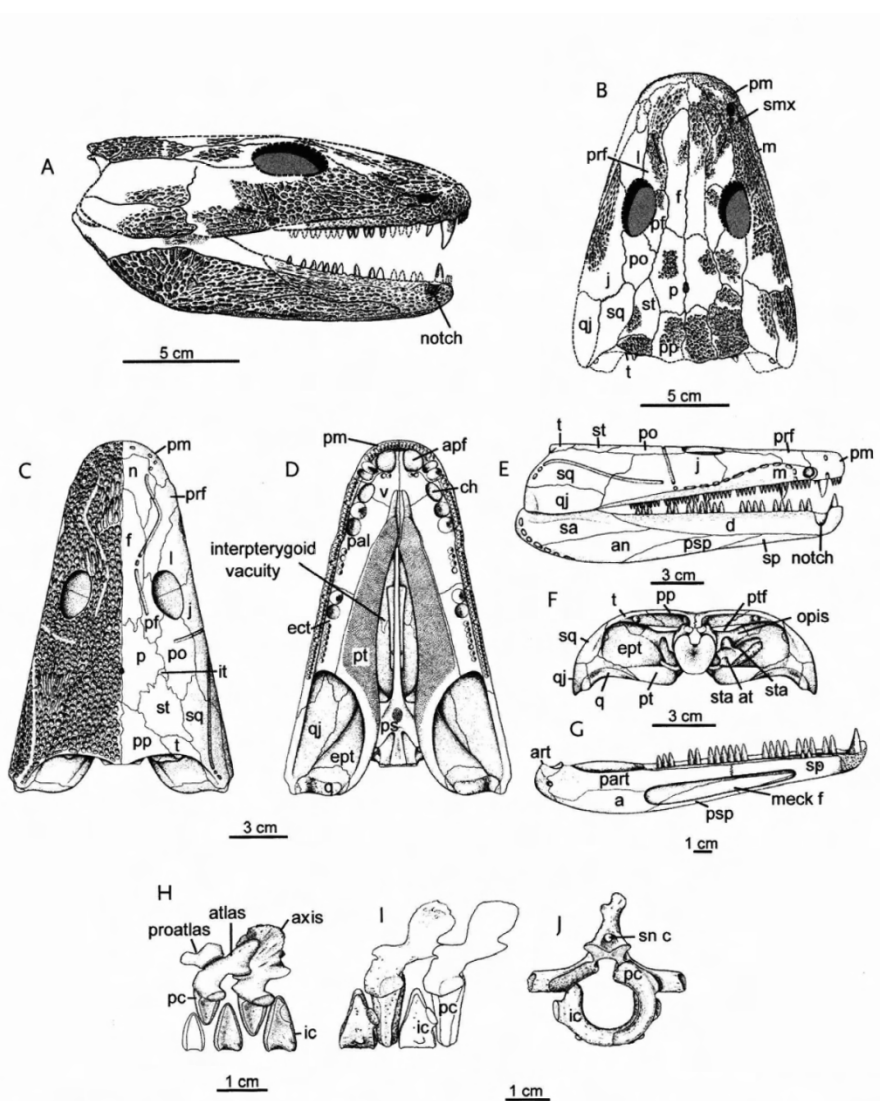


Figure 4.13. The colosteids *Pholidogaster* and *Greererpeton*. A and B, The skull of *Pholidogaster pisciformis* in lateral and dorsal views, from the Upper Viséan Gilmerton Ironstone, near Edinburgh. A and B from Panchen 1975; C–G from Smithson, 1982; H–J from Godfrey, 1989.

views. G, Jaw in medial view. H–J, Anterior cervicals and trunk vertebrae in lateral and posterior views. A and B from Panchen 1975; C–G from Smithson, 1982; H–J from Godfrey, 1989.

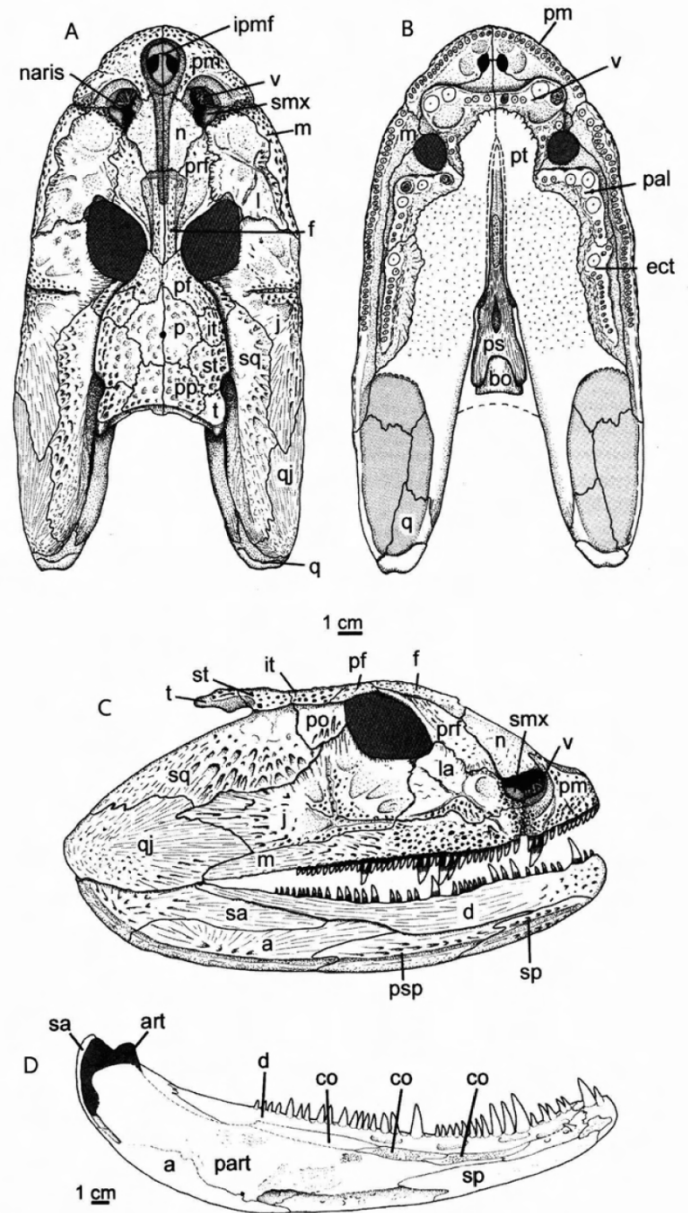
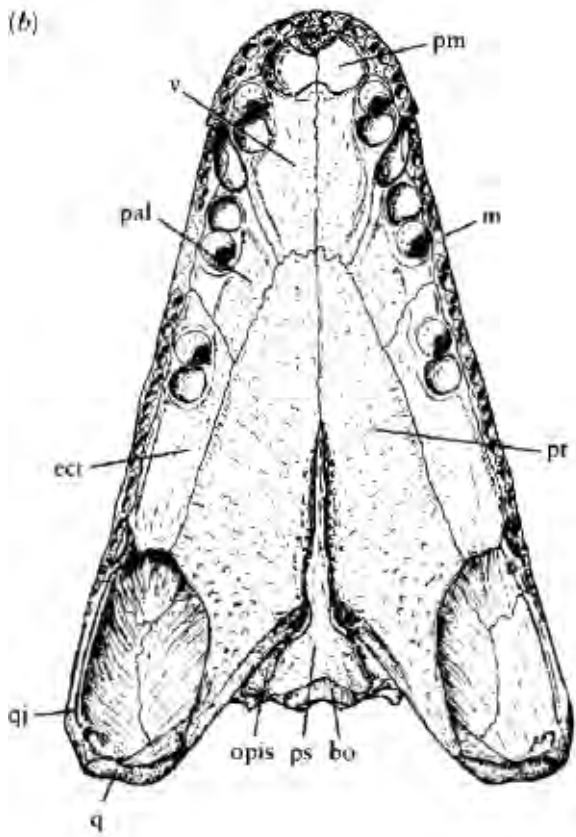
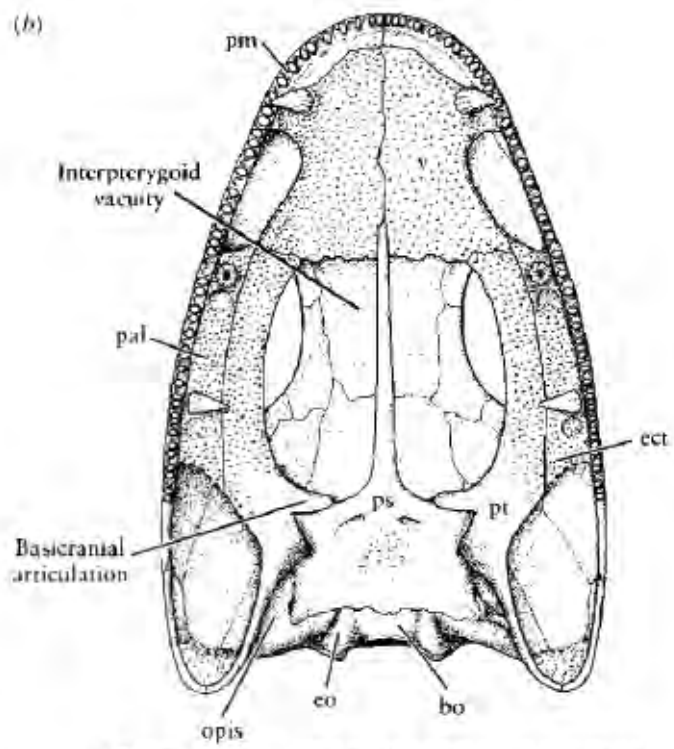


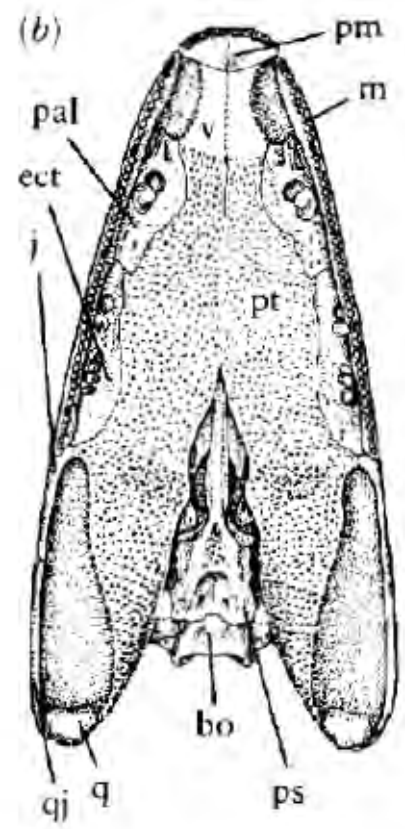
Figure 4.22. A–C, Skull of *Crassigyrinus* from the upper Viséan and lower Namurian of Scotland, in dorsal, palatal, and lateral views. From Clack, 1998a. D, Medial view of lower jaw. From Ahlberg and Clack, 1998.



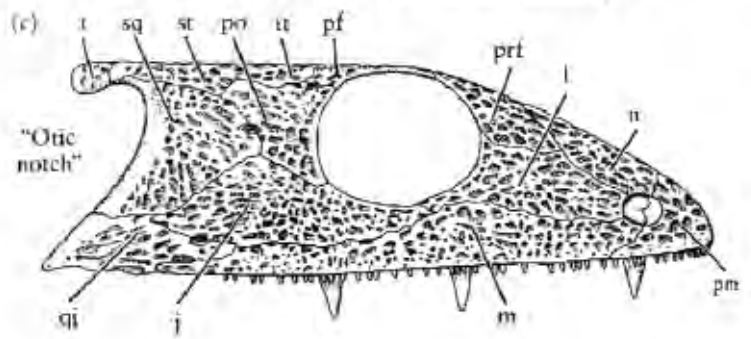
Megalocephalus
(stem
neotetrapoda)

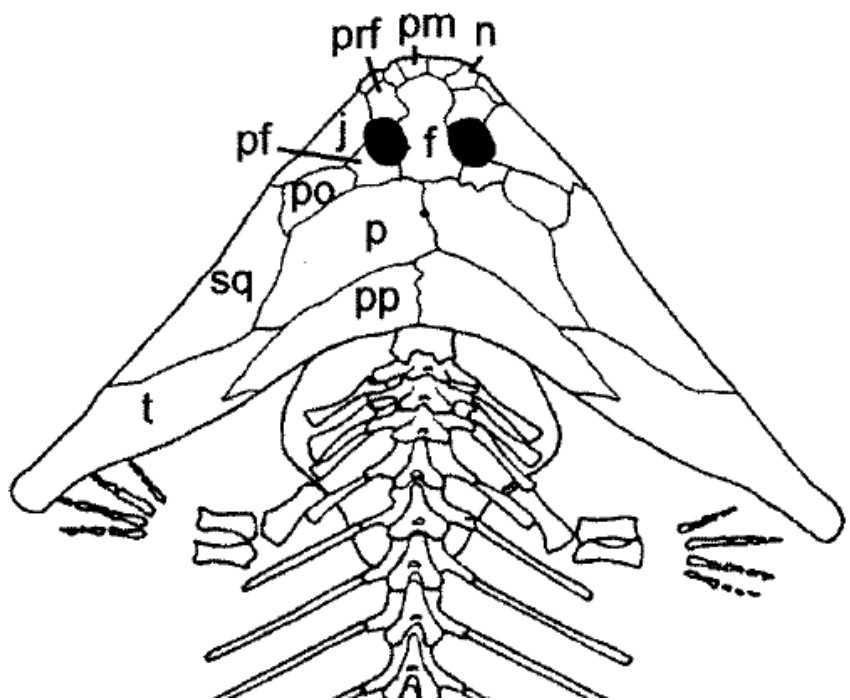
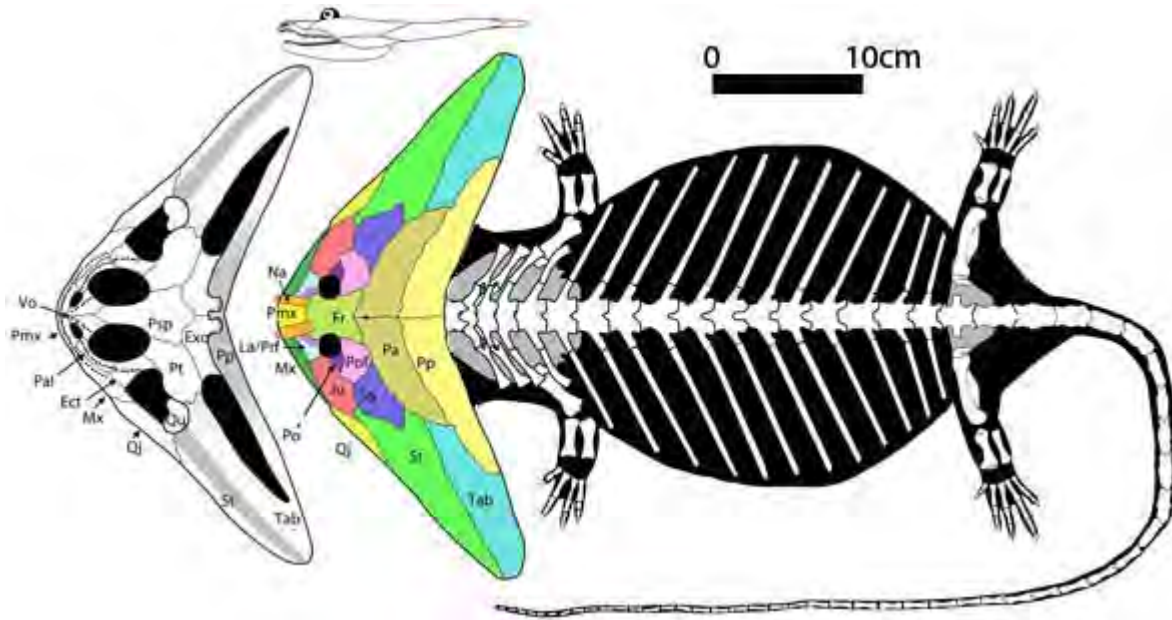


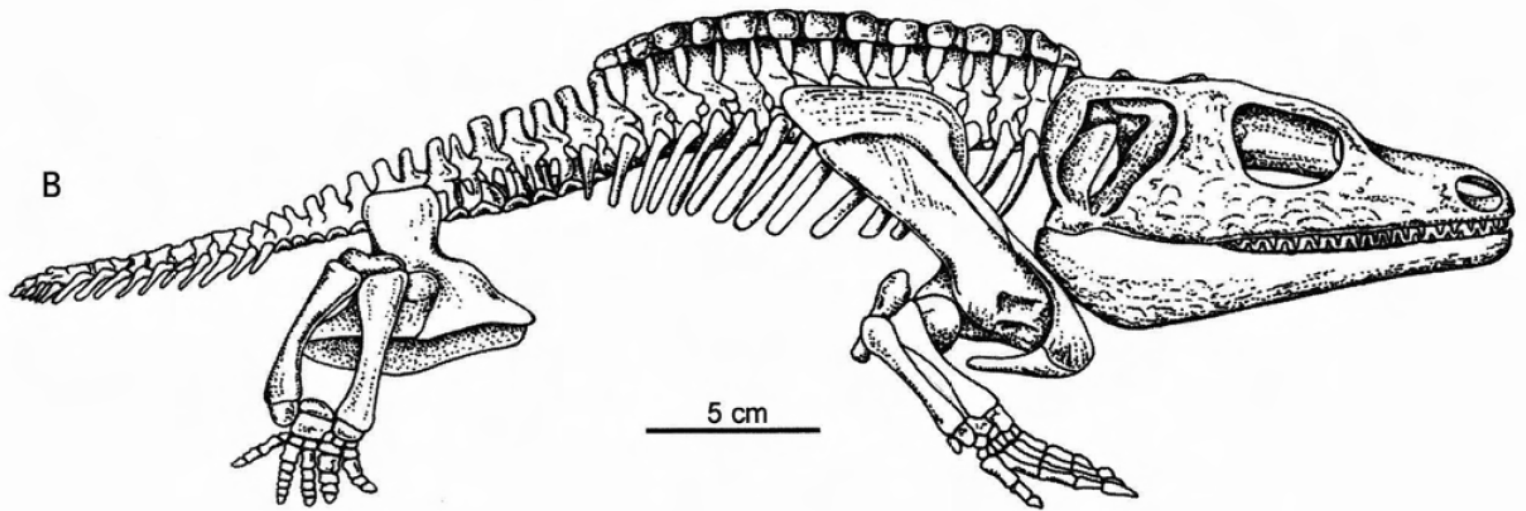
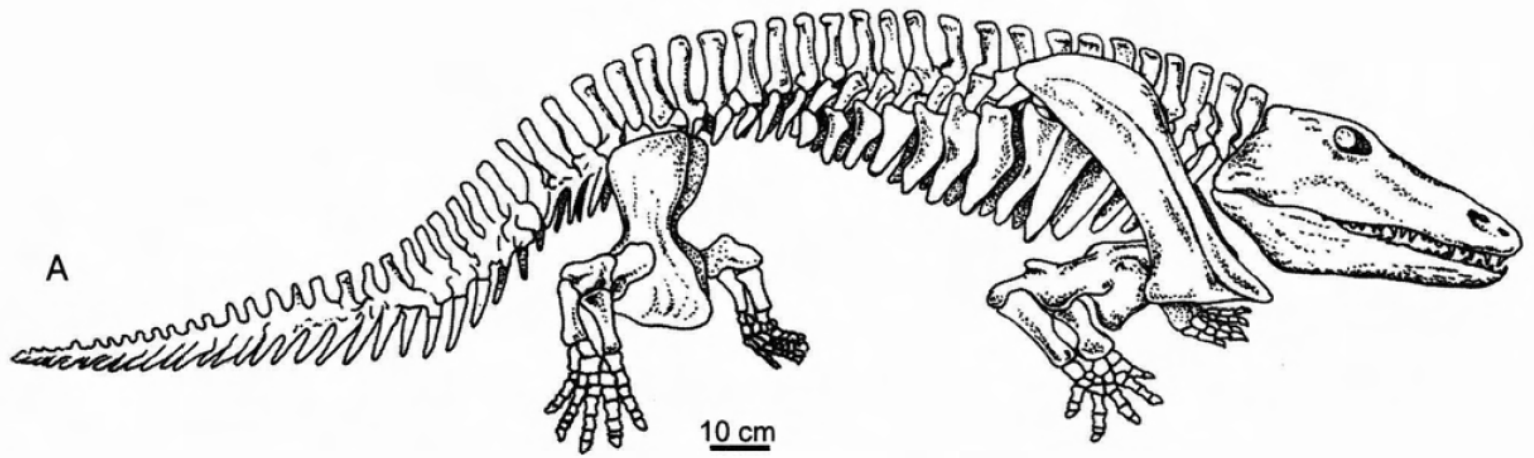
Dendroerpeton (temnospondyl)



Proterogyrinus
("anthracosaur")







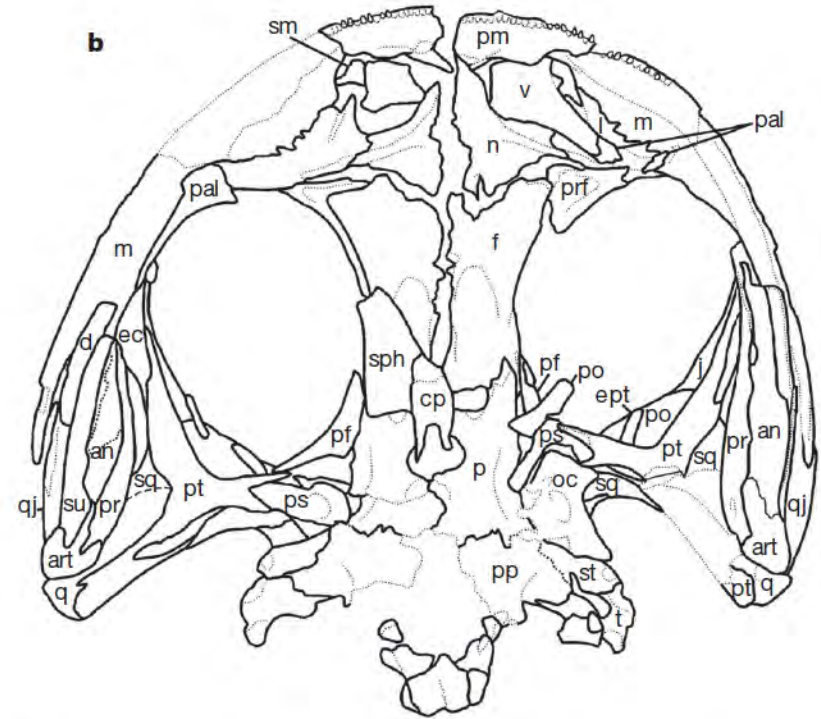
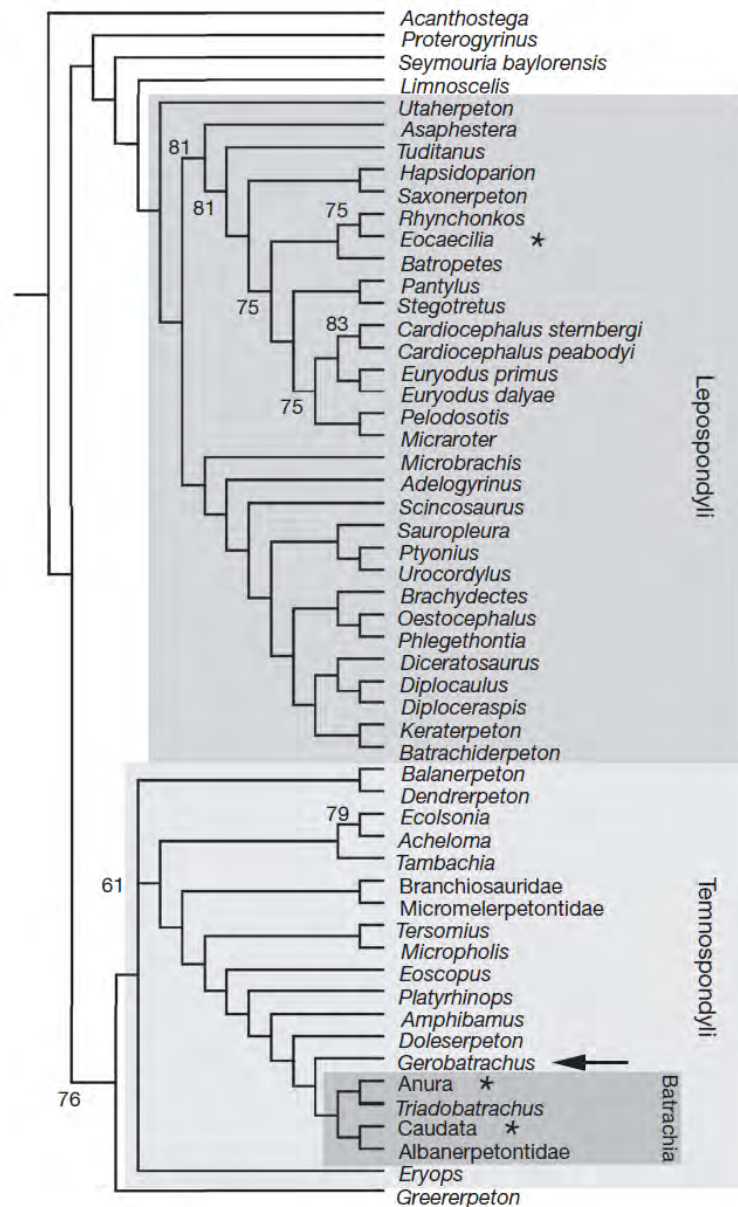
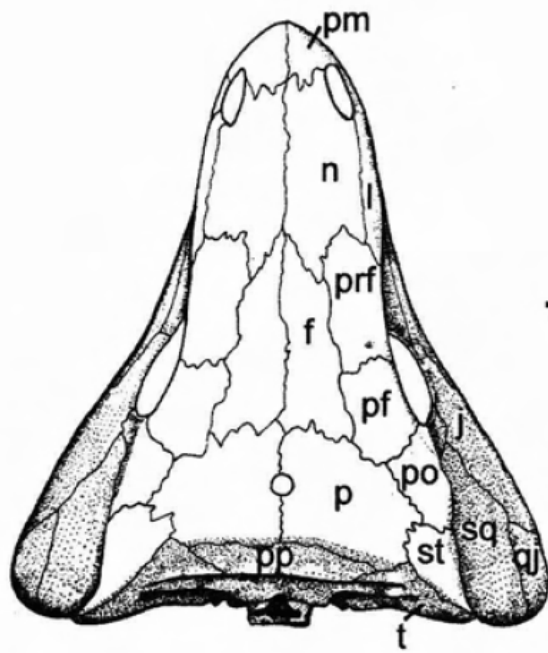
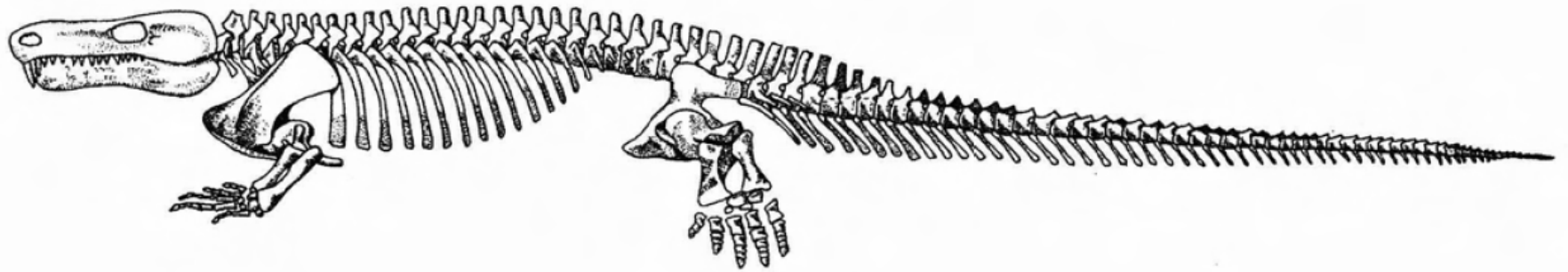
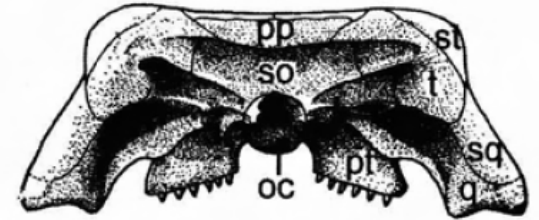
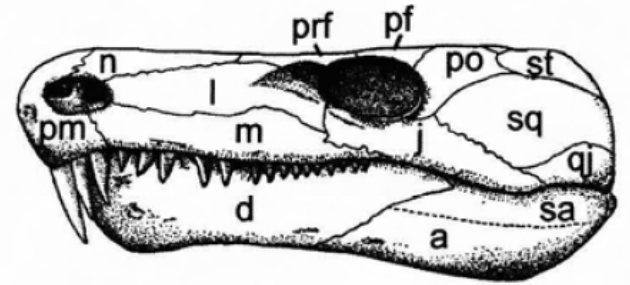
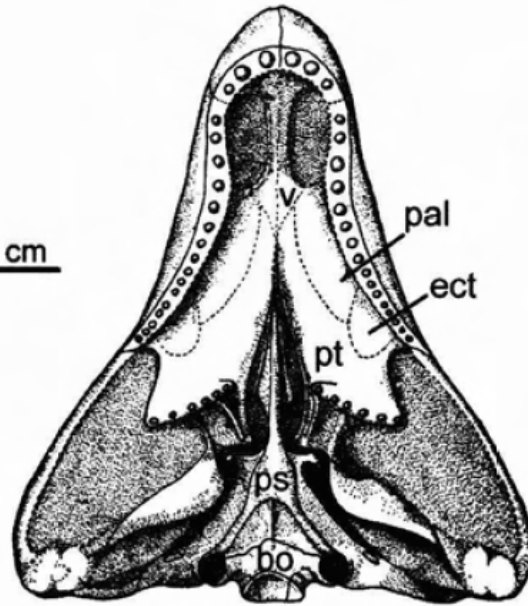
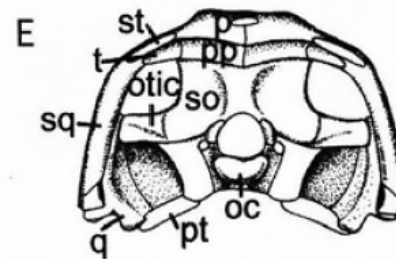
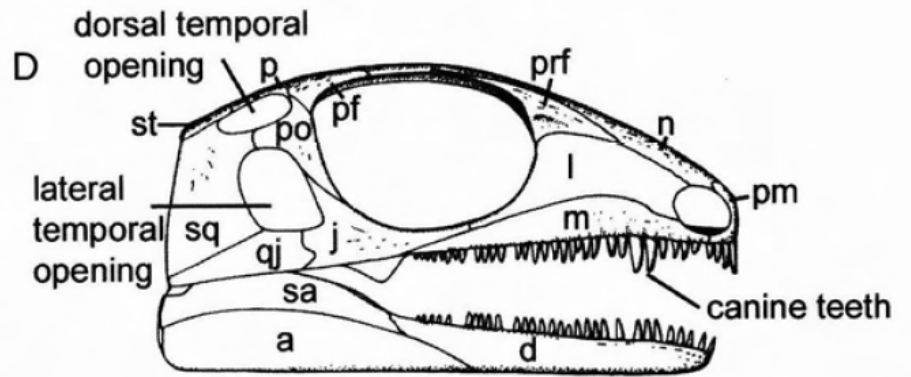
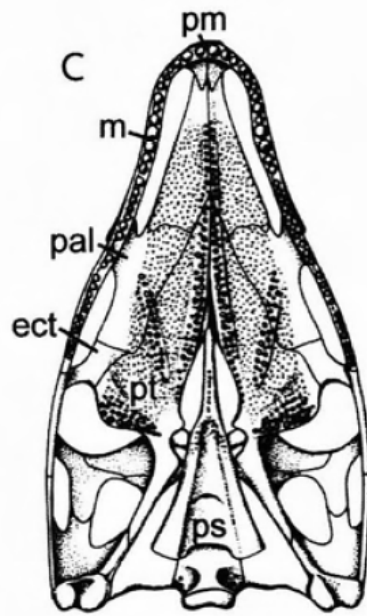
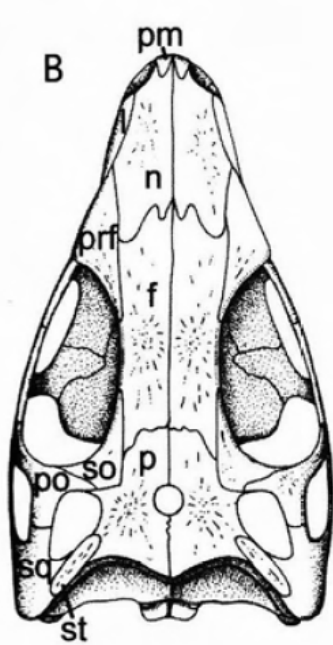
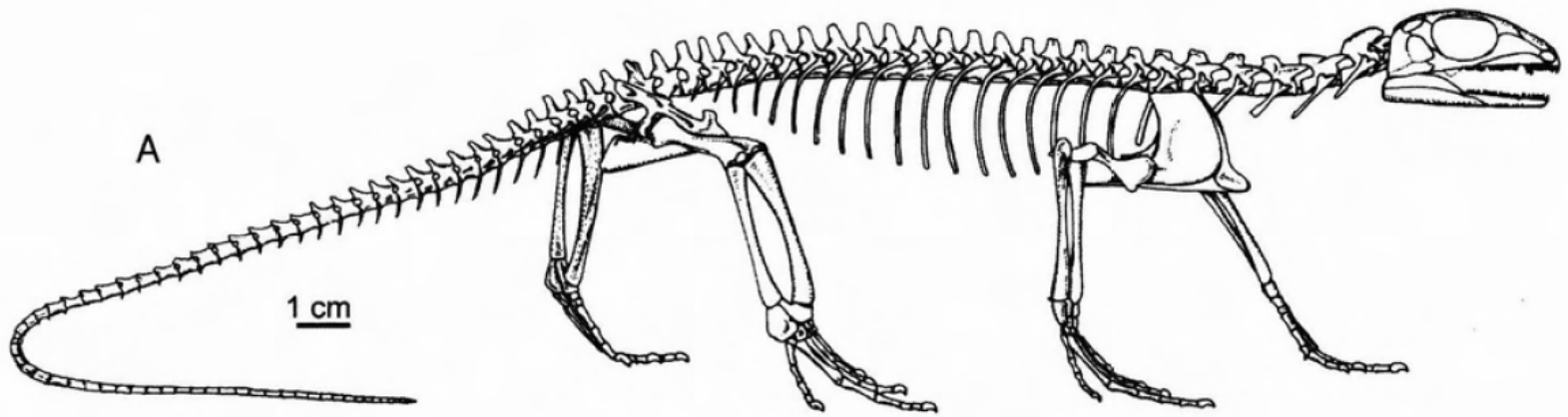


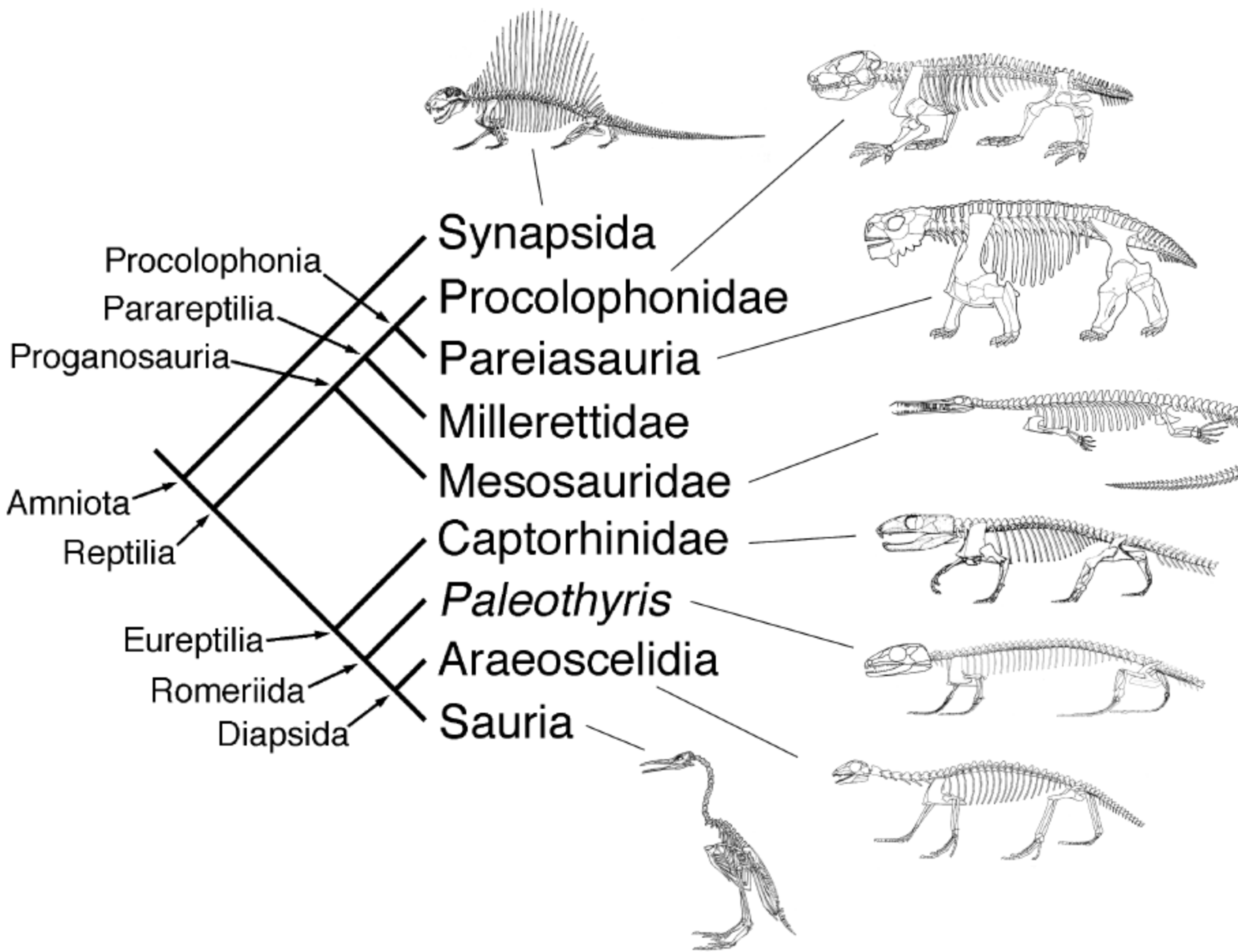
Figure 2 | *Gerobatrachus hottoni*, gen. et sp. nov., holotype specimen USNM 489135. **a**, Close-up interpretive specimen, and **b**, outline drawing of skull in ventral view. Abbreviations are the same as for Fig. 1 and: an, angular; art, articular; cp, cultriform process of parasphenoid; d, dentary; ec, ectopterygoid; ept, epipterygoid; f, frontal; j, jugal; l, lacrimal; m, maxilla; n, nasal; oc, portion of otic capsule; p, parietal; pal, palatine; pf, postfrontal; pm, premaxilla; po, postorbital; pp, postparietal; pr, prearticular; prf, prefrontal; ps, parasphenoid; pt, pterygoid; q, quadrate; qj, quadratojugal; sm, septomaxilla; sph, sphenethmoid; sq, squamosal; st, supratemporal; su, surangular; t, tabular; v, vomer.



4 cm







Dermatocráneo Amnioto: configuración de las fenestras

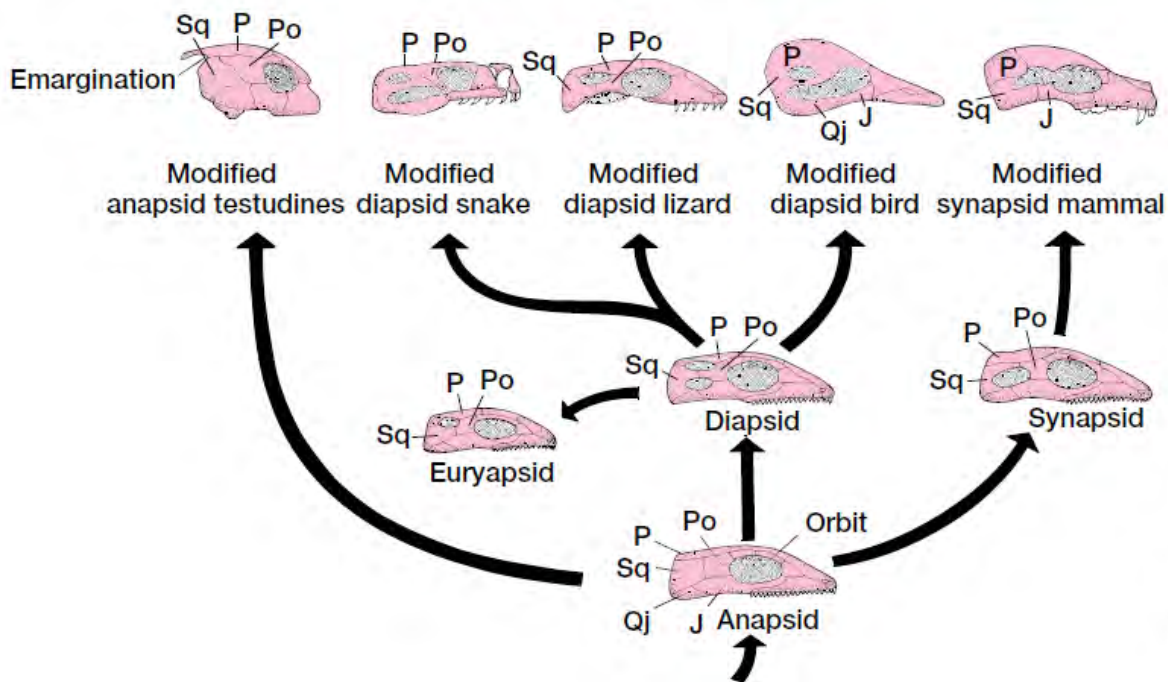


FIGURE 7.34 Major lineages of dermatocranium evolution within amniotes. The anapsid skull occurs in cotylosaurs and their modern descendants, turtles and tortoises. Two major groups, the diapsids and synapsids, independently evolved from the anapsids. *Sphenodon* and crocodylians retain the primitive diapsid skull, but it has been modified in diapsid derivatives such as snakes, lizards, and birds. Shading indicates positions of temporal fenestrae and orbit. Abbreviations: jugal (J), parietal (P), postorbital (Po), quadratojugal (Qj), squamosal (Sq).

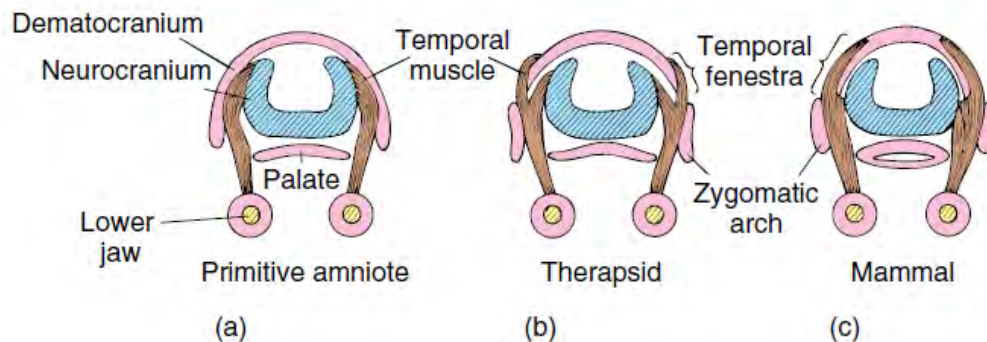


FIGURE 7.35 Temporal fenestrae. The shift in jaw muscle attachment to the skull is shown. (a) Anapsid skull. In early amniotes, temporal muscles run from the neurocranium to the lower jaw. Such a skull is retained in modern turtles. (b) Perforation in the dermatocranium opens fenestrae, and attachment of jaw muscles expands to the edges of these openings. (c) Extensive attachment of jaw muscles to the surface of the dermatocranium. Such development of fenestrae characterizes the diapsid and synapsid radiations.

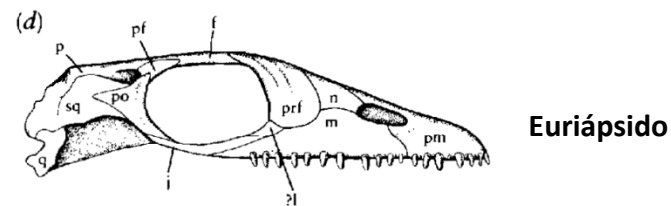
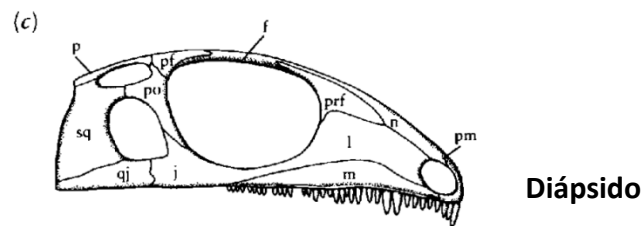
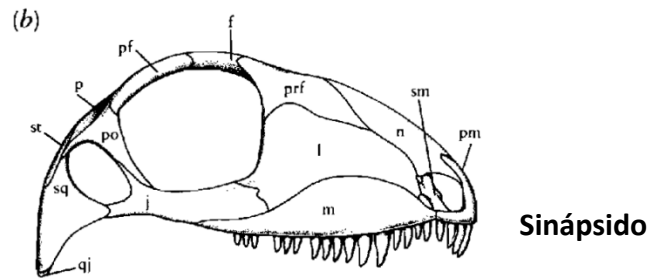
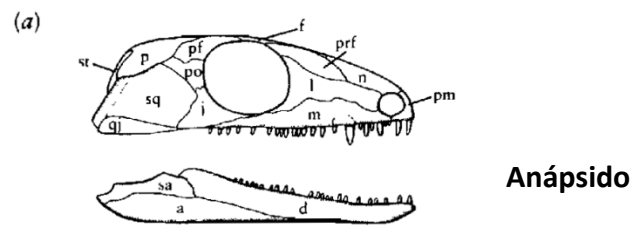


Figure 10-11. SKULLS OF EARLY AMNIOTES SHOWING THE PATTERN OF TEMPORAL OPENINGS THAT DISTINGUISH THE MAJOR GROUPS. (a) The anapsid condition, illustrated by the prothyrid *Paleothyris*. (b) The synapsid condition, exemplified by the early mammal-like reptile *Haptodus*. (c) The diapsid condition, shown by *Petrolacosaurus*. (d) The nothosaur *Neusticosaurus*, illustrating the parapsid or euryapsid condition. The diapsid and synapsid configurations are thought to have evolved separately from the anapsid condition. The euryapsid pattern has evolved from the diapsid pattern by loss of the lower temporal bar. Abbreviations as in Figure 8-3.

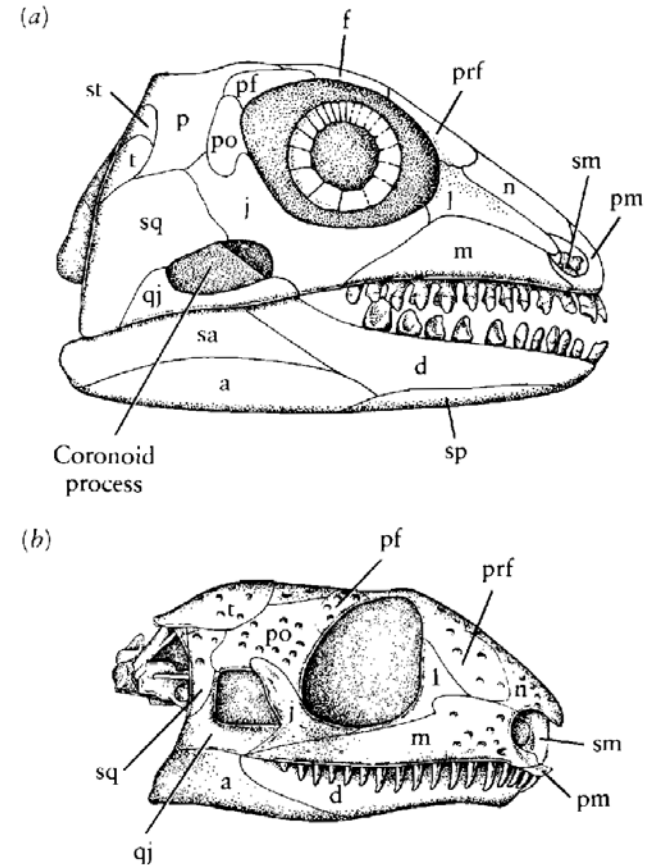
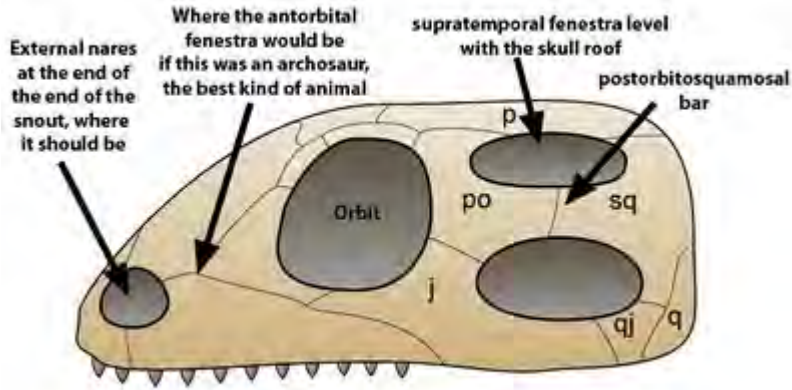
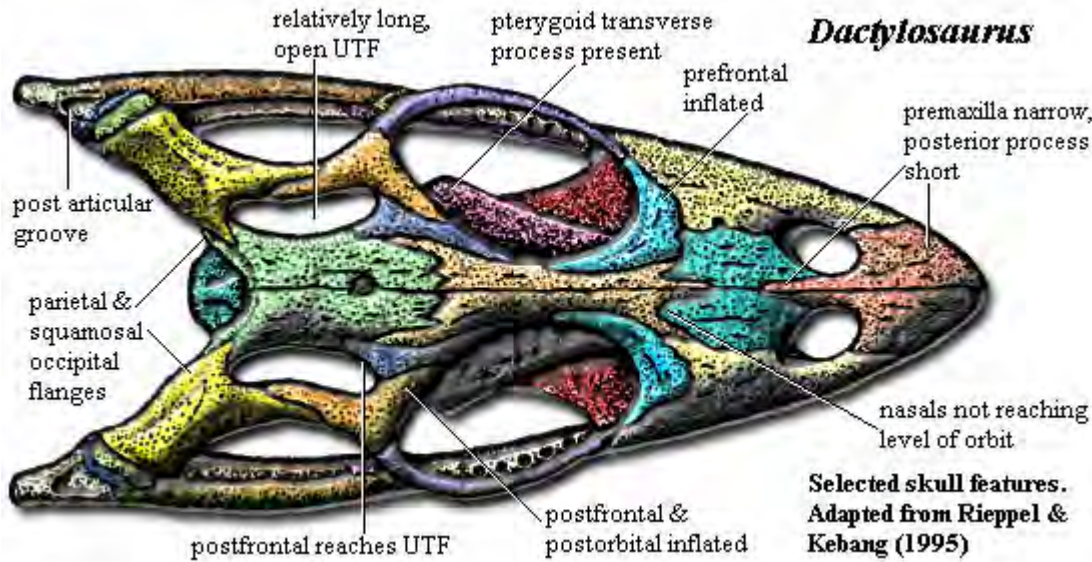
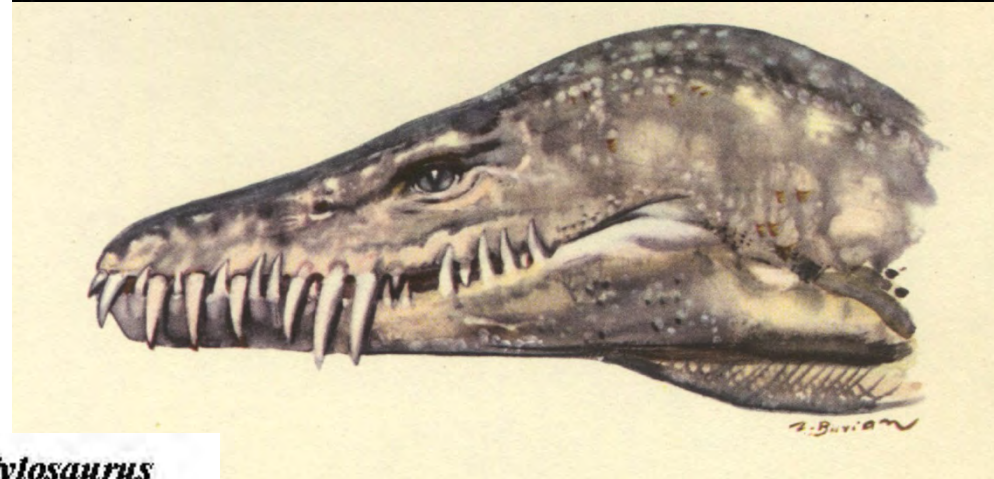
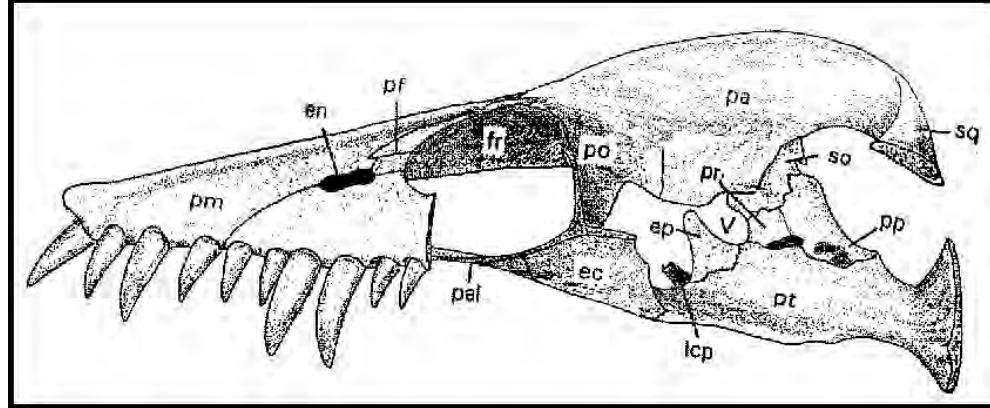


Figure 10-13. SKULLS OF TWO PRIMITIVE AMNIOTES FROM THE LOWER PERMIAN SHOWING LATERAL TEMPORAL OPENINGS. They show no close affinities with other groups. (a) *Bolosaurus*, in which the cheek teeth are expanded and show precise occlusion; note also the high coronoid process. (b) *Aceleistorhinus*. Abbreviations as in Figure 8-3. From Daly, 1969.

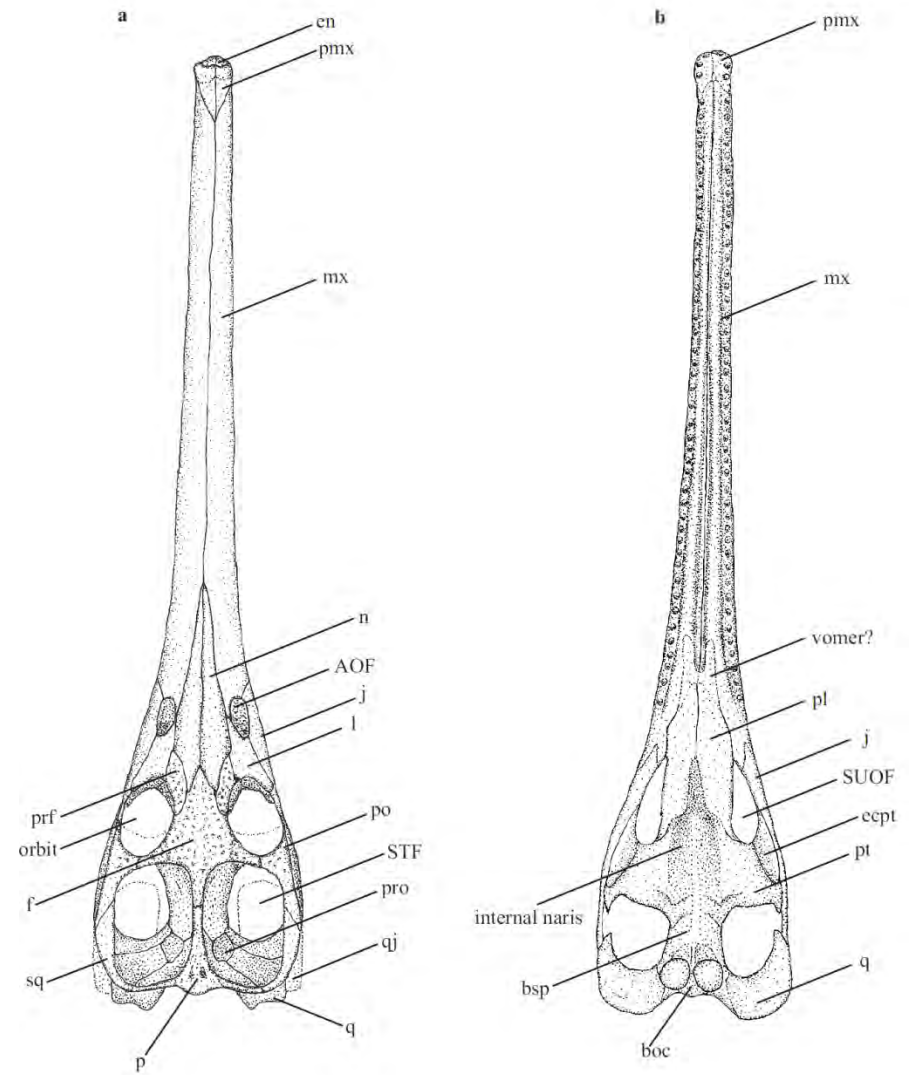
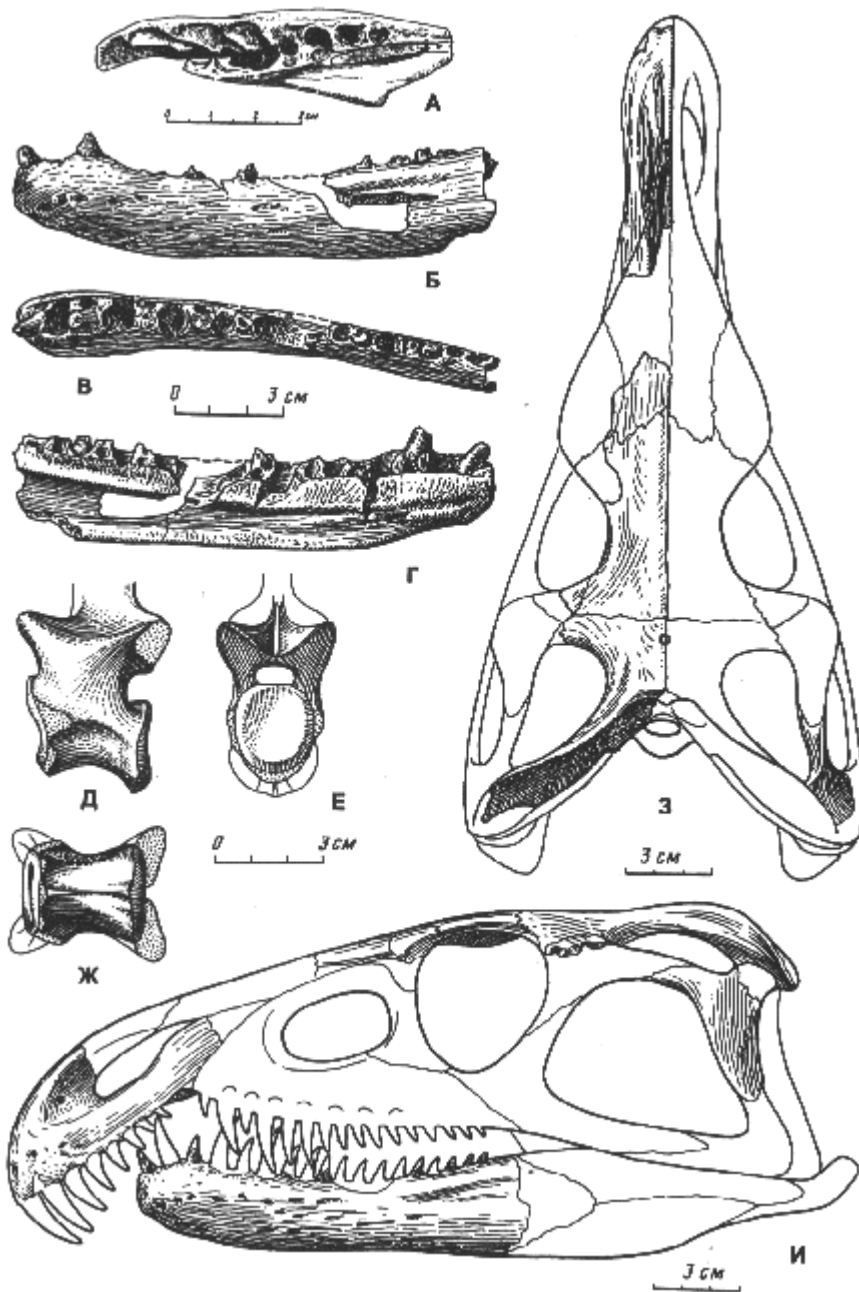
A GENERIC DIAPSID SKULL



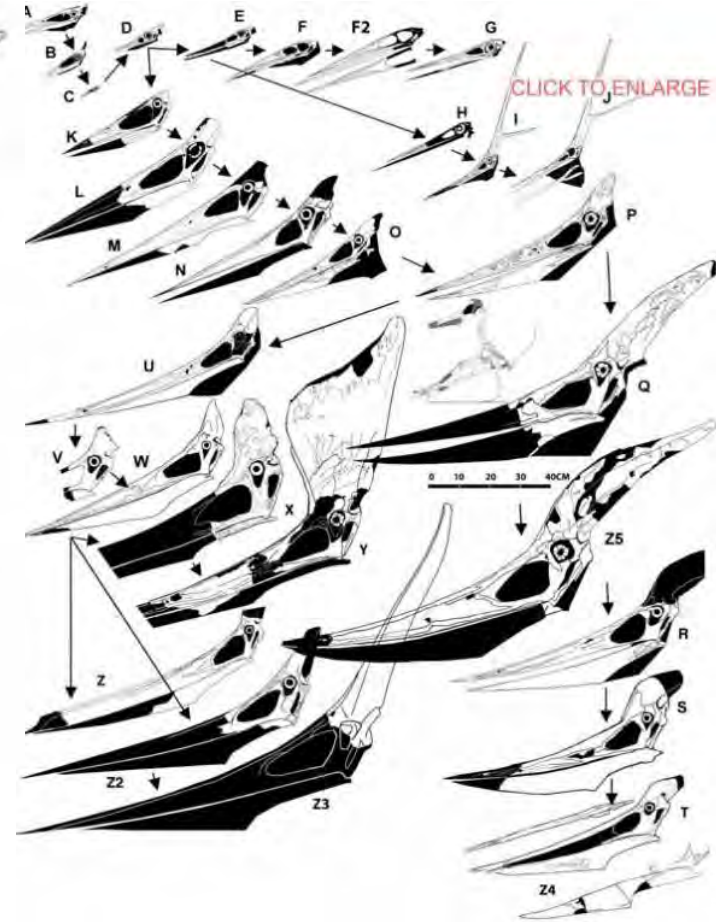
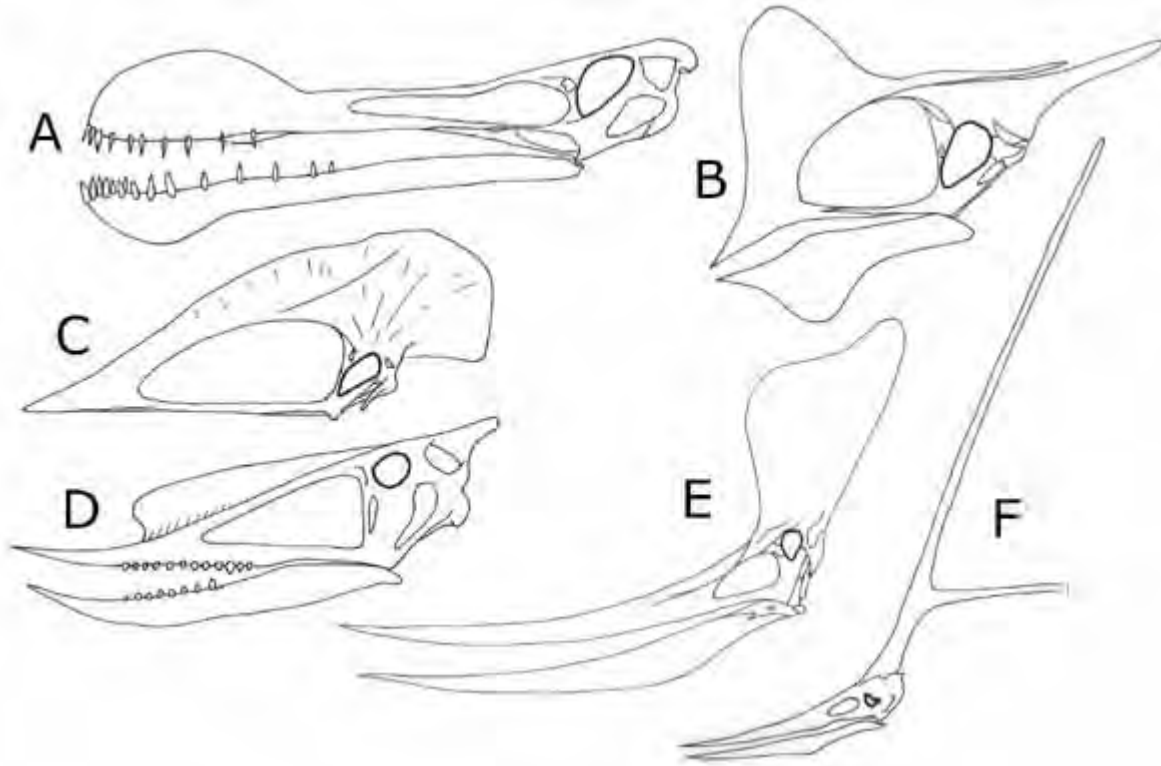
This image was stolen from Wikipedia. Hey archosaur workers. I think we should get on those Wikipedia entries, ay?



Archosauria: fenestra anterorbital



Pterosauria



A selected of crested pterodactyloid pterosaurs. A. Ornithocheirid ornithocheiroid *Ornithocheirus*. B. Tapejarid azhdarchoid *Tapejara*. C. Thalassodromid azhdarchoid *Tupuxuara*. D. Dsungaripterid *Dsungaripterus*. E. Pteranodontid ornithocheiroid *Pteranodon*. F. Nyctosaurid ornithocheiroid *Nyctosaurus*

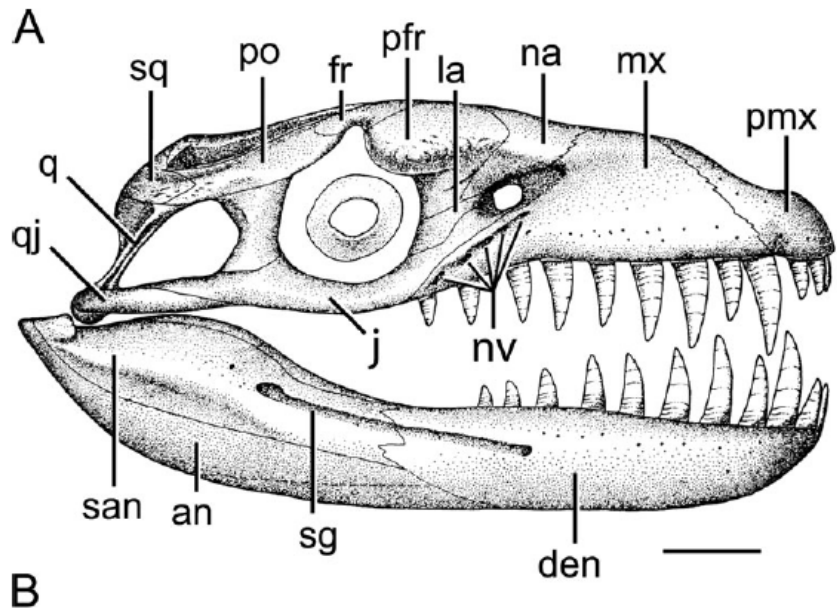


Figure 2 Skull of *Dakosaurus andiniensis* in lateral view. **A**, reconstruction of the right side based on information from available specimens. **B**, right side of MOZ 6146P. **C**, left side of MOZ 6146P. Abbreviations: **an**, angular; **den**, dentary; **fr**, frontal; **j**, jugal; **la**, lacrima; **mx**, maxilla; **na**, nasal; **pfr**, prefrontal; **pmx**, premaxilla; **po**, postorbital; **q**, quadrate; **qj**, quadratojugal; **san**, surangular; **sg**, surangular groove; **sq**, squamosal. Scale bar = 10 cm.

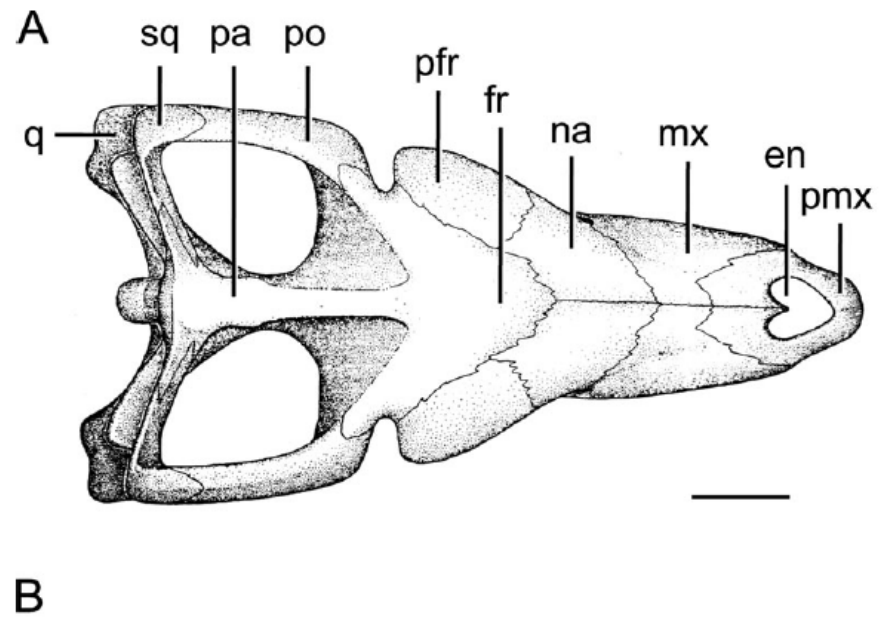
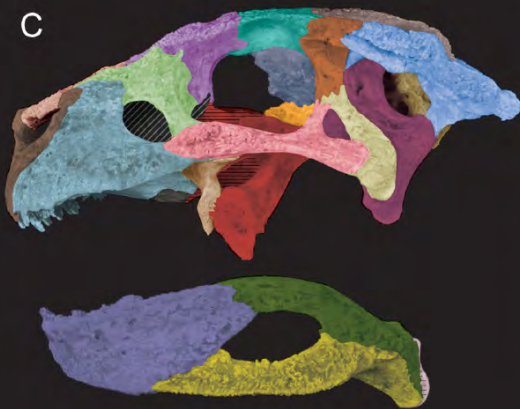
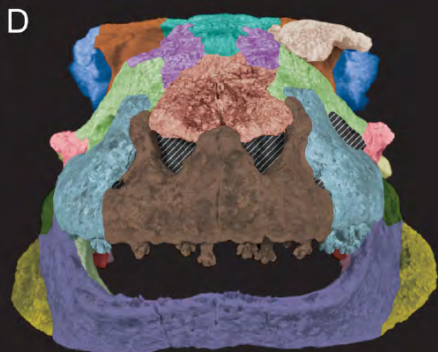


Figure 3 Skull of *Dakosaurus andiniensis* in dorsal view. **A**, reconstruction based on information from available specimens and **B**, specimen MOZ 6146P. Abbreviations: **en**, external nares; **fr**, frontal; **mx**, maxilla; **na**, nasal; **pa**, parietal; **pfr**, prefrontal; **pmx**, premaxilla; **po**, postorbital; **q**, quadrate; **sq**, squamosal. Scale bar = 10 cm.



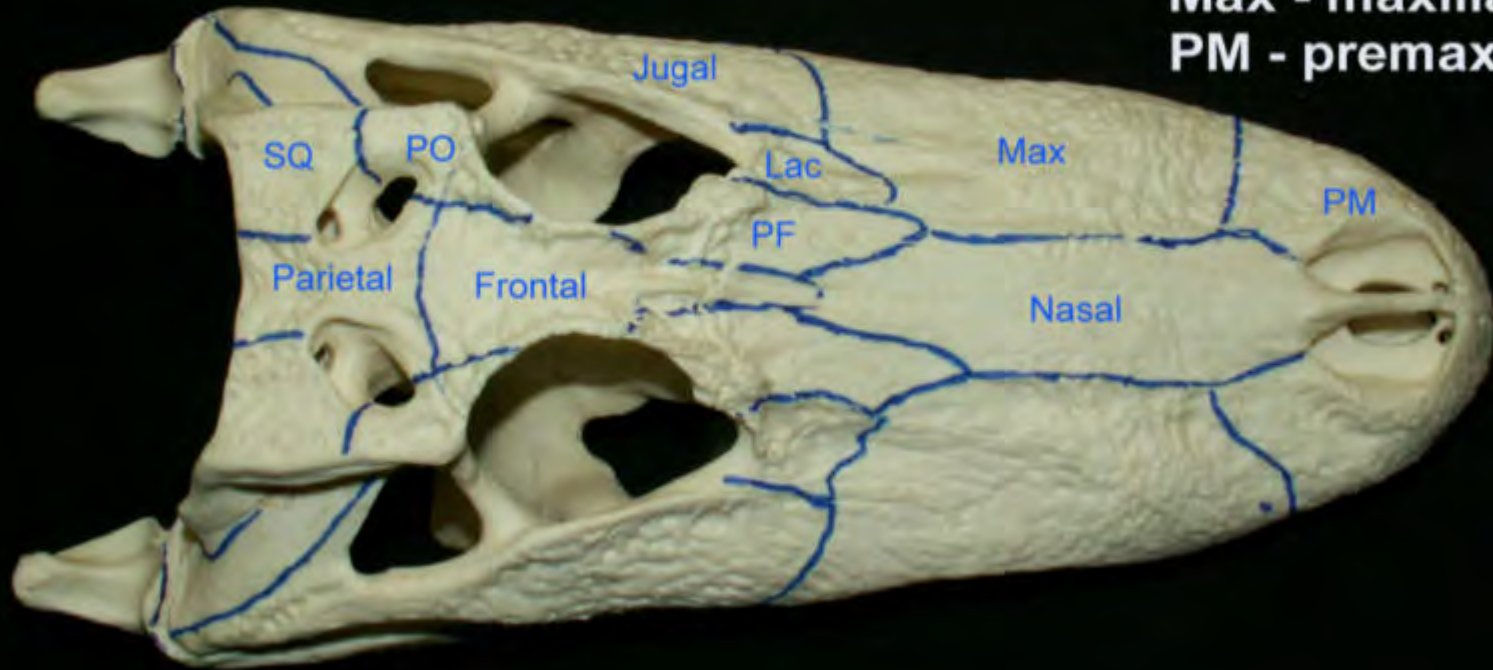
Angulars	Parabasisphenoid
Articulars	Parietal
Basioccipital	Postorbitals
Dentaries	Prefrontals
Ectopterygoids	Premaxillae
Frontal	Pterygoid
Jugals	Quadrates
Lacrimal	Quadratojugals
Laterosphenoids	Splenials
Maxillae	Squamosals
Nasals	Supraoccipital
Otococcipital	Supratemporal Ossifications
Palatines	Surangulars
Palpebrals	Vomers



2 cm

Alligator Skull Dorsal View

SQ - squamosa
PO - postorbital
PF - prefrontal
Lac - lacrimal
Max - maxilla
PM - premaxilla



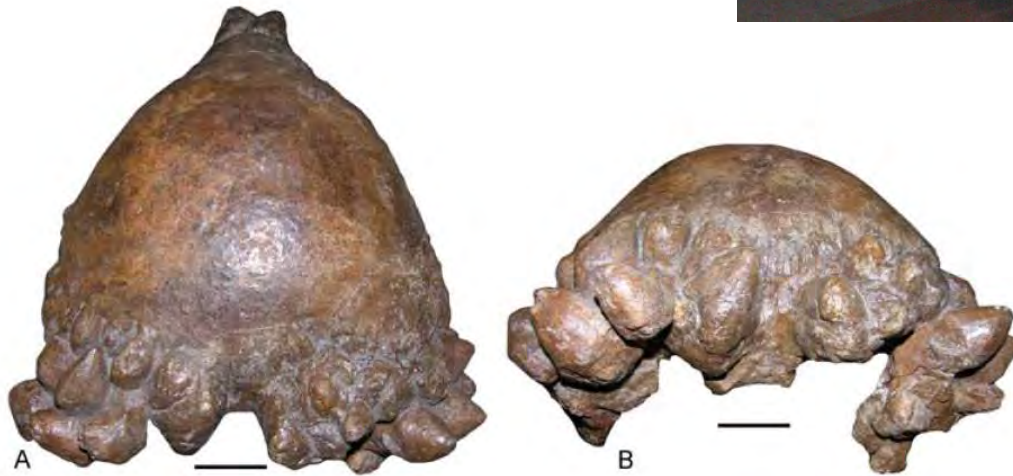


Figure 6. The holotype adult skull of *Pachycephalosaurus "reinheimeri"* (DMNS 469). (A) Asymmetrical clusters of massive, slightly pointed to rounded nodal ornaments on the dorsal surface of the squamosals dominate the posterior skull. (B) The squamosal nodes in posterior view. Scale bars are 5 cm.
doi:10.1371/journal.pone.0007626.g006

Ontogenia craneal en Marginocéfalos

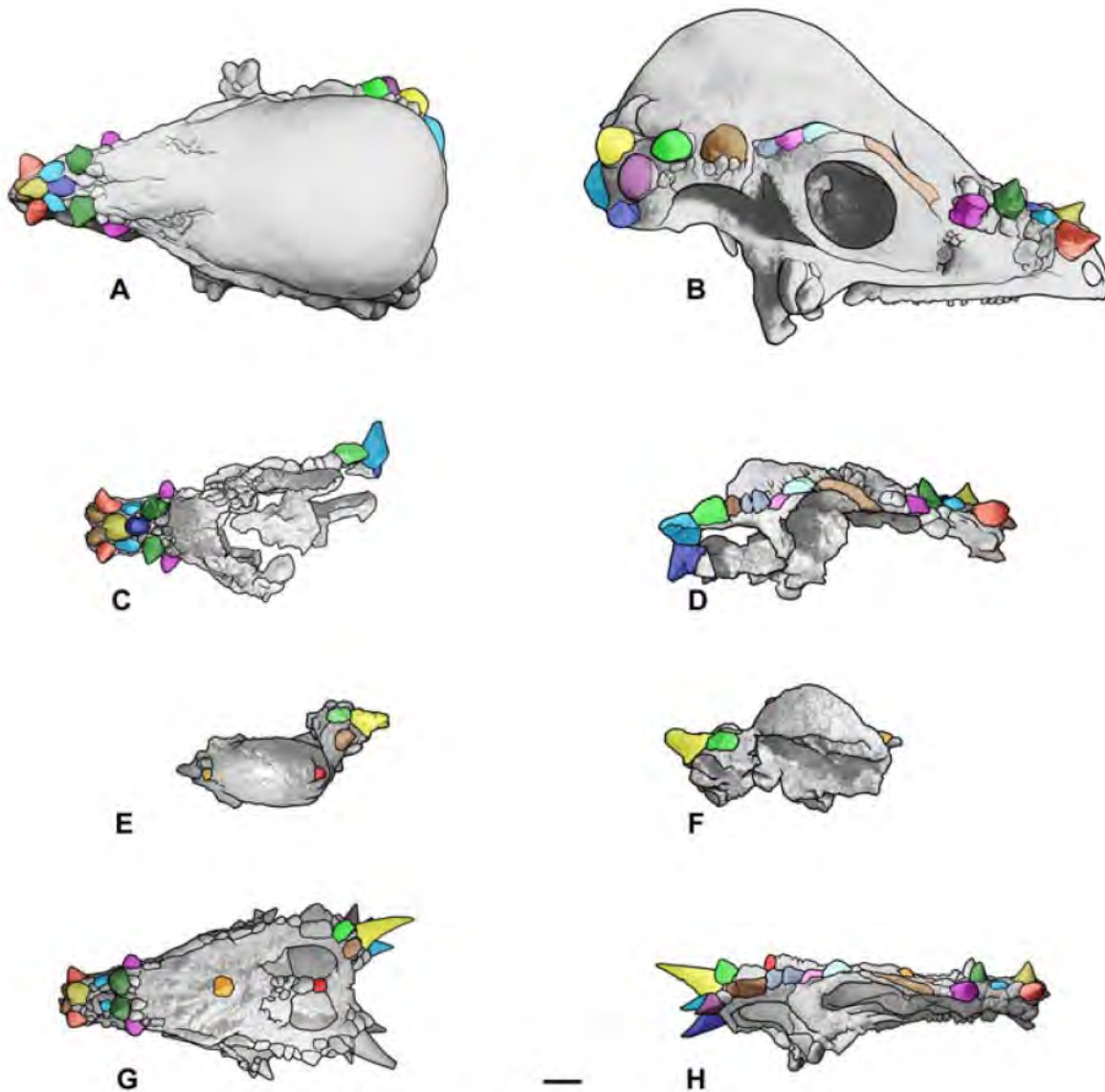


Figure 3. Cranial ontogenetic sequence of *Pachycephalosaurus wyomingensis* with morphological landmarks highlighted in color. The ontogenetically oldest adult, AMNH 1696, in (A) dorsal and (B) right lateral views. A younger adult, UCMP 556078 (cast) with inflation of the frontoparietal dome+lateral cranial elements and mature nasal and squamosal nodal ornamentation in (C) dorsal and (D) right lateral views. MPM 8111, a partial skull of "*Stygimoloch*" in (E) dorsal and (F) left lateral views (reversed) illustrates the high narrow frontoparietal dome, squamosal nodes and horns characteristic of the subadult growth stage. Landmarks on the dorsal skull of MPM 8111 in orange (anterior) and red (posterior) constrain the position of the dome. The youngest growth stage in this cranial ontogenetic series is "*Dracorex*", TCNI 2004.17.1 (cast) in (G) dorsal and (H) right lateral views. The position of the squamosal horns and nasal nodes are consistent in these four pachycephalosaurid skulls, which increase in overall length and size from youngest (G,H) to oldest (A,B). Scale bar is 5 cm.

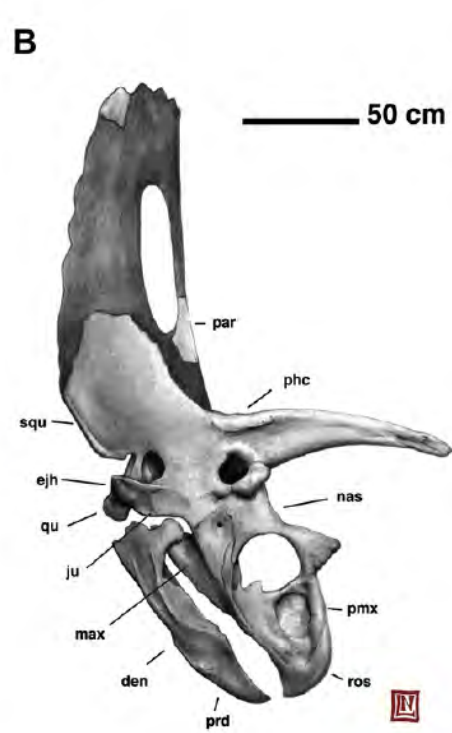


Fig. 4. A. OMNH 10165, holotype skull of *Titanoceratops ouranos*, with the posterior frill reconstructed to resemble that of *Pentaceratops stembergi*. B. Illustration showing missing parts of the frill (shaded). Abbreviations: den, dentary; ejh, epijugal horncore; ju, jugal; max, maxilla; nas, nasal; par, parietal; phc, postorbital horncore; pmx, premaxilla; qu, quadrate; ros, rostral; squ, squamosal.



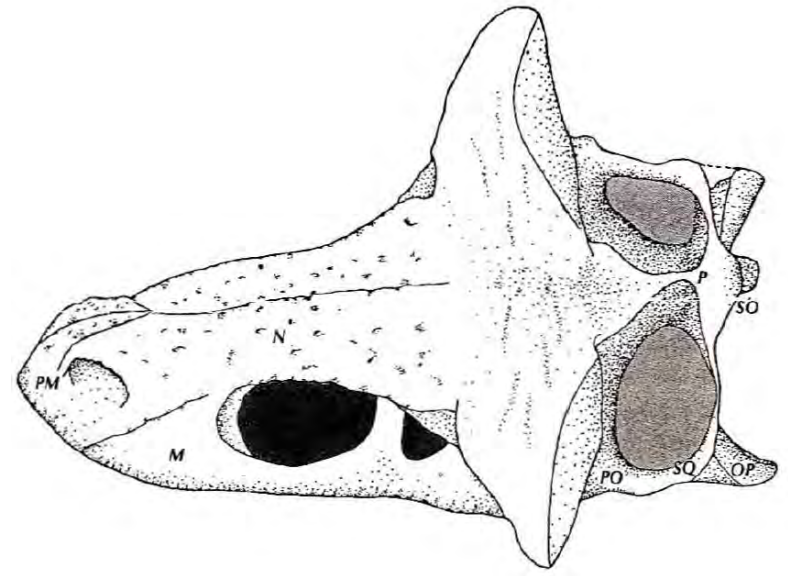
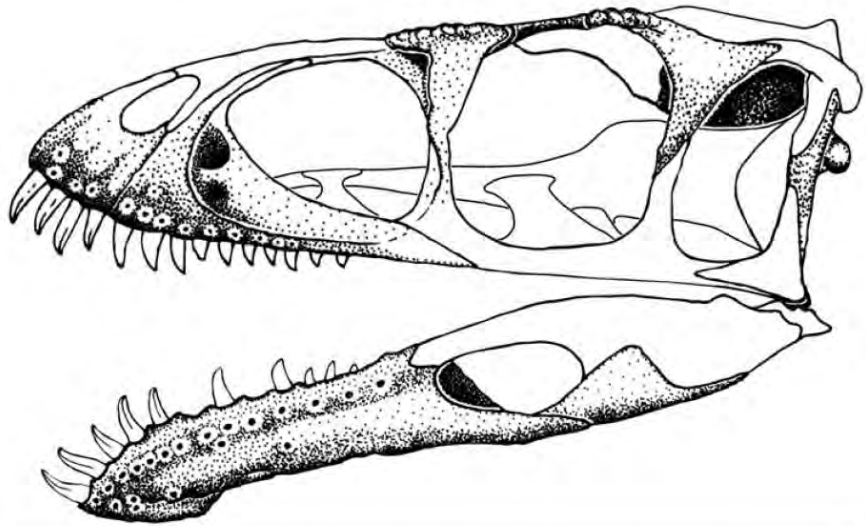


FIGURE 11. Reconstructed skull of *Masiakasaurus bnotifleri* in left lateral view. Known elements

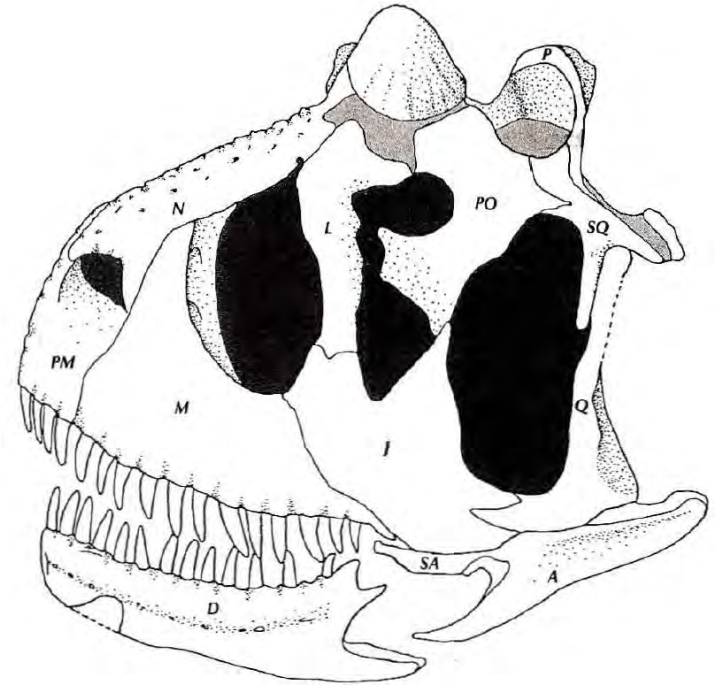
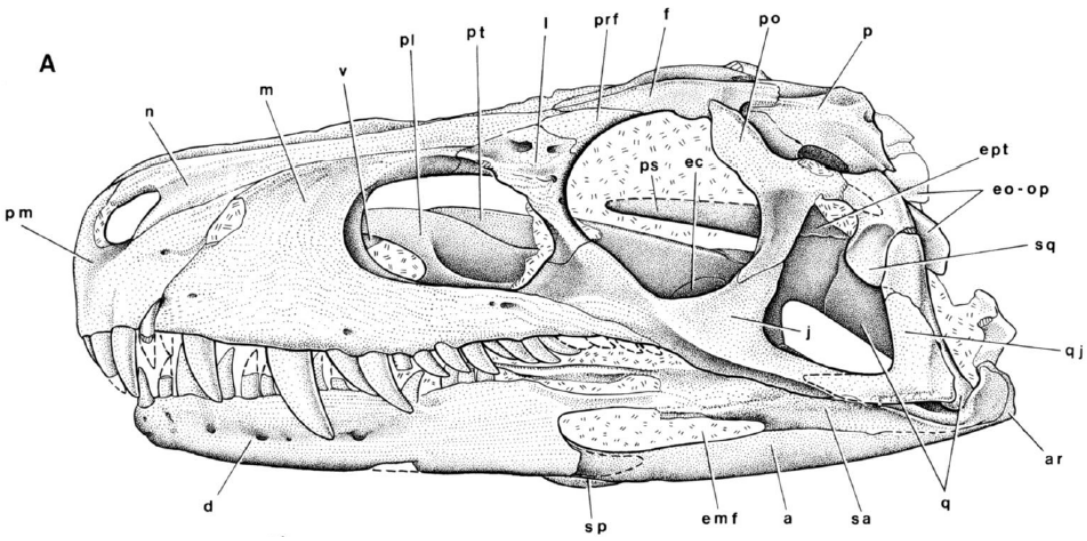
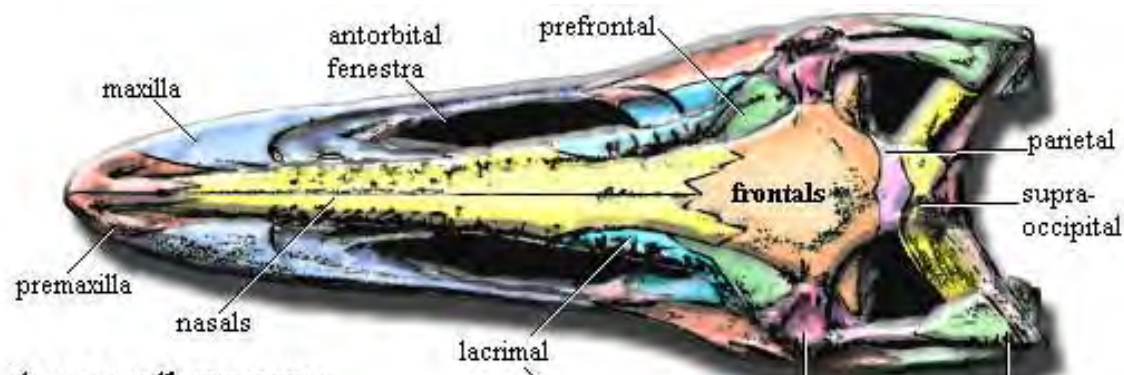
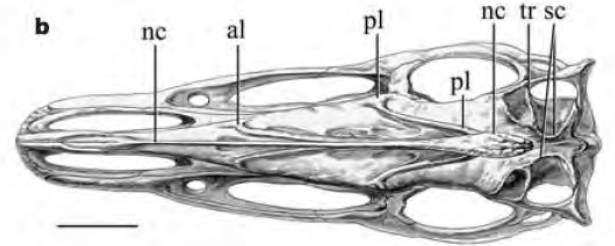
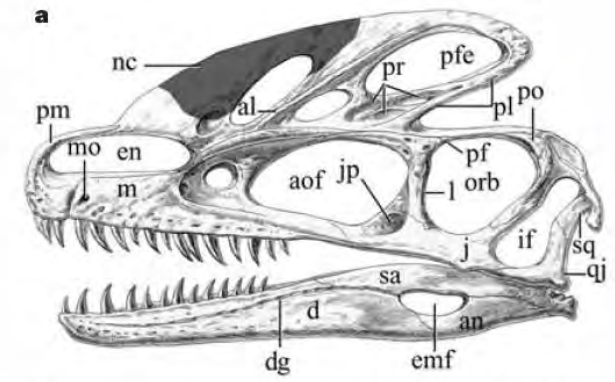
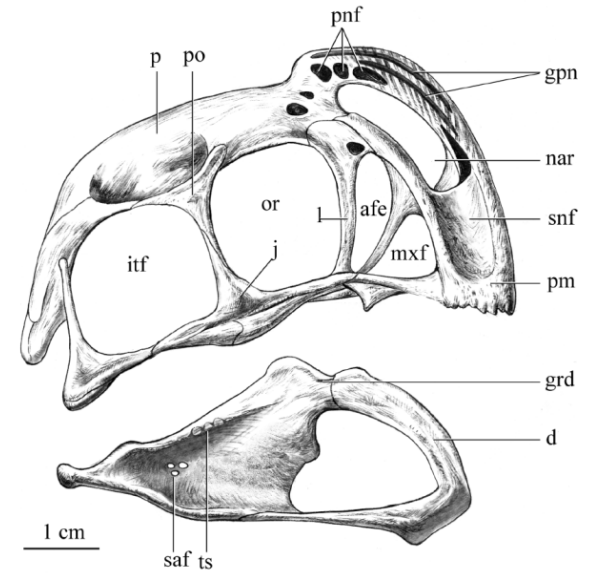
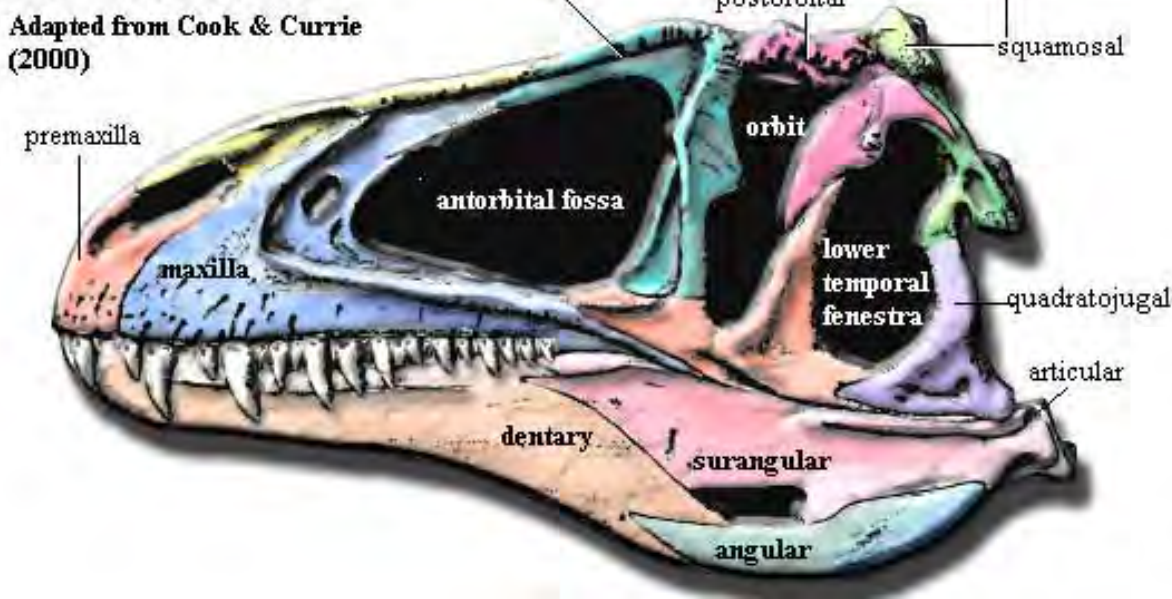
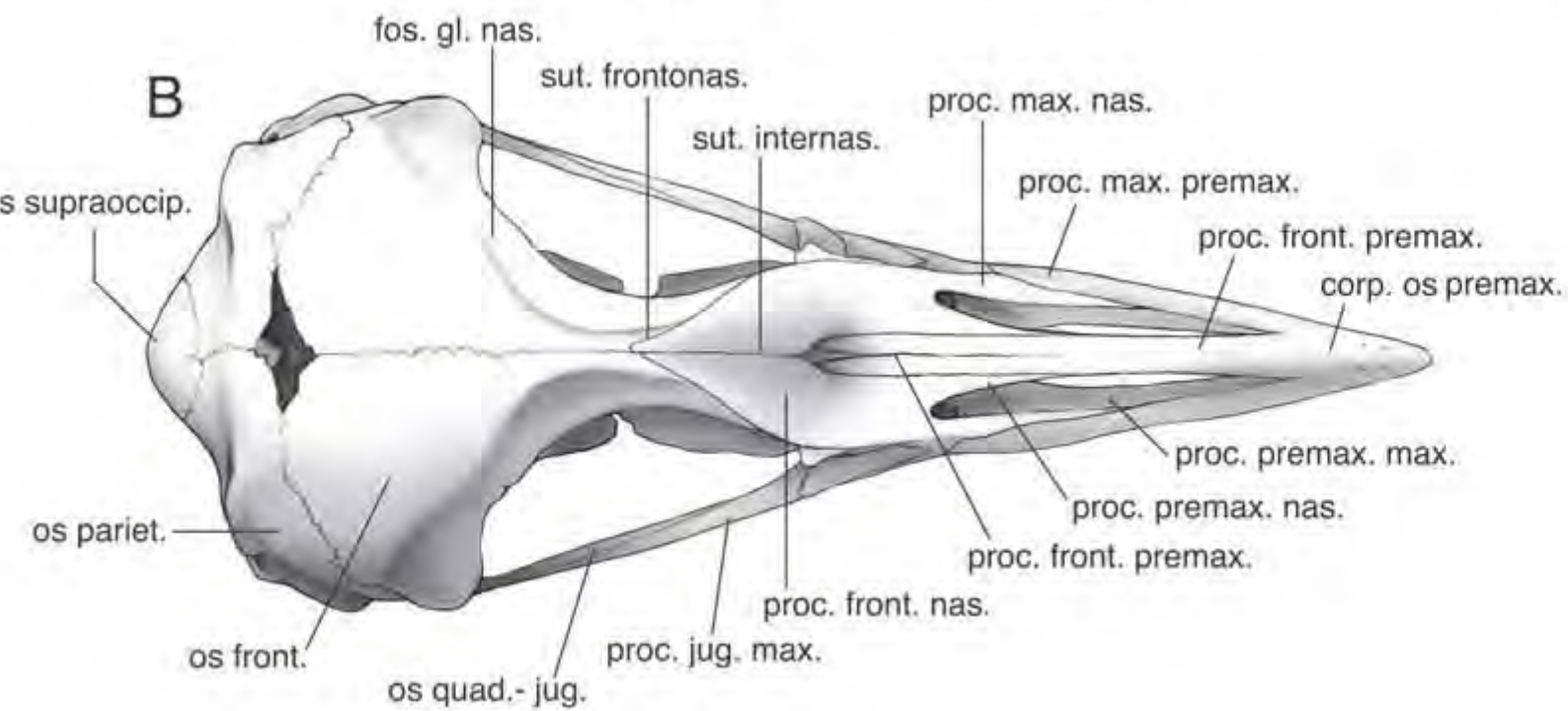
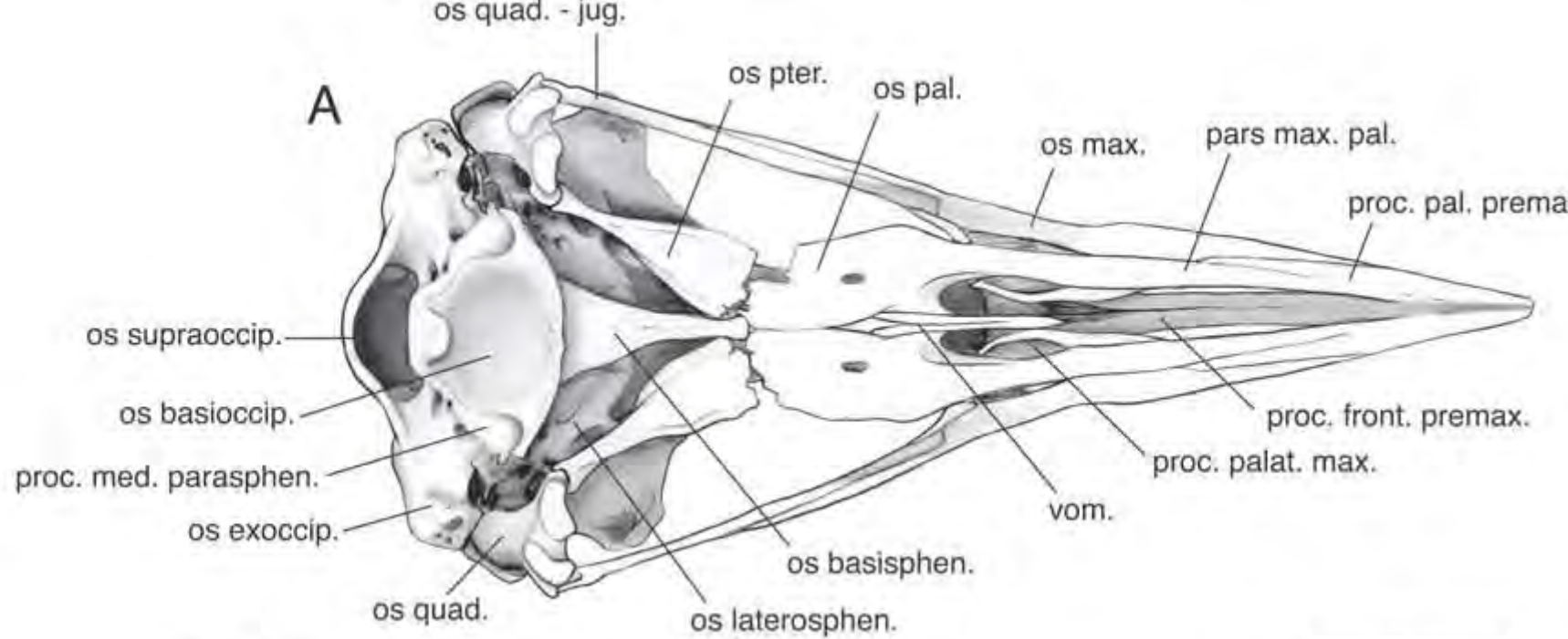


Figure 1. Dorsal view and left lateral view of holotype of *Carnotaurus sastrei*, actual length 57cm. Standard letter abbreviations are used for the elements of the skull.

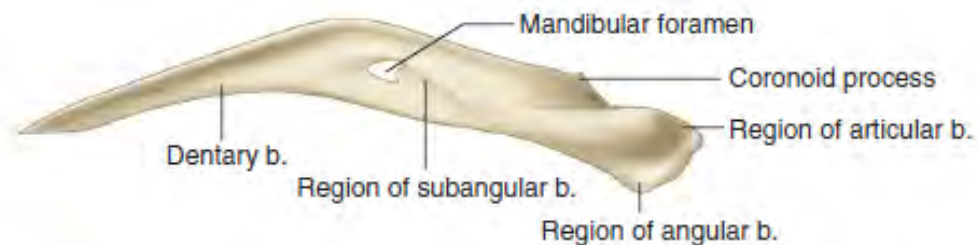
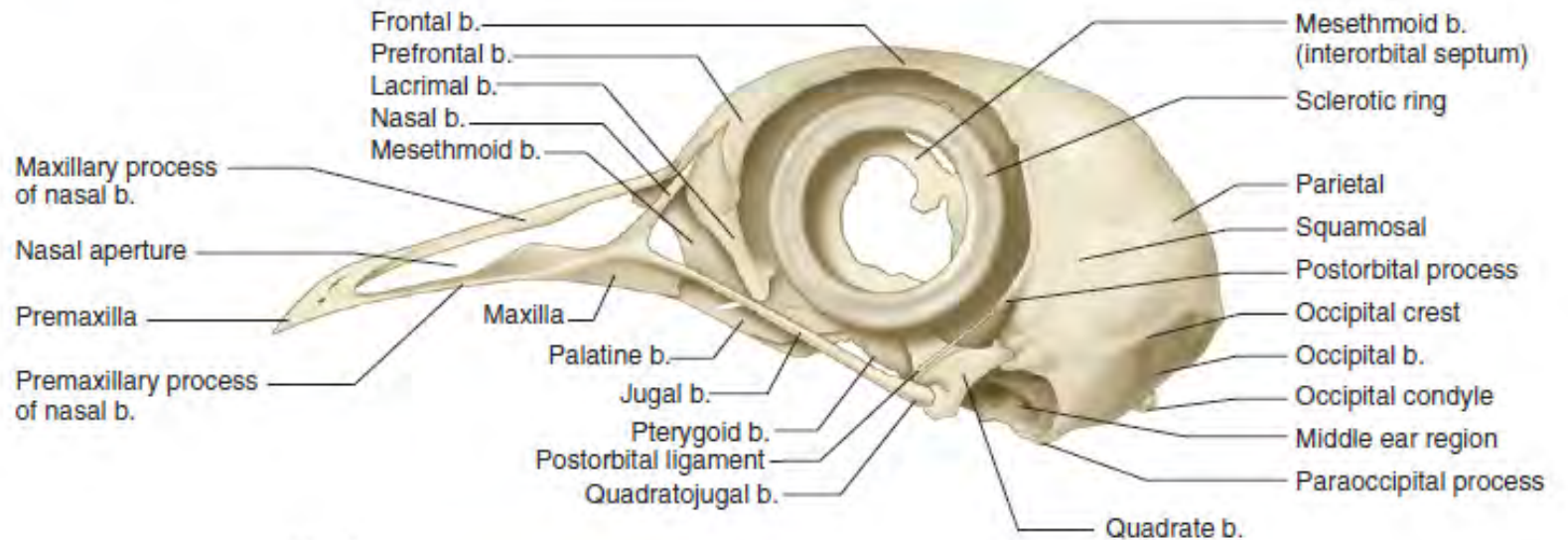
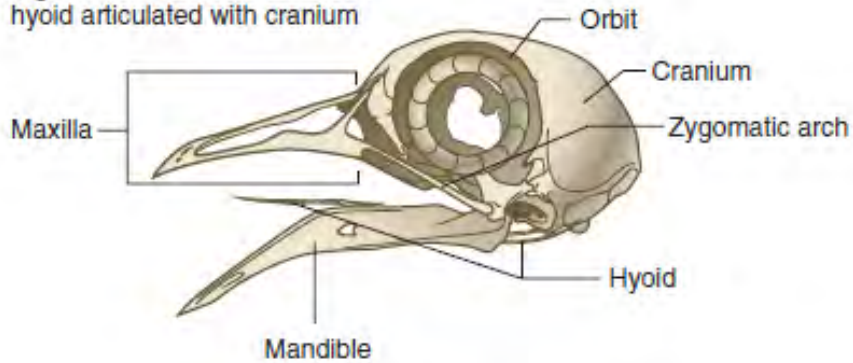


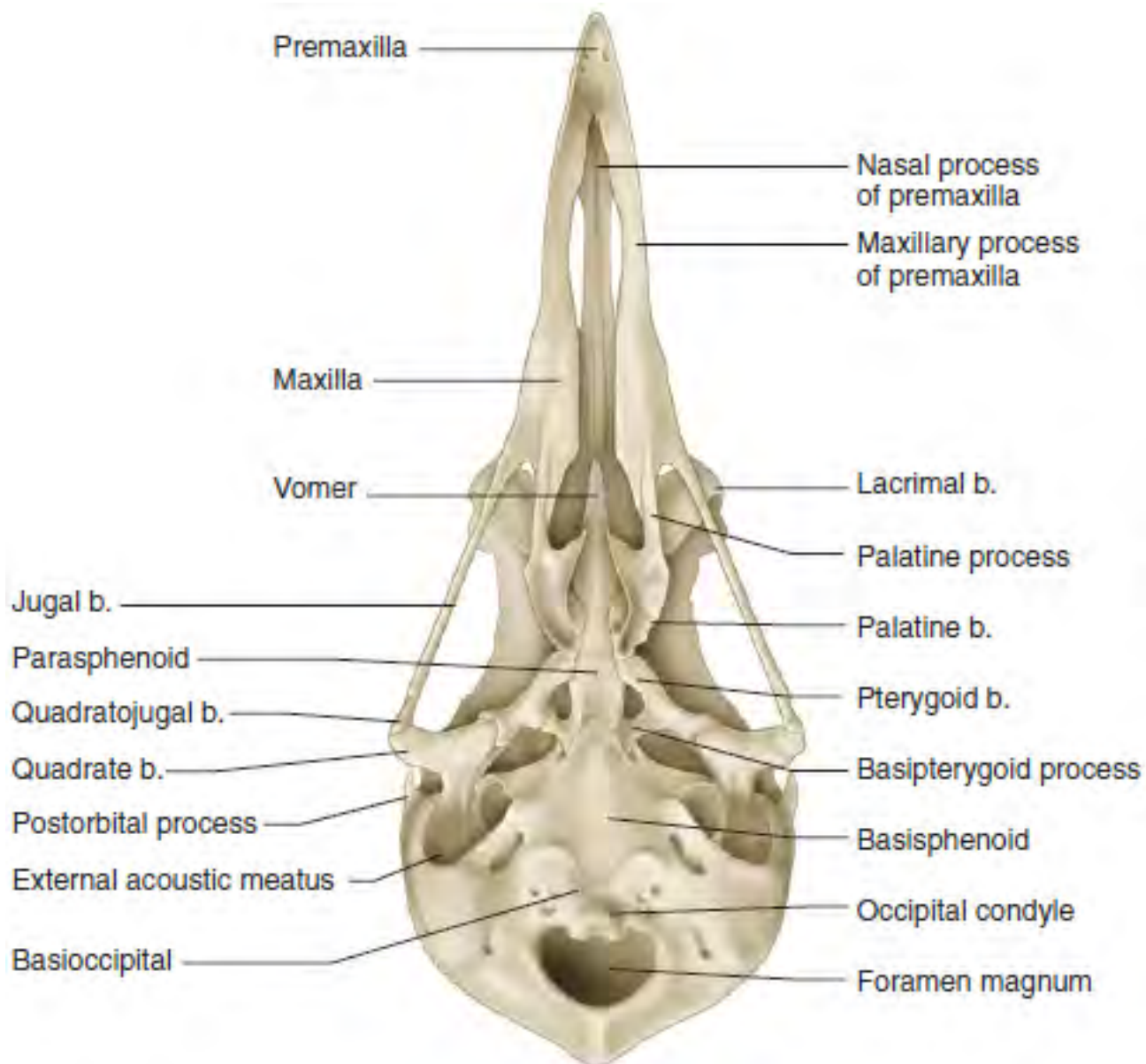
Acrocanthosaurus
Adapted from Cook & Currie (2000)



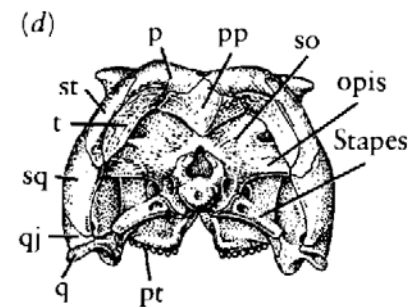
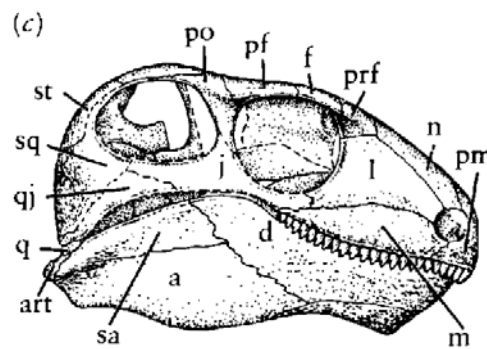
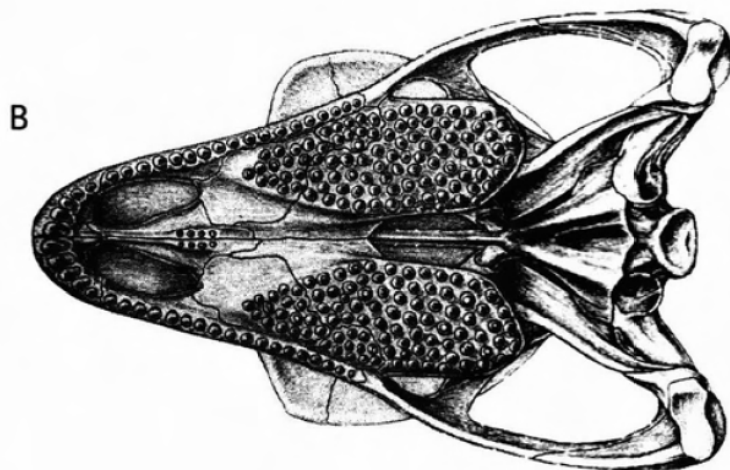
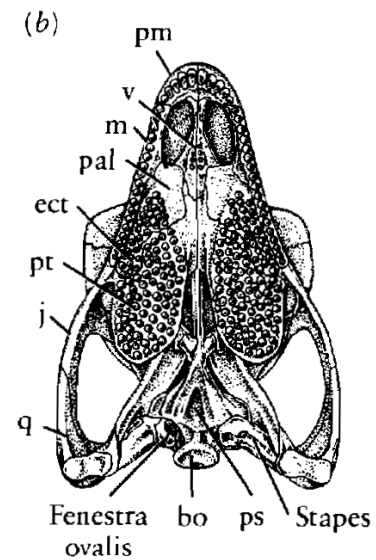
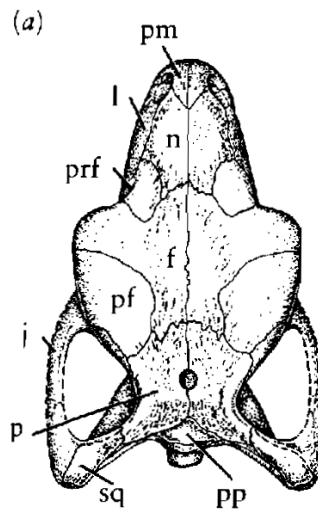
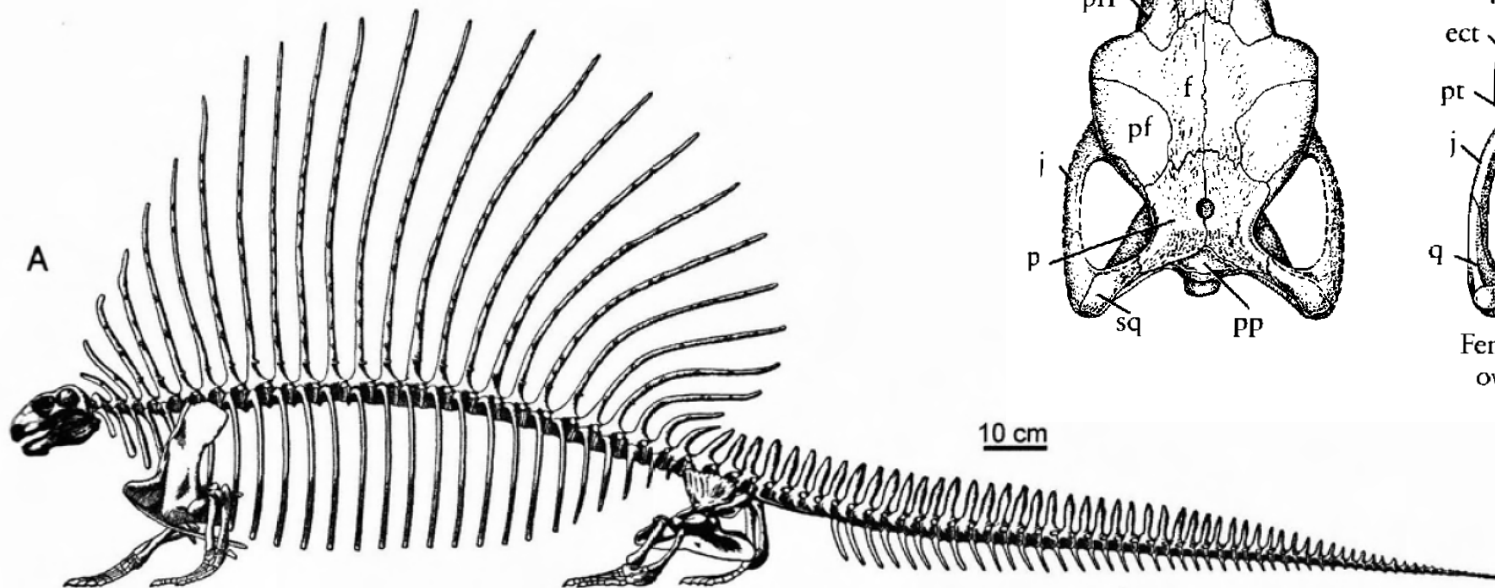


Pigeon skull with mandible and hyoid articulated with cranium





Synapsida



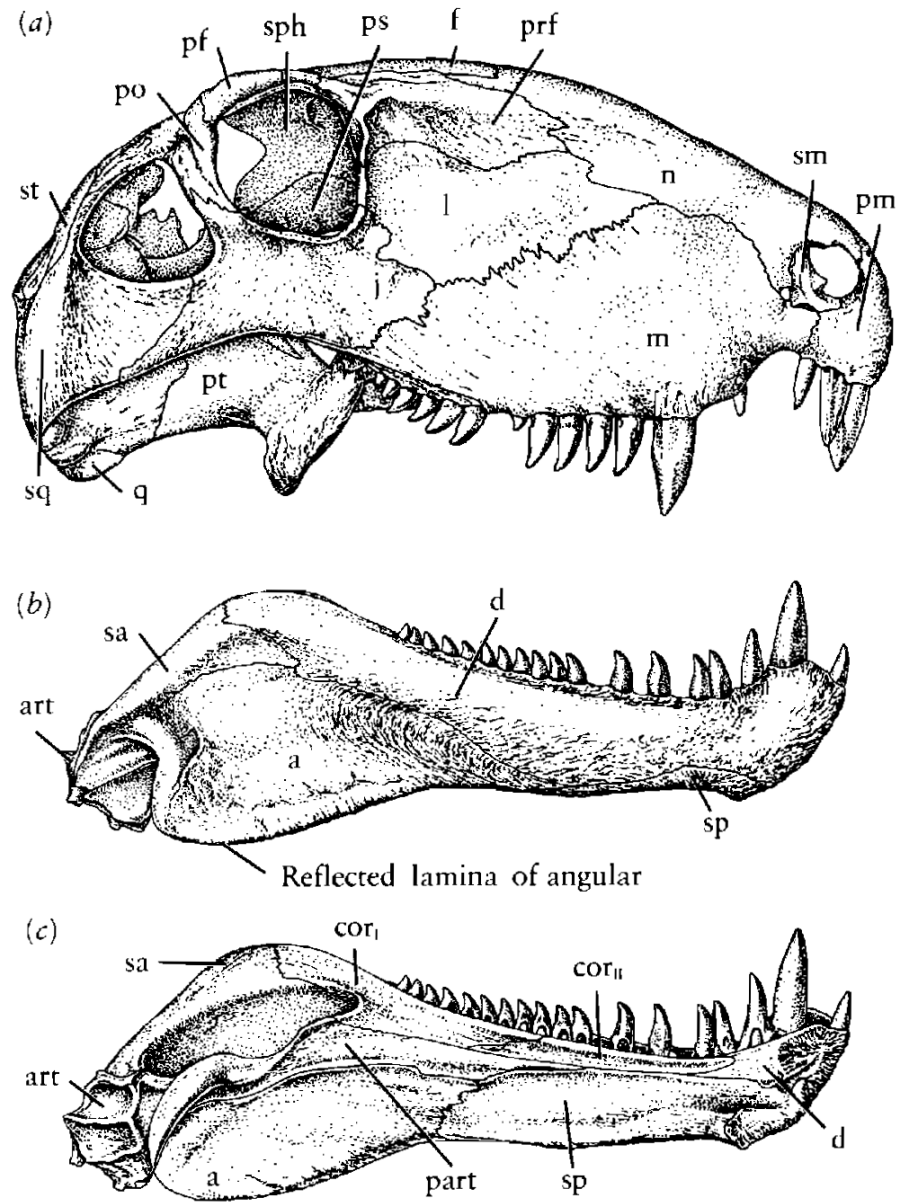


Figure 17-6. (a) Skull of *Dimetrodon*, in lateral view. (b) Lateral and (c) medial views of the lower jaw, $\times \frac{1}{4}$. Abbreviations as in Figure 8-3. From Romer and Price, 1940.

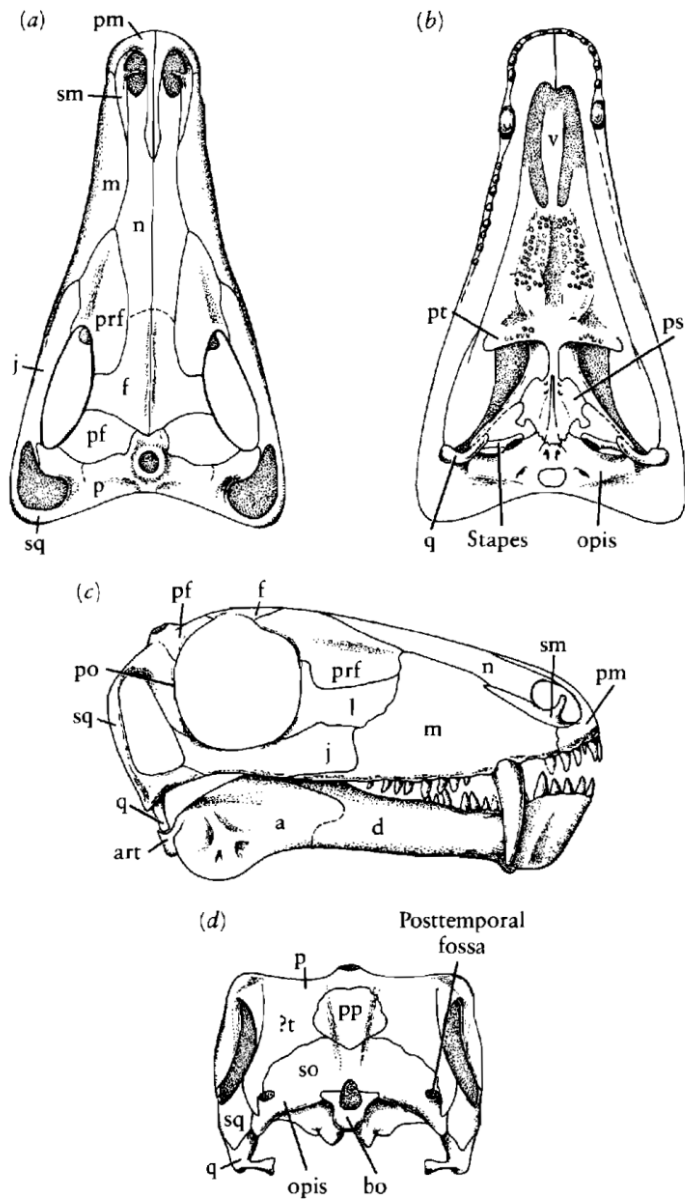


Figure 17-13. SKULL OF THE PRIMITIVE THERAPSID BIARINOSUCHUS. (a) Dorsal, (b) palatal, (c) lateral, and (d) occipital views, $\times \frac{1}{2}$. Abbreviations as in Figure 8-3. From Sigogneau and Chudinov, 1972.

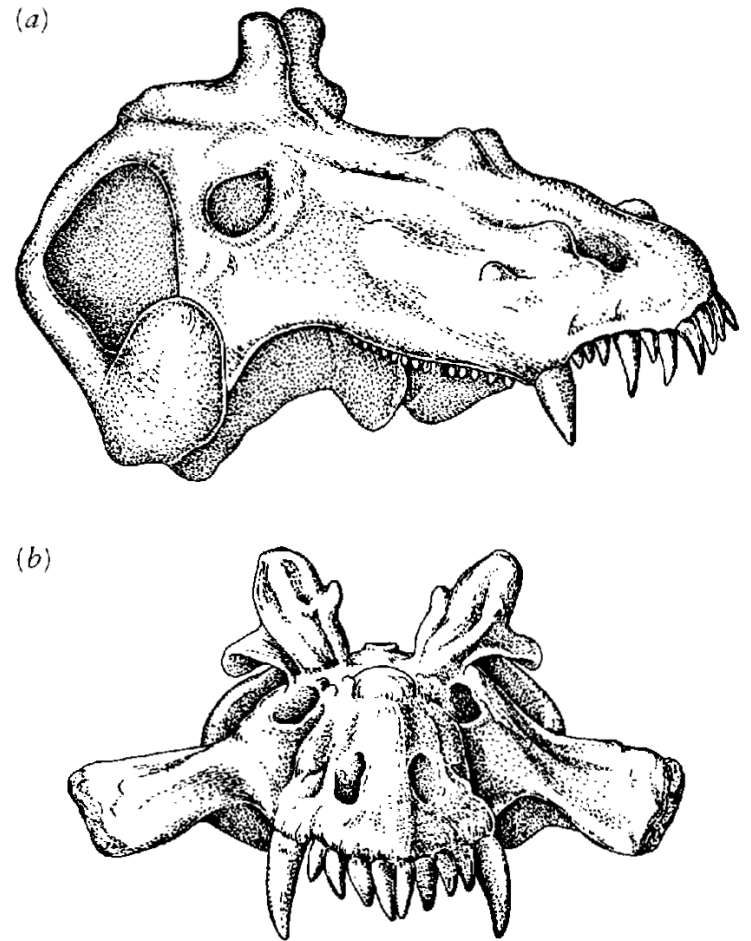


Figure 17-16. THE SKULL OF *ESTEMMENOSUCHUS*. (a) Lateral and (b) anterior views. It is one of the oldest-known therapsids, coming from the lowermost Upper Permian of Russia. The small size of the cheek teeth suggests that it was a herbivore. Its specific affinities are unknown. From Chudinov, 1965. By permission of the University of Chicago Press. Skull 80 cm long.

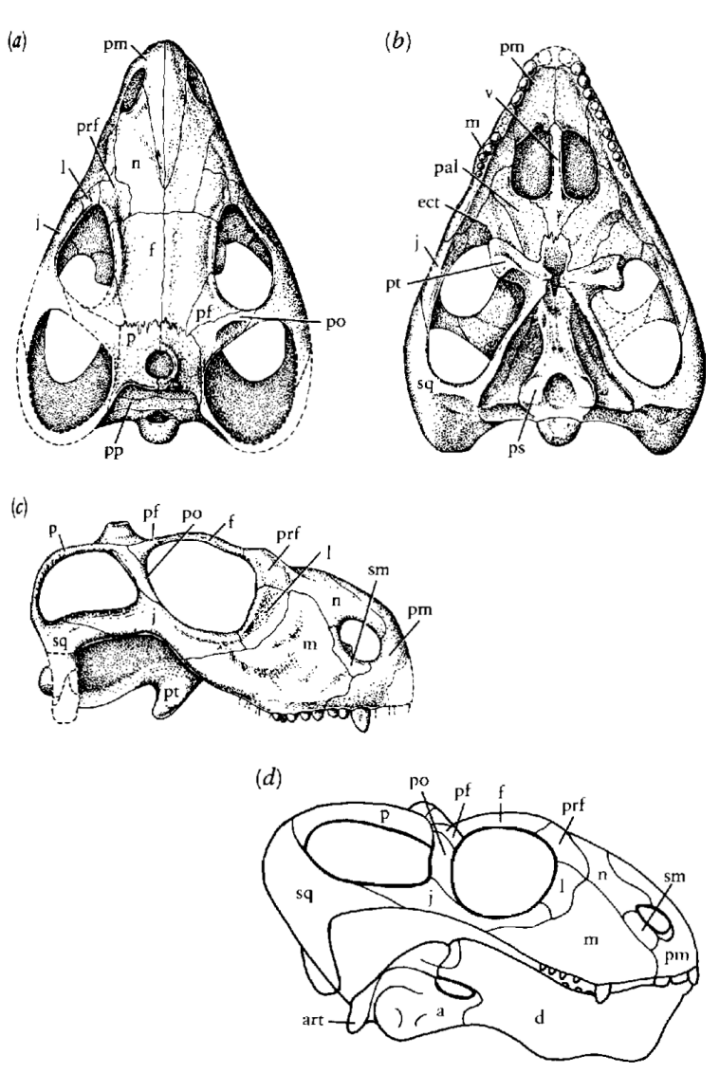


Figure 17-20. SKULLS OF PRIMITIVE UPPER PERMIAN ANOMODONTS. *Otsheria* in (a) dorsal, (b) palatal, and (c) lateral views, $\times \frac{1}{2}$. From Chudinov, 1960. (d) *Venjukovia* in lateral view, $\times \frac{1}{2}$. From Barghusen, 1976. Abbreviations as in Figure 8-3.

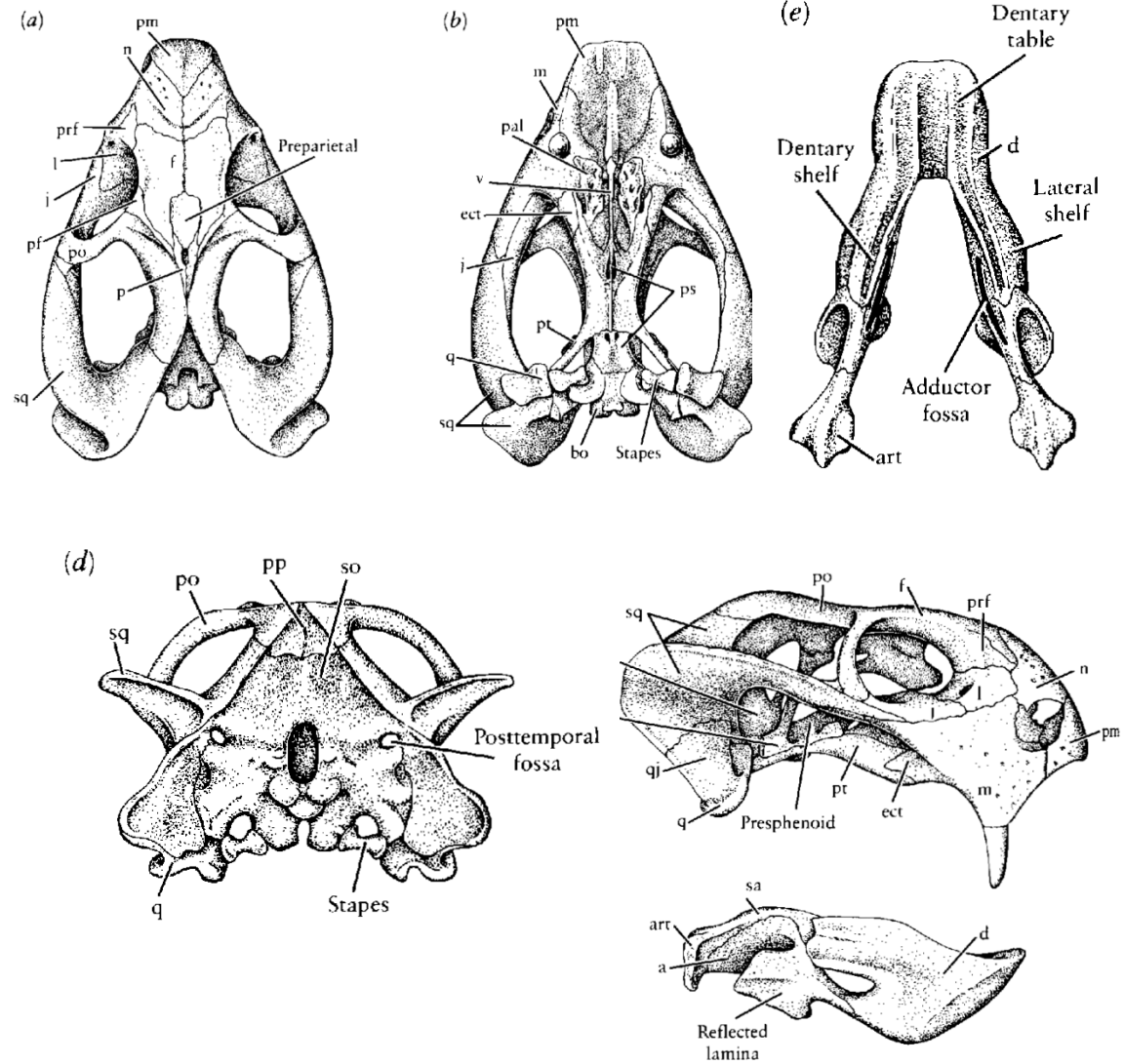


Figure 17-22. SKULL AND LOWER JAWS OF THE ADVANCED ANOMODONT *DICYNODON*. Skull in (a) dorsal, (b) palatal, (c) lateral, and (d) occipital views, $\times \frac{3}{2}$. (e) Lower jaw in dorsal view, $\times \frac{3}{2}$. Abbreviations as in Figure 8-3. From Cluver and Hotton, 1981.

Cynodontia

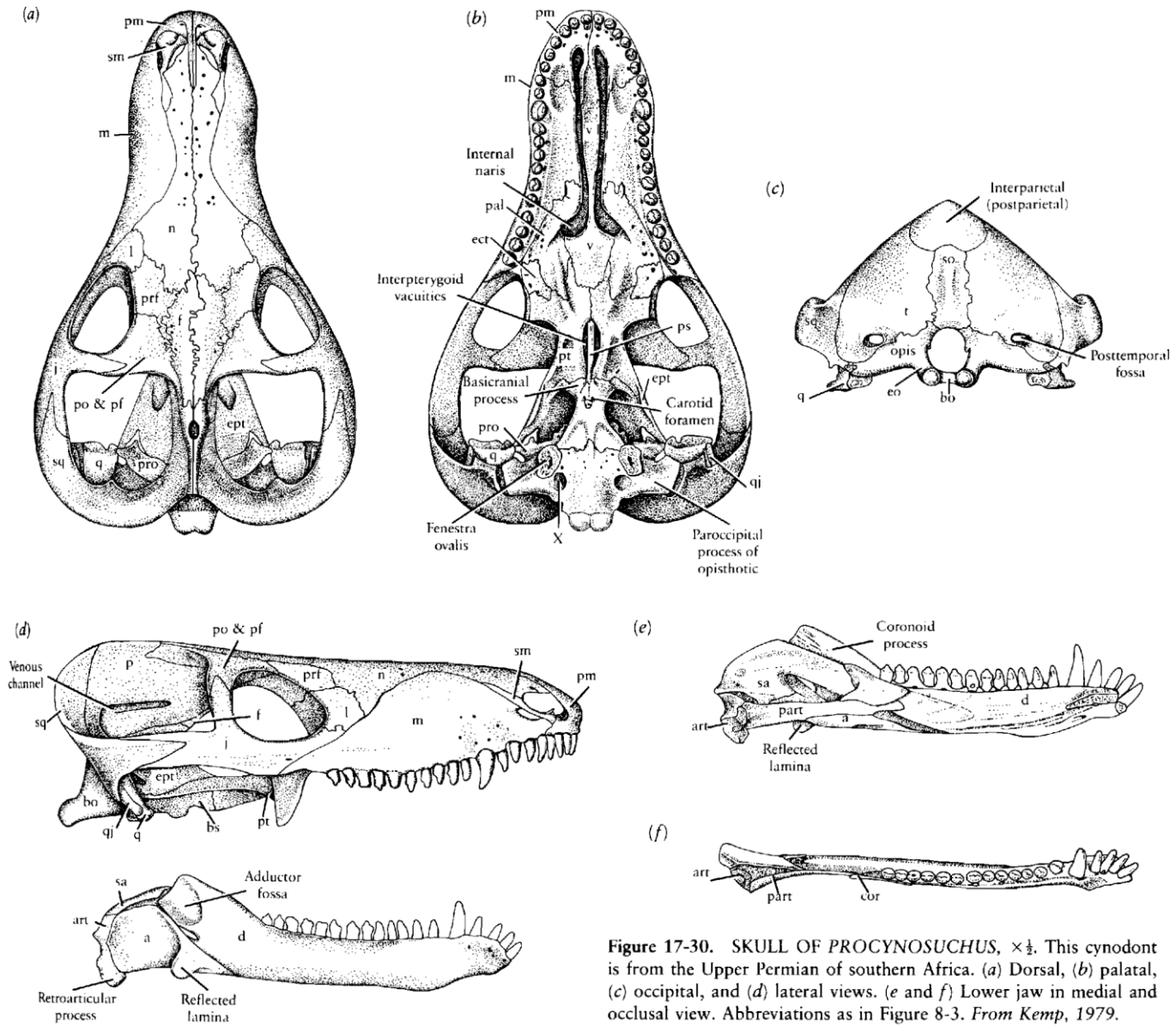


Figure 17-30. SKULL OF *PROCYNOSUCHUS*, $\times \frac{1}{2}$. This cynodont is from the Upper Permian of southern Africa. (a) Dorsal, (b) palatal, (c) occipital, and (d) lateral views. (e and f) Lower jaw in medial and occlusal view. Abbreviations as in Figure 8-3. From Kemp, 1979.

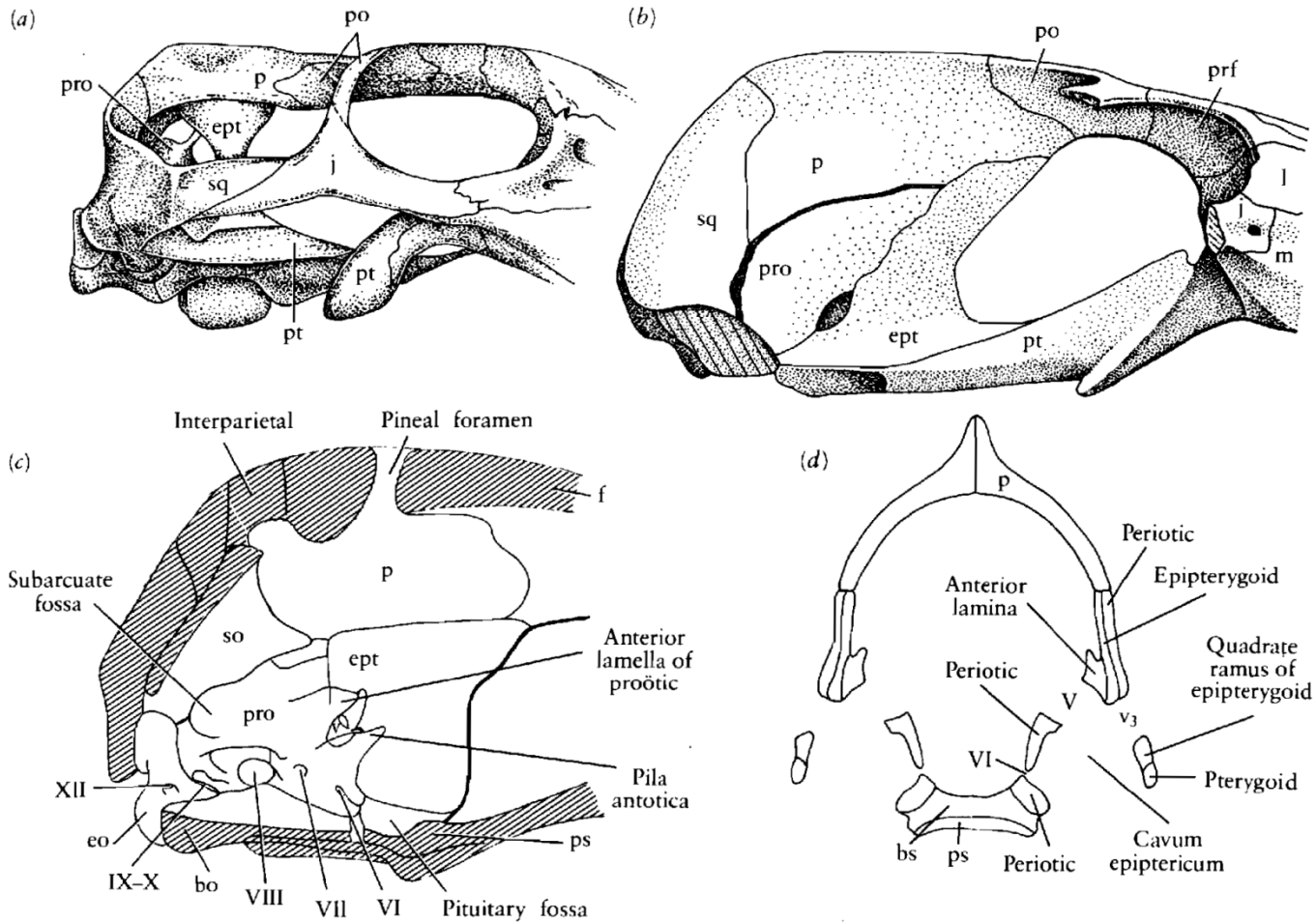
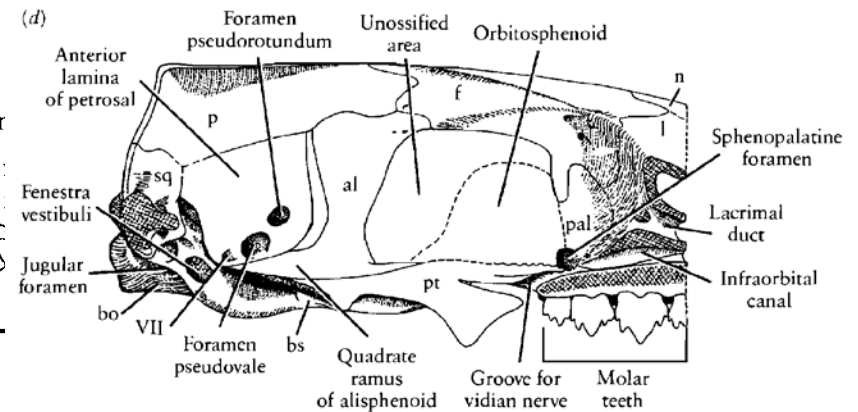
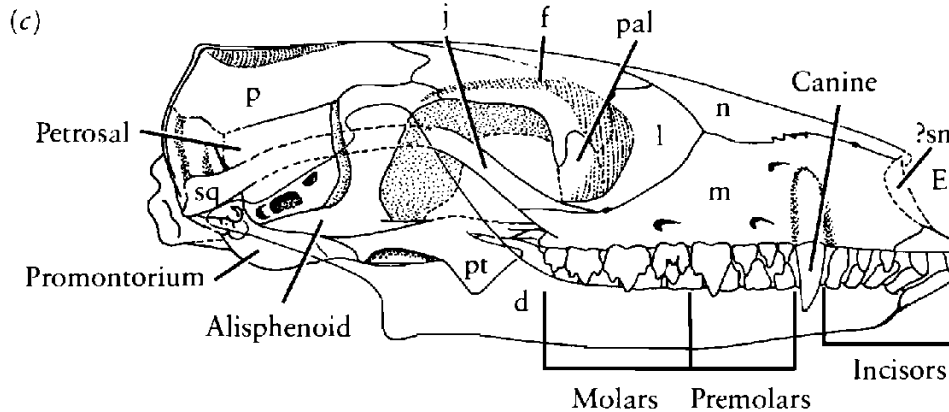
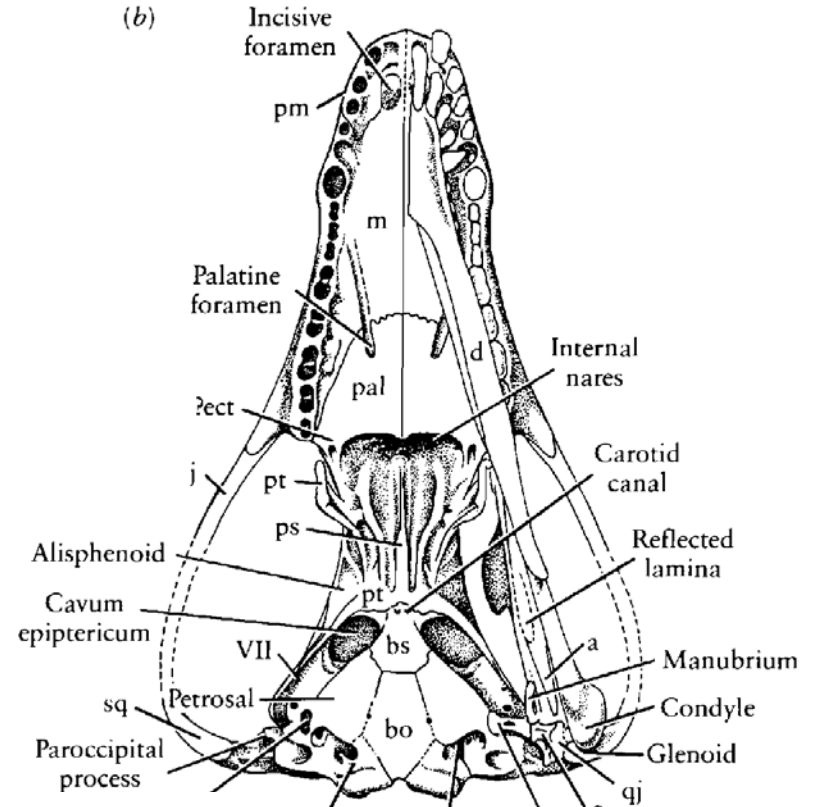
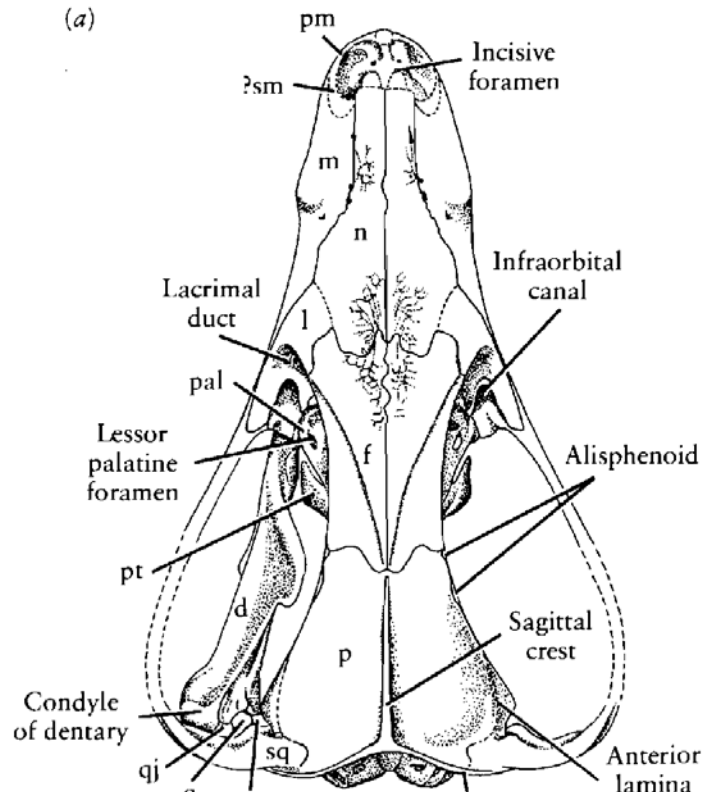


Figure 17-46. EVOLUTION OF THE MAMMALIAN BRAINCASE. (a) Posterior portion of the skull in the primitive therapsid *Regisaurus*. As in primitive amniotes, the braincase is still formed primarily by endochondral bones and cartilage. The parietal and squamosal are primarily superficial elements. The epipterygoid forms a broad vertical pillar that is lateral to the brain. *From Mendrez, 1972.* (b) Lateral view of the braincase in *Probainathus*, a Middle Triassic cynodont. The parietal and squamosal have spread ventrally to provide additional surface for the origin of the jaw musculature. They reach the otic capsule to form a continuous wall of the braincase posteriorly. The epipterygoid is sutureally attached to both the otic capsule and the parietal to form

a partial wall, lateral to the original cartilagenous braincase. The area of the braincase medial to the orbit remains unossified. *From Romer, 1970.* (c) Medial view of the lateral wall of the braincase in the Lower Triassic cynodont *Thrinaxodon*. *From Crompton and Jenkins, 1979.* (d) Transverse section through the back of the right side of the braincase in *Thrinaxodon* to show the position of the cavum epiptericum between the periotic and the epipterygoid. *From Crompton and Jenkins, 1979.* (c and d) By permission of the University of California Press. Abbreviations as in Figure 8-3, plus: V₃ opening for mandibular ramus of Vth nerve.

Mammalia



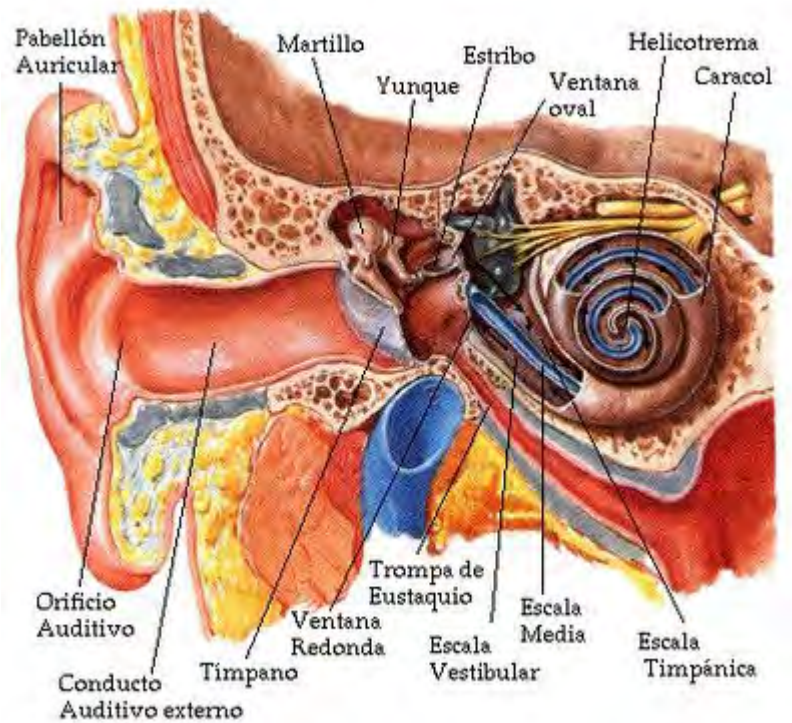
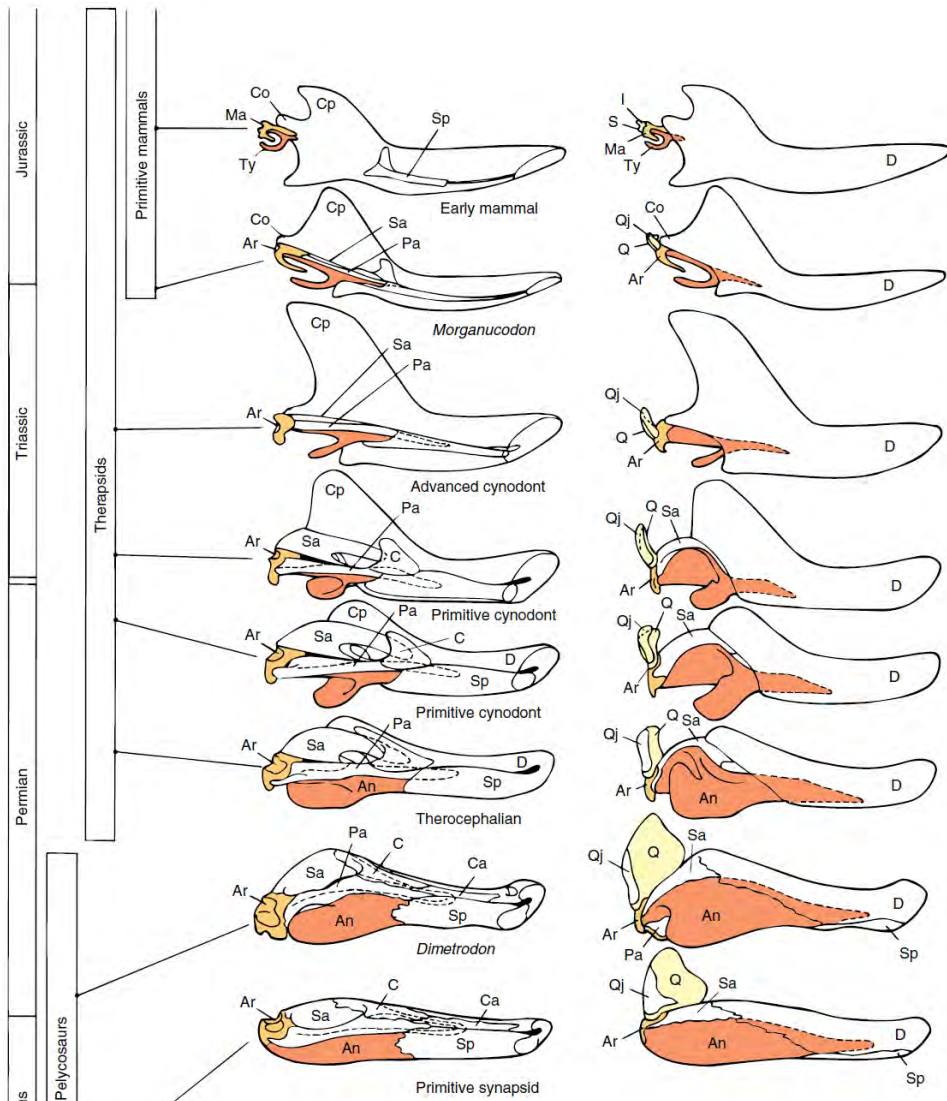


FIGURE 7.5 Evolution of the mammalian middle ear bones. Left column a medial view of the left mandibular ramus; right column lateral view of right mandibular ramus and quadrate. No teeth are shown to make comparisons clear. From primitive pelycosaurs, to therapsids, to first mammals, changes in the postdentary bones are indicated along with incorporation of the quadrate (incus) and articular (malleus) into the middle ear. The fossil species used to follow these changes are shown in relationship to their occurrence in the geological record. Abbreviations: angular (An), articular (Ar), coronoid (C), anterior coronoid (Ca), condyle of dentary (Co), coronoid process (Cp), dentary (D), incus (I), malleus (Ma), prearticular (Pa), quadrate (Q), quadratojugal (Qj), stapes (S), surangular (Sa), splenial (Sp), tympanic annulus (Ty).

Based on the research of James A. Hopson and Edgar F. Allin.

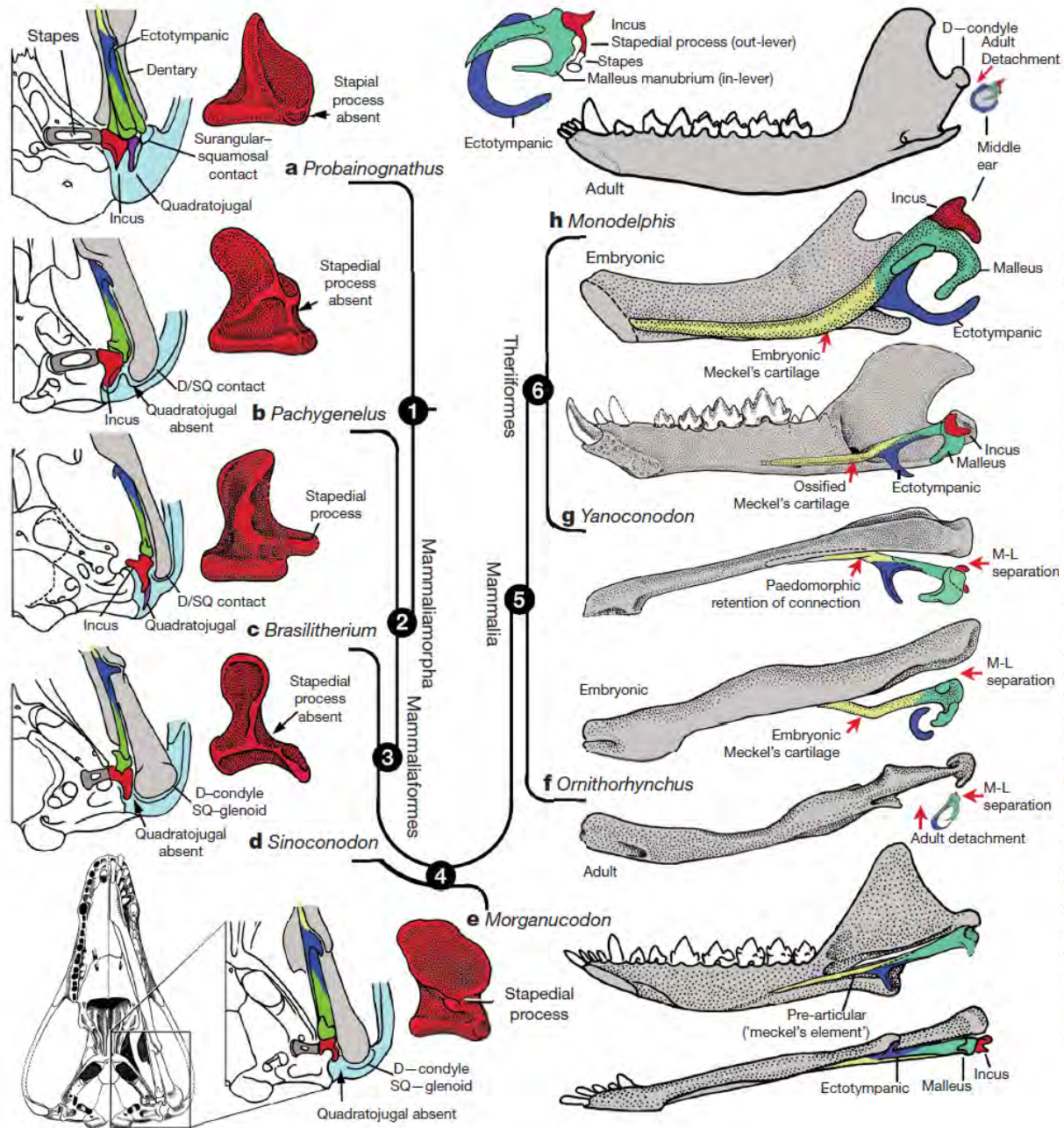
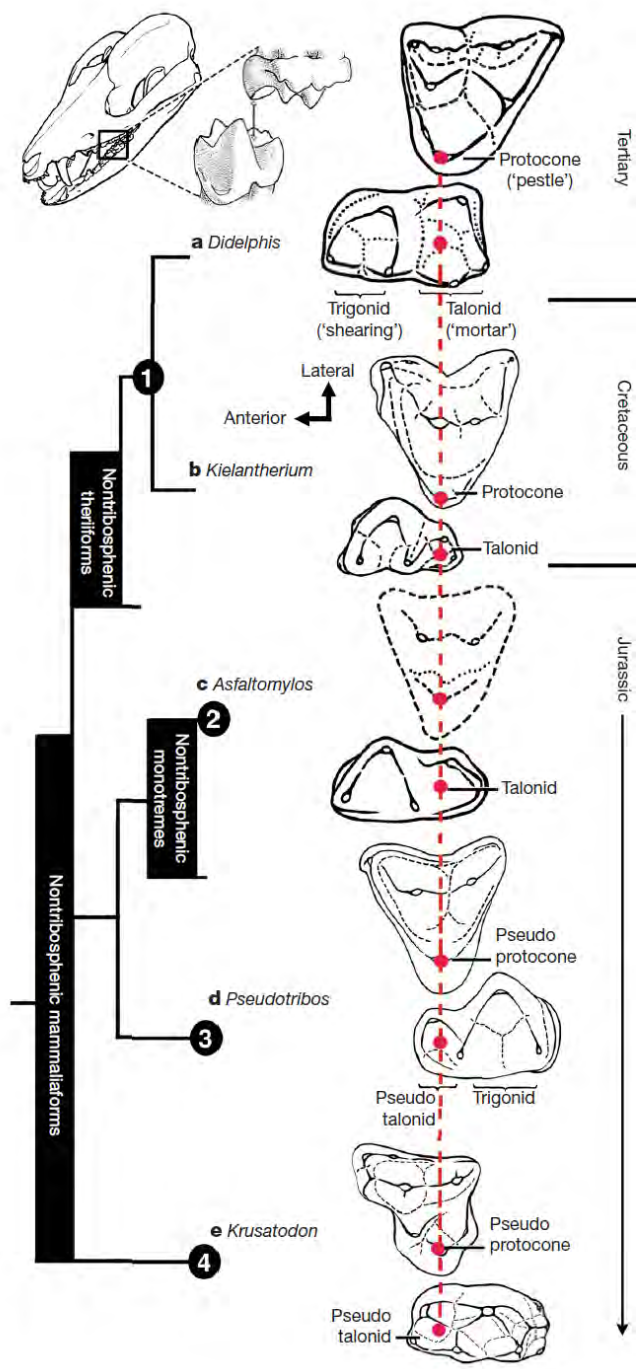
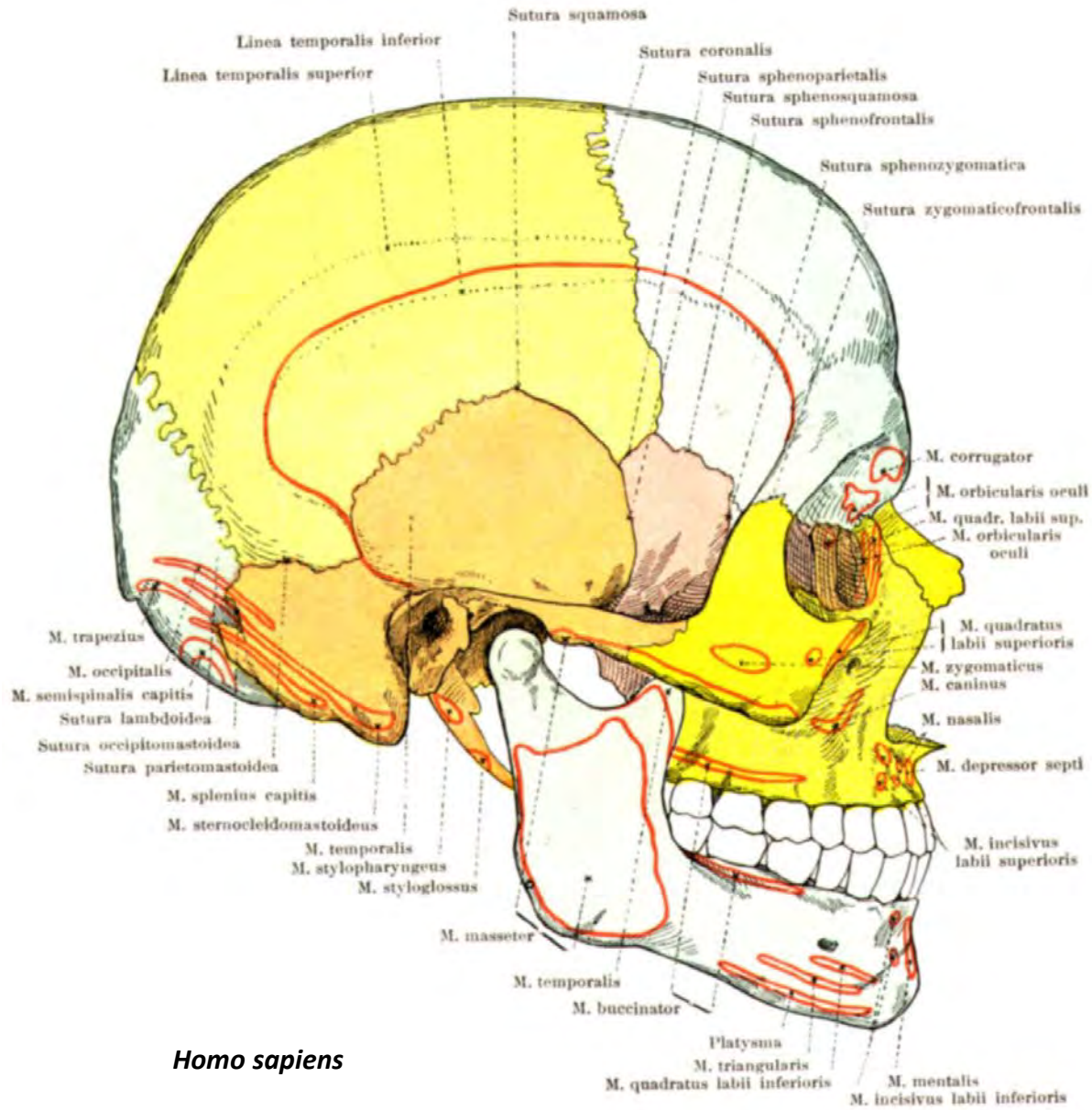
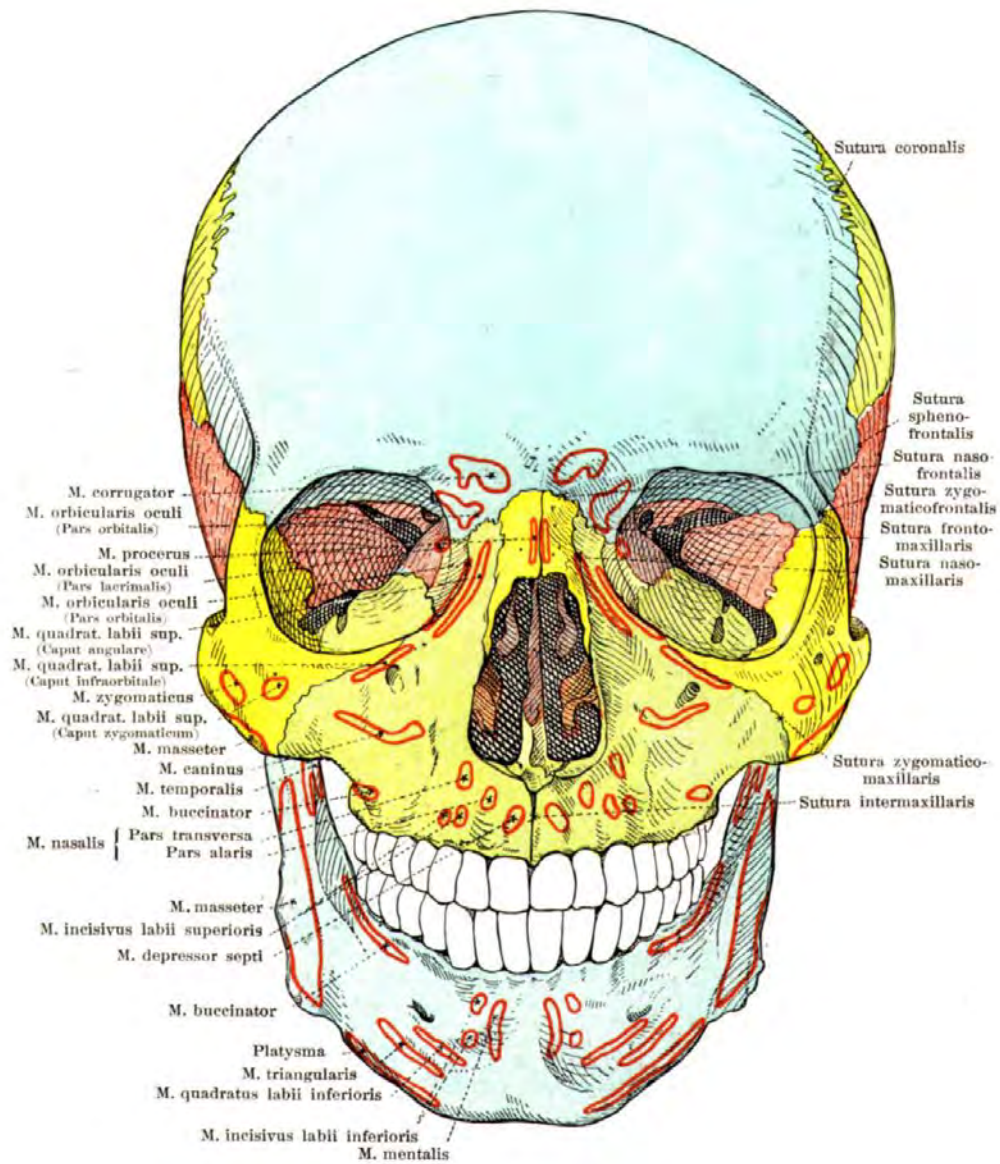
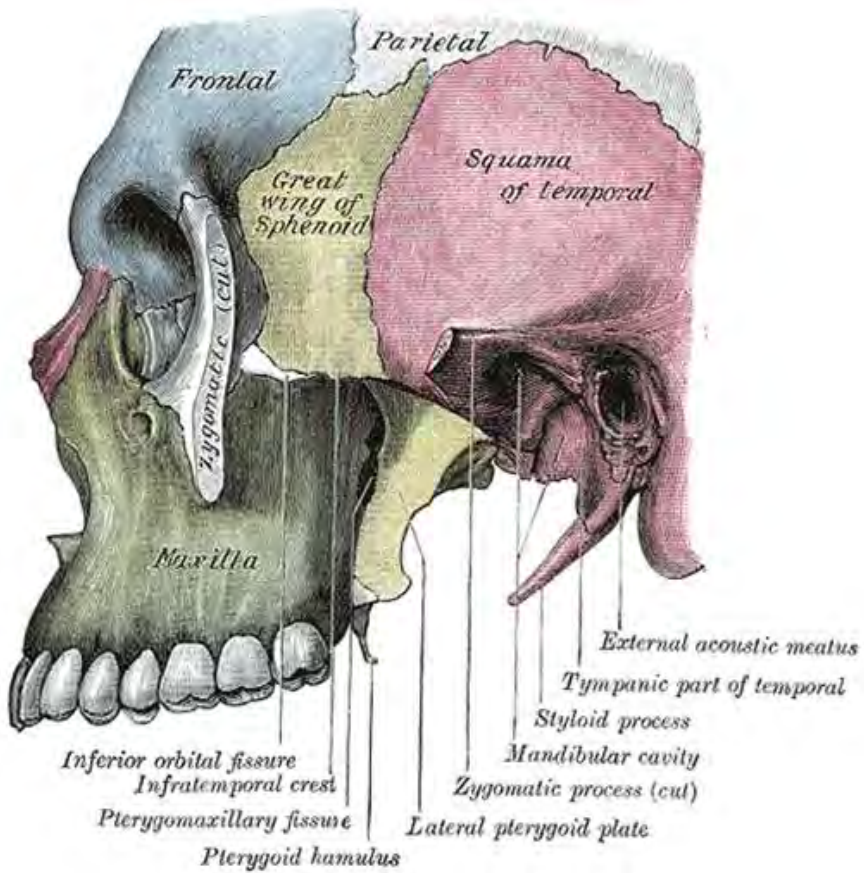


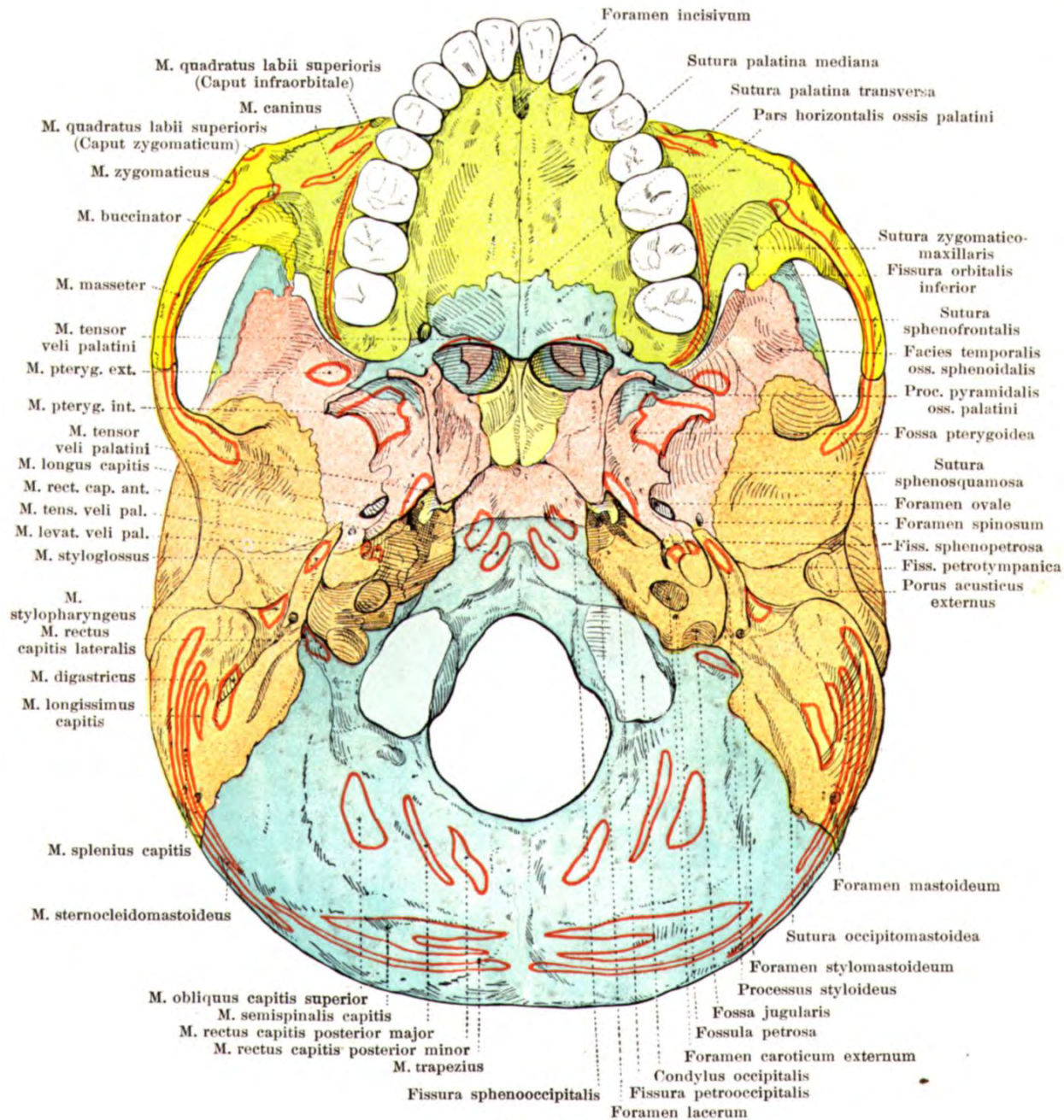
Figure 3 | Evolution of the mammalian cranio-mandibular joint and the definitive mammalian middle ear through the cynodont-mammal transition. Homoplasies occurred for the simplification of the incus articulation, the stapedial process of the incus and the detachment of the ectotympanic from mandible. **a**, The cynodont *Probainognathus*^{51,53}; ventral view of left basicranium and posterior view of the incus (quadrate). **b**, The mammaliaform *Pachygenelus*^{51,55}. **c**, The mammaliaform *Brasilitherium* (modified from ref. 57 by personal observation). **d**, The mammaliaform *Sinoconodon*. **e**, *Morganucodon* (redrawn from refs 53 and 54): left panel, left basicranium, ventral view; middle panel, left incus, posteromedial view; and right panel, the mandible and 'mandibular' middle ear in ventral (below) and medial (above) views. **a–e**, Homoplastic loss of the quadratojugal for a more mobile incus occurs in *Pachygenelus* (**b**) and mammaliaforms (**d, e**), but not in *Probainognathus* (**a**), tritylodontids (not shown) and *Brasilitherium* (**c**). The stapedial process of the incus, the out-lever for the middle ear, is present in tritylodontids (not shown), *Brasilitherium* (**c**) and *Morganucodon* (**e**), but not in other taxa (**a, b, d**). **f**, The monotreme *Ornithorhynchus* lower jaw (ventral view): the middle ear attached anteriorly to the mandible by Meckel's cartilage in the embryonic stage⁵⁹, but detached from the mandible after re-absorption of Meckel's cartilage in the adult. **g**, The eutriconodont *Yanacoconodon* lower jaw (lower panel, ventral view; upper panel, medial view): the middle ear is medio-laterally (M-L) separated from, but anteriorly connected to, the mandible by the prematurely ossified Meckel's cartilage, similar to the embryonic condition of monotremes of medio-lateral (M-L) separation of the ear from the mandible, and to the monotreme configuration of the ectotympanic and malleus. **h**, The medial view of the mandible and middle ear of the marsupial *Monodelphis*: the middle ear is attached to the mandible by Meckel's cartilage in the embryonic stage^{60,61}, but detached from the mandible after the re-absorption of Meckel's cartilage in the adult. Because *Yanacoconodon* (**g**) is nested between extant monotremes (**f**) and therians (**h**), both of which have separation of the middle ear from the mandible, the Meckel's connection of the ectotympanic to the mandible in *Yanacoconodon* shows that some Mesozoic mammals had homoplastic evolution of the definitive mammalian middle ear, defined by full detachment of the ectotympanic from the dentary. The ossified Meckel's cartilage of *Yanacoconodon* is very similar to the embryonic Meckel's cartilage of extant monotremes, and has paedomorphic resemblance to the embryonic condition of extant mammals. The homoplastic attachment of the mandible and the middle ear in *Yanacoconodon* is correlated with changes in the timing and rate of development. D, dentary; SQ, squamosal; D/SQ, the dentary-squamosal contact or joint.

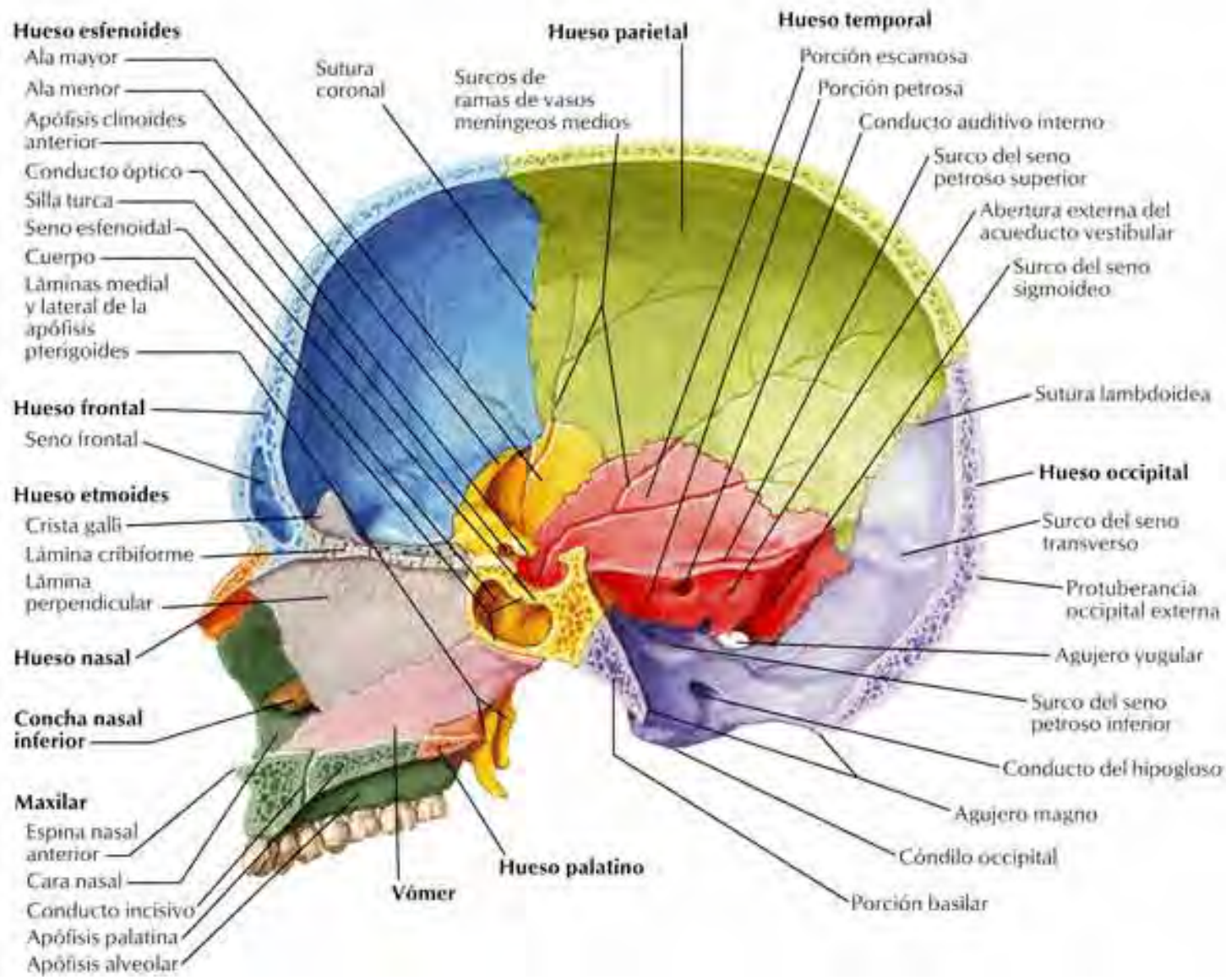


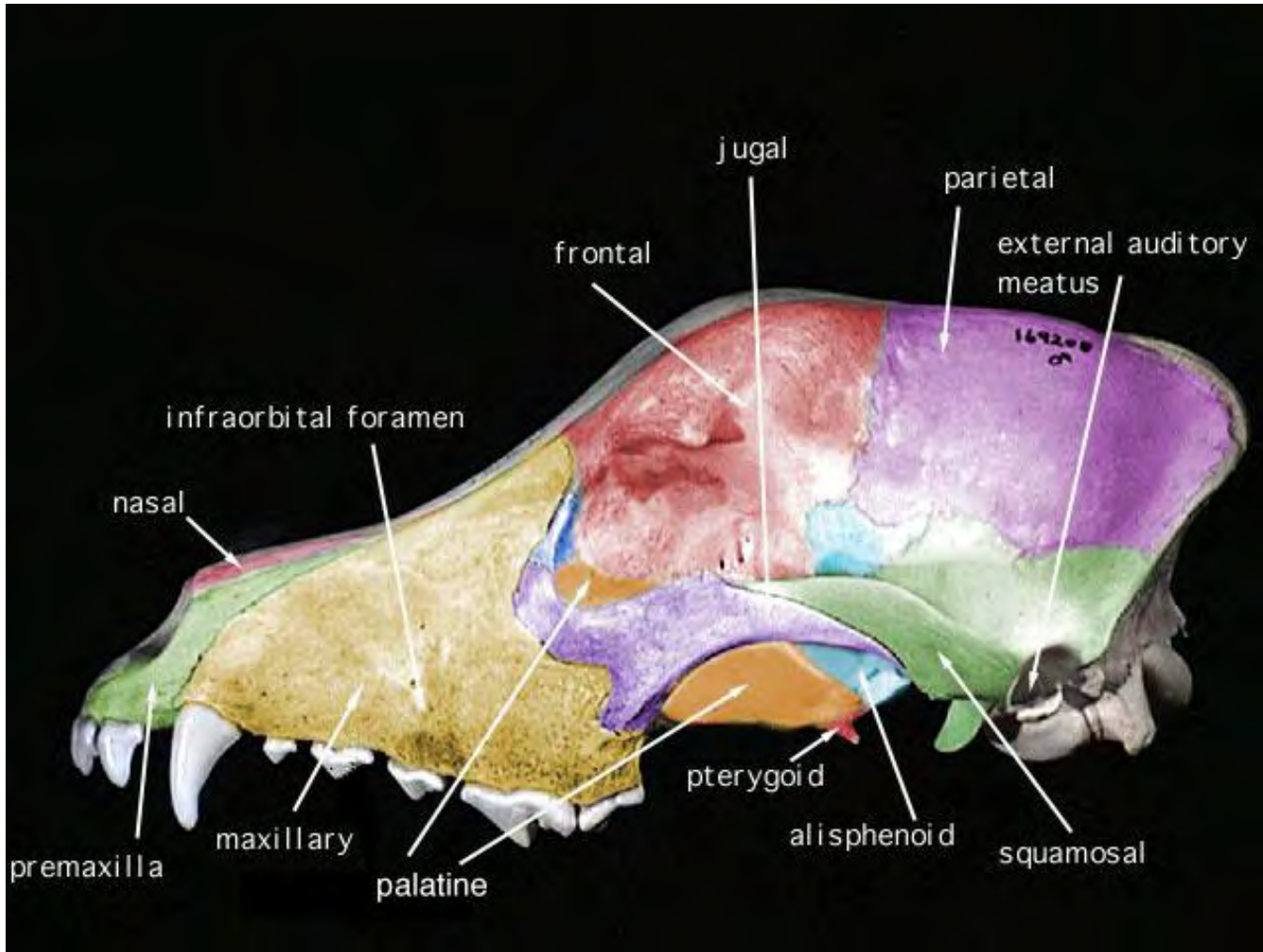


Homo sapiens

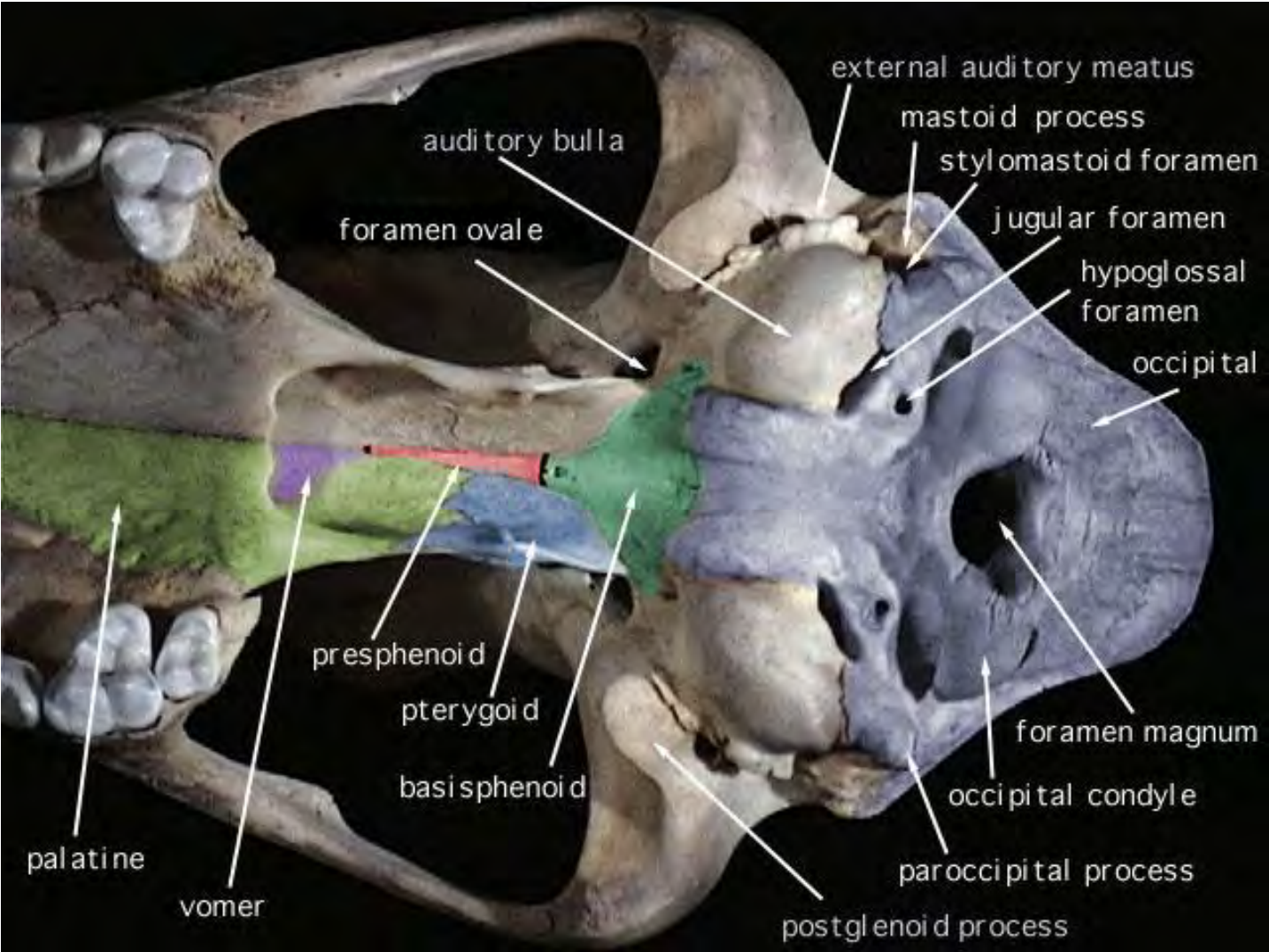


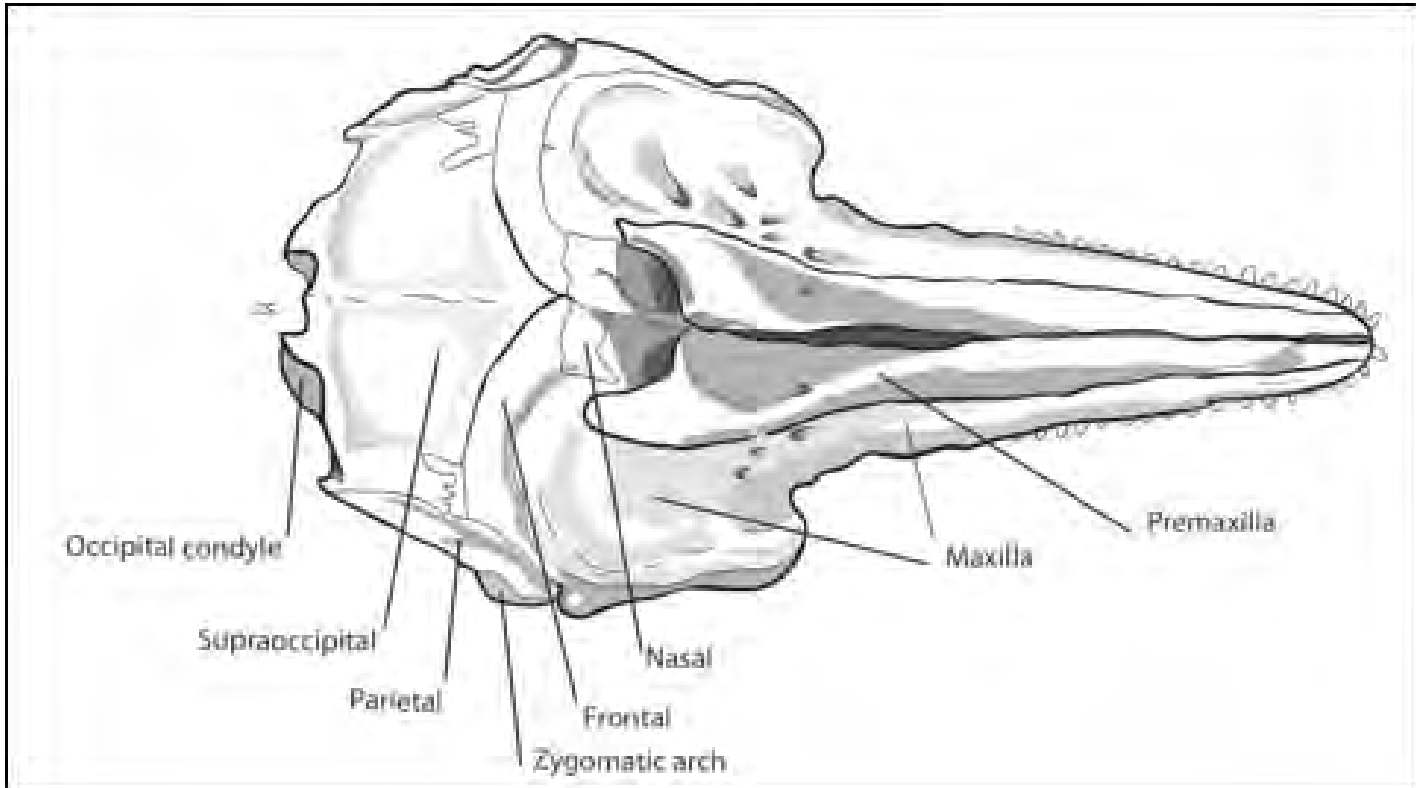




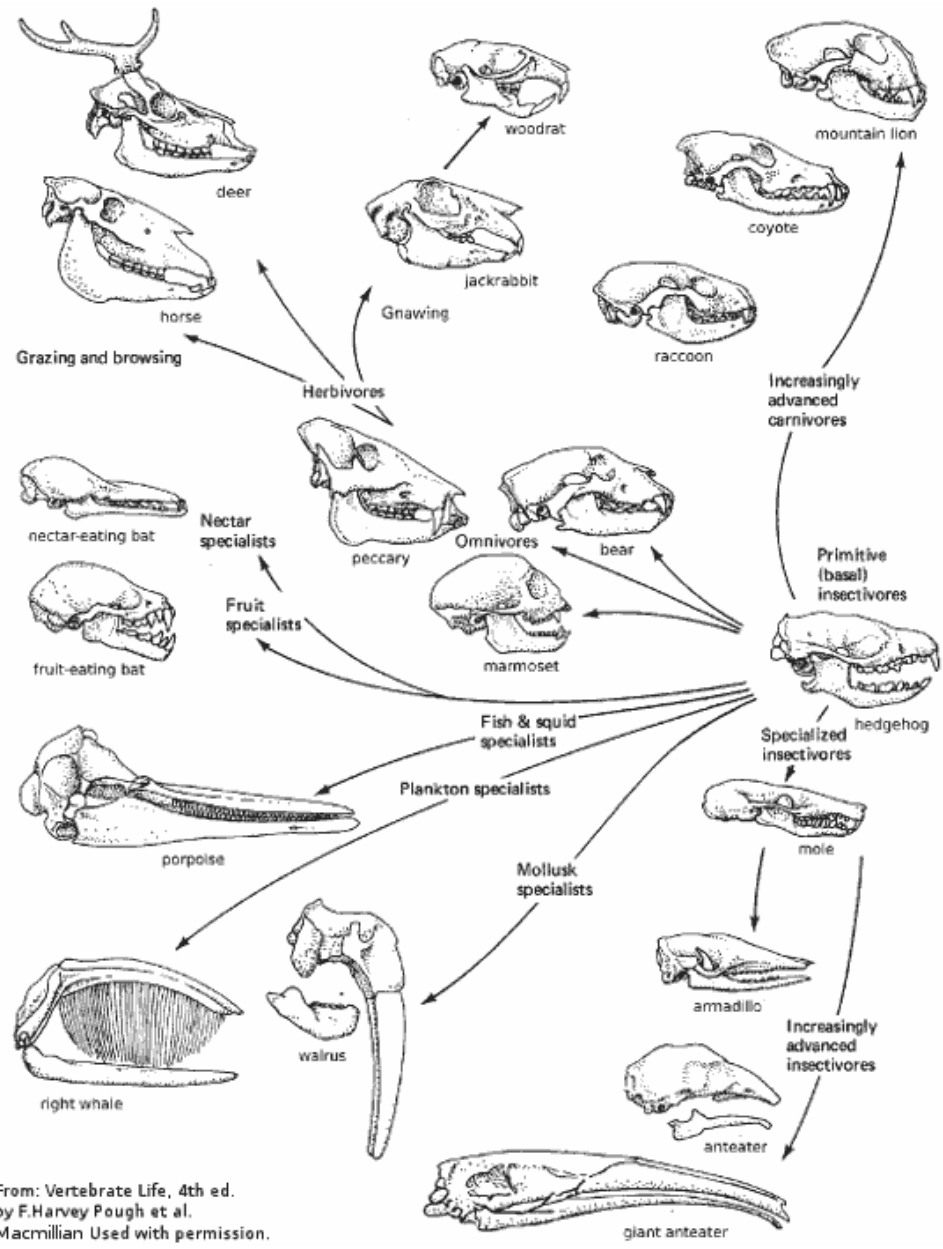


Canis lupus





Odontocetii



From: Vertebrate Life, 4th ed.
 by F. Harvey Pough et al.
 Macmillian Used with permission.